Investigations on Membrane Fouling and Cleaning in Ultrafiltration Processes in Lignocellulosic Biorefineries

Rudolph, Gregor

2021

Document Version:
Publisher's PDF, also known as Version of record

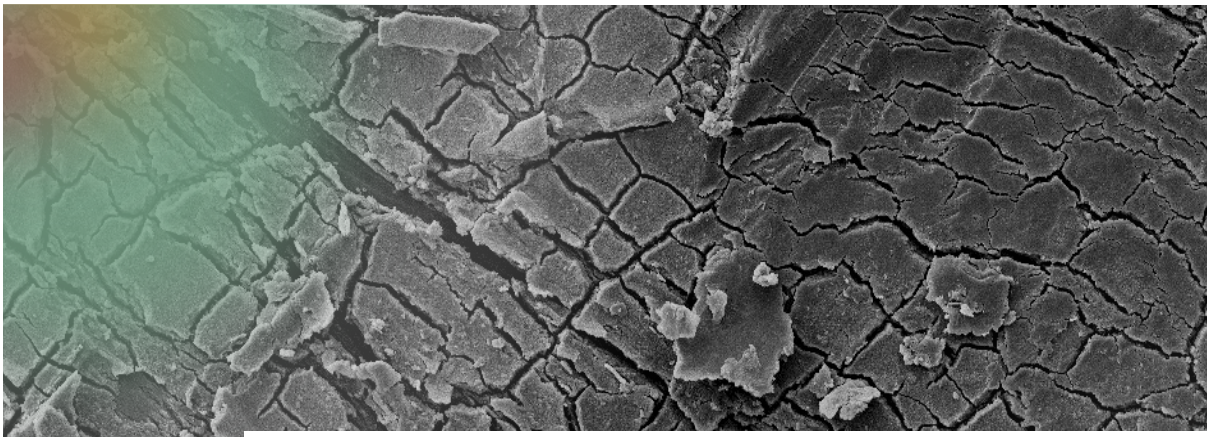

Investigations on Membrane Fouling and Cleaning in Ultrafiltration Processes in Lignocellulosic Biorefineries

GREGOR RUDOLPH | CHEMICAL ENGINEERING | LUND UNIVERSITY

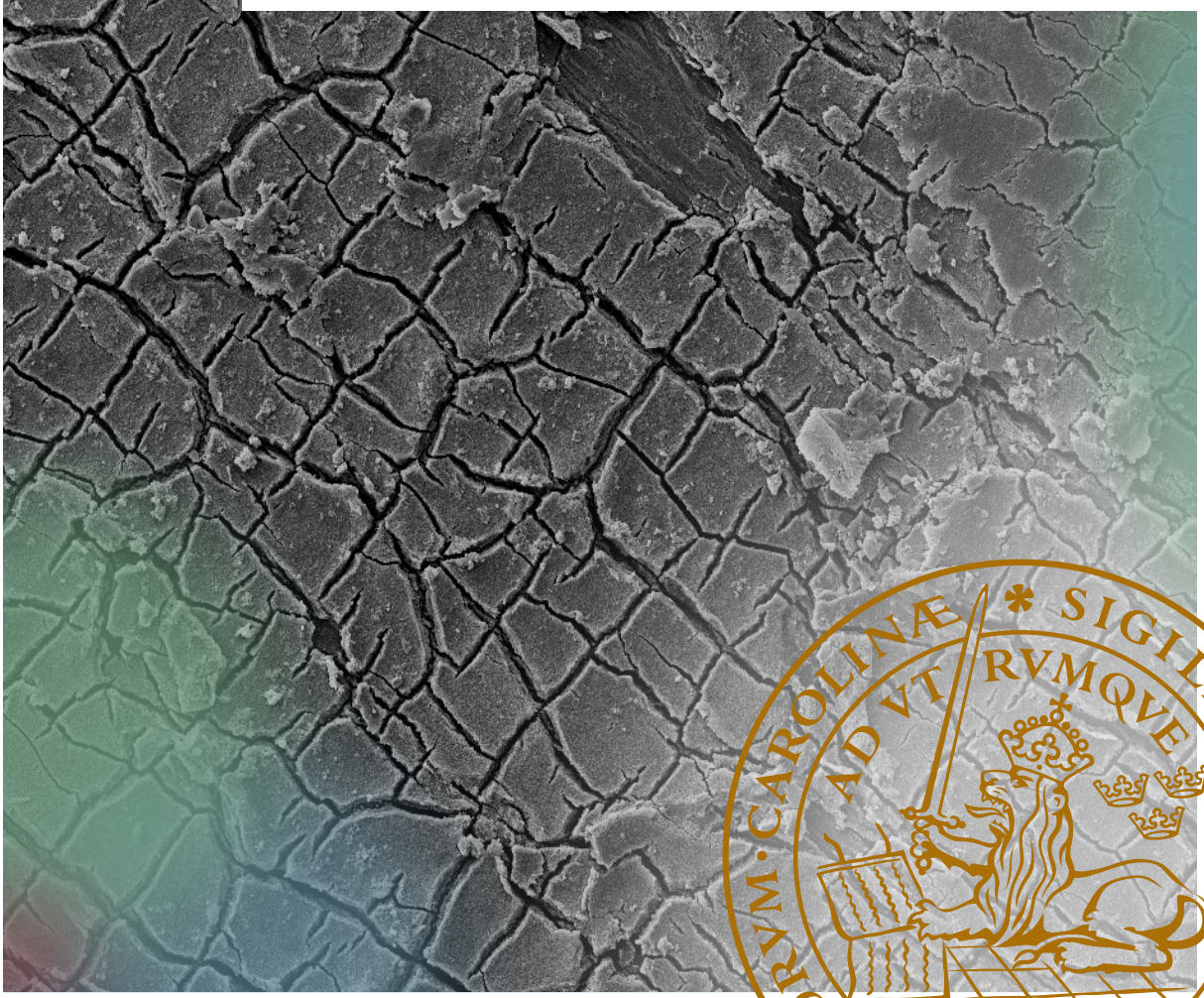

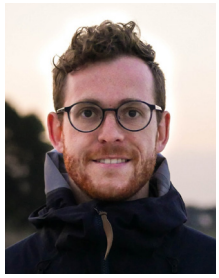

GREGOR RUDOLPH holds a bachelor's degree in mechanical engineering and a master's degree in chemical engineering from RWTH Aachen University, Germany. In 2016, he started his doctoral studies at the Department of Chemical Engineering at Lund University. His research has been focusing on improving the extraction of valuable compounds from process streams in pulp and paper mills, so-called lignocellulosic biorefineries, by membrane filtration, a cost- and energy-efficient filtration process. The greatest challenge in this task is that the membranes tend to clog during the filtration. This is usually referred to as "membrane fouling" and can only be overcome by regular membrane cleaning.

In the work presented in this thesis, membrane fouling was analyzed with a number of analytical techniques to understand why and how membrane fouling takes place, and what is actually fouling the membranes. In addition, cleaning of fouled membranes in new environmentally friendly ways was investigated. The research presented in this thesis supports the improvement of membrane technology in lignocellulosic biorefineries, making it more attractive to implement it, hereby constituting an important contribution in the transformation of society from a fossil-based to a sustainable bio-based one.

Printed by Media-Tryck, Lund 2021 NORDIC SWAN ECOLABEL 3041 0903

ISBN: 978-91-7422-808-3

Chemical Engineering
Faculty of Engineering
Lund University

Investigations on Membrane Fouling and Cleaning in Ultrafiltration Processes in Lignocellulosic Biorefineries

Investigations on Membrane Fouling and Cleaning in Ultrafiltration Processes in Lignocellulosic Biorefineries

by Gregor Rudolph

LUND
UNIVERSITY

Thesis for the degree of Doctor of Philosophy in Engineering

by due permission of the Faculty of Engineering, Lund University, Sweden.
To be defended on Friday, 11th June 2021 at 09:15 in Lecture Hall KC:B at the Department of Chemical Engineering, Lund University.

Faculty opponent

Prof. João Crespo
Department of Chemistry, Universidade Nova de Lisboa, Portugal

Organization	Document name
LUND UNIVERSITY Department of Chemical Engineering P O Box 124 SE–221 00 LUND Sweden	**DOCTORAL DISSERTATION** Date of disputation 2021-06-11 Sponsoring organization None
Author(s) Gregor Rudolph	

Title and subtitle

Investigations on Membrane Fouling and Cleaning in Ultrafiltration Processes in Lignocellulosic Biorefineries

Abstract

The current fossil-based economy must be transformed into a bio-based circular economy. A cornerstone of this transformation is the conversion of pulp and paper mills into lignocellulosic biorefineries that allow not only the production of pulp, paper, and electricity, but also novel biochemicals. Highly selective, electrifiable, and low-energy-consuming separation technologies will be key in the complete and economically feasible utilization of valuable compounds from lignocellulosic biomass such as wood. These requirements are met by the pressure-driven membrane processes microfiltration, ultrafiltration (UF), nanofiltration and reverse osmosis. The greatest challenge to the broad implementation of membrane processes in lignocellulosic biorefineries is membrane fouling. Membrane fouling not only alters the capacity and selectivity of the membrane, but also increases the investment and operational costs of the separation process. Membrane fouling can often only be overcome by chemical cleaning. Improvements in chemical cleaning processes would result in a reduction in operational costs and lessen the environmental impact of the process.

In the work presented here, the fouling and cleaning of membranes used for the UF of process streams from lignocellulosic biorefineries were investigated. This was done with the help of *ex situ* and *in situ* analytical methods. Suitable *in situ* real-time monitoring techniques for this task were identified and evaluated through a literature review and a survey carried out among industrial membrane users and analytical equipment suppliers. Membrane fouling was studied *ex situ* using techniques such as scanning electron microscopy, atomic force microscopy, attenuated total reflectance-Fourier transform infrared spectroscopy, and Brunauer-Emmett-Teller surface analysis. Quartz crystal microbalance with dissipation monitoring was used for *in situ* real-time adsorption studies. UF of thermomechanical pulping process water with the commercially available UFX5-pHt membrane from Alfa Laval was used as a reference system. This process water contained hemicelluloses, lignin, wood extractives, and inorganic residues. UF of other solutions associated with lignocellulosic biorefineries, such as black liquor from Kraft pulping, hot water extract from sawdust, and bleach plant effluent from sulfite pulping, were also investigated. For the reference system, it was found that especially hemicelluloses were immediately adsorbed on the membrane, forming a thin rigid fouling layer. This layer became thicker and softer over time, due to the incorporation of droplets of colloidal extractive stabilized by hemicelluloses, until equilibrium was reached. After reaching equilibrium, water was lost from the fouling layer, and it became thinner and more rigid again. It was also found that foulants entered the inner structure of the membranes, blocking the pores or being adsorbed on the pore walls. Rinsing with water revealed that a very thin fouling layer consisting not only of hemicelluloses, but also of wood extractive residues such as fatty and resin acids, remained adsorbed on the membrane polymer. Alkaline cleaning with a commercial cleaning agent removed irreversible fouling, and the initial membrane permeability was recovered. However, this was only possible after one filtration cycle. When the same membrane was used for several filtration cycles and subjected to several cleaning cycles, alkaline cleaning was no longer effective. A home-made enzyme cocktail was investigated as an alternative and more environmentally sound cleaning agent. The membrane permeability was not completely recovered when this cocktail was used alone, but promising results were obtained when it was used in combination with the alkaline cleaning agent.

Overall, the findings presented in this thesis will help improve membrane filtration processes in lignocellulosic biorefineries. It was shown that detailed analysis of membrane fouling allowed the processes leading to reductions in capacity and selectivity during UF of process streams to be identified. Comprehensive knowledge on the causes of membrane fouling will make it easier to tailor membrane cleaning processes. This will prolong the membrane lifetime, and reduce plant downtime and the usage of chemicals and water, resulting in a reduction in process costs and a more environmentally sound process. The findings of this work will also contribute to the wider implementation of membrane processes in the transition from a fossil-based economy to a fossil-free bio-based circular economy.

Key words

Membrane fouling, membrane cleaning, ultrafiltration, online monitoring, galactoglucomannan, wood extractives, QCM-D, lignocellulosic biomass, pulp and paper

Classification system and/or index terms (if any)

Supplementary bibliographical information	Language
	English
ISBN (print) 978-91-7422-808-3	ISBN (pdf) 978-91-7422-809-0
Recipient's notes	Number of pages 212 / Price
	Security classification

Investigations on Membrane Fouling and Cleaning in Ultrafiltration Processes in Lignocellulosic Biorefineries

by Gregor Rudolph

LUND
UNIVERSITY

This doctoral thesis consists of two parts. A summary puts the research into context and presents the main findings and conclusions. The publications themselves are then reproduced. All but one of these papers have been published in peer-reviewed journals.

Cover illustration by
Gregor Rudolph

Faculty of Engineering, Department of Chemical Engineering,

ISBN: 978-91-7422-808-3 (print)
ISBN: 978-91-7422-809-0 (pdf)

Printed in Sweden by Media-Tryck, Lund University, Lund 2021

Det har jag aldrig provat förut, så det klarar jag säkert.
(I've never tried this before, so I'm sure I can do it.)
– Pippi Långstrump

Acknowledgments

First and foremost, I would like to thank my supervisors, Prof. Frank Lipnizki and Prof. Ann-Sofi Jönsson, from the depth of my heart. This work would not have been possible without their support and guidance. Thank you for being open to all my ideas and problems. Frank, I am very grateful for all the funny, insightful and enlightening talks that usually went on way too long and had to be terminated abruptly because you had to go to a meeting that started 5 minutes ago. Ann-Sofi, without your trust in me I would not have been able to carry out at PhD in Lund at all. I am deeply grateful for your critical, but always encouraging views on my work. The positive energy you kindled with every new finding I presented was pure motivation.

I would also like to thank my co-supervisors, Dr. Herje Schagerlöf and Prof. Ola Wallberg. Thank you, Herje, for always being available for discussions on every analytical method and for your help in solving my analytical problems. Thank you, Ola, for being so welcoming, and for making my time in the Biorefinery Group so productive.

Special thanks go to Dr. Tiina Virtanen from LUT University, Finland. Thank you for your friendship, fruitful cooperation, and the important impact of our collaboration on my thesis. Thanks also to Prof. Mari Kallioinen for our fruitful collaboration, and for the fantastic time you and Prof. Mika Mänttäri gave me during my visit to the Membrane Technology Laboratory at LUT University.

I would like to thank Dr. Tatiana Plisko and Prof. Alexander Bildyukevich, for their friendship and the wonderful experiences I had in Minsk, Belarus. Without this opportunity, I would not have learned how to cast membranes.

I owe a huge debt of gratitude to Prof. Tommy Nylander for granting me access to the endless analytical facilities of the Division of Physical Chemistry at the Department of Chemistry, Lund University. Thanks to Dr. Polina Naidjonoka, Prof. José Campos Terán, Dr. Ben Humphreys and Dr. Axel Rüters for their guidance during my journey in physical chemistry. In this context, I would like to express special thanks to Dr. Roberto Ortiz from CR Competence for fruitful discussions on my ideas and problems. I am extremely grateful that you shared your extensive knowledge of QCM-D with me.

Thank you also to Dr. Emanuel Larsson, at the Division of Solid Mechanics, Lund University, for sharing your extensive knowledge on tomography and image analysis. It was great working with you, and I hope our journey has not come to an end. Warm thanks to all my colleagues at the Department of Chemical Engineering,

especially the members of the Membrane Group. It was so much fun and motivating to carry out my PhD studies with you. I would like to especially thank Miguel Sanchis-Sebastiá, Dr. Johan Thuvander and Dr. Basel Al-Rudainy. Without your support, I would have drowned. Thanks to Dr. Mats Galbe and Dr. Borbála Erdei for lending a helping hand whenever I needed it; and to Dr. Anton Löfgren for all our enlightening political discussions and for teaming up with me in the sustainable event team. Thanks to Dr. Federico Micolucci for all the amazing nights out! Thanks to Maja Ekblad for being the best roommate and for teaching me so much about Sweden and Swedish culture; and to Ellen Edefell and Michael Persson, for the productive time we spent together on the Departmental Board representing our fellow PhD students. I wish to thank Leif Stanly, Maria Messer and Gitty Yahoo for making working at the Department so smooth, and for helping whenever anyone needs you. Special thanks to Gertrude Persson for the great chats we had about anything and everything, and your wonderful open heart. Lena Nielsson you are missed!

I am grateful to all the students who helped me and challenged me during my PhD studies: Marta Lemos Ferreira, Catarina Oliveira, Ferry Oomen, Astrid Hermansson, Linnéa Petersson, and Sofia Correia. Thank you to the KTEK40 students that I was honored to teach the wonders of mass transfer processes.

I wish to thank my collaborators and everyone I came to know through the courses, workshops, conferences, and summer schools I attended, and who made those events such great experiences.

Finally, I would like to thank my paternal grandmother and my maternal grandfather, who both passed away during my time in Sweden, for having been such great grandparents. I miss you! I would like to thank my family for their support and trust along this journey; and my friends, especially Balzi, and Jan, whom I talked to most about the ups and downs of my work. Last, but by no means least, I thank my loving Marie from the bottom of my heart. Without your warm-hearted support and critical reviews, I would not have grown into a confident researcher and a very happy man. I would like to thank the funding agencies that supported my travels all over the world: the Åforsk Foundation, Civilingenjören Hakon Hanssons stiftelse, the Erasmus+ Teaching Staff Mobility programme, the European Membrane Society, and the Royal Physiographic Society of Lund. Thanks to Alfa Laval, Denmark; Banmark, Finland; Ecolab, Germany; Novozymes, Denmark; and Stora Enso, Sweden, for providing various kinds of material used in this work.

Popular Scientific Summary

Transforming society with bio-based products: mastering the separation process is key

The transition to a circular, non-fossil-based economy is the main priority of many scientists within engineering worldwide, through necessity. We need every possible contribution to prevent the climate crisis we are facing. Producing new bio-based products from wood represents such a contribution. We can extract valuable compounds from wood thanks to a process called membrane filtration.

Let's create new materials from wood

To utilize all the valuable compounds in wood, it must be decomposed into its chemical building blocks. Industrial plants for this process already exist in the form of pulp mills that produce the raw materials for paper, cardboard, and textile production. Incorporating membrane technology into pulp mills transforms them into "lignocellulosic biorefineries", enabling us to extract even more useful chemicals that would otherwise end up as waste. The work presented in this thesis helps lignocellulosic biorefineries come one step closer to the circular economy, but the process demands advanced technology.

During the processing of wood, some of its chemical constituents dissolve in water. One of the challenges is to extract and concentrate these compounds for further use. An efficient and energy-smart way of doing this is by using membrane filtration. Membranes are very dense filters that can be used to separate the molecules in a solution according to their size, in much the same way as a filter is used to hold back ground coffee beans when making filter coffee, but on a much smaller scale. The greatest problem in using membranes for this task is that they tend to become clogged during filtration. This is usually referred to as "membrane fouling".

A closer look at the problem and how it can be solved

I have studied the fouling and cleaning of membranes in lignocellulosic biorefineries. I used a number of analytical techniques to understand why and how membrane fouling takes place, and what is actually fouling the membranes. I analyzed the membranes after use and after cleaning, and studied the development of fouling during filtration. Finally, I investigated new ways of cleaning fouled membranes in an environmentally friendly way.

My work showed that a group of compounds found in the solution obtained from mechanical pulping at high temperatures, became attached to the membrane surface forming a thin layer. This layer grew over time and other components became incor-

porated into it. These compounds also entered the pores of the membranes. Rinsing with water removed most of the fouling, but a very thin layer remained. It was possible to remove this remaining fouling with an environmentally friendly mixture of enzymes, followed by cleaning with an alkaline cleaning agent.

My vision is that this research will improve membrane processes in lignocellulosic biorefineries, making it more attractive to implement them. This would constitute an important contribution in the transformation of society from a fossil-based to a sustainable bio-based one.

Populärvetenskaplig sammanfattning

Omvandla samhället med biobaserade produkter: det är viktigt att behärska separationsprocessen

Övergången till en cirkulär, fossilfri ekonomi är den viktigaste prioriteringen för många forskare inom ingenjörsvetenskap världen över, av nödvändighet. Vi behöver alla möjliga bidrag för att förebygga den klimatkris vi står inför. Att producera nya biobaserade produkter från trä är ett sådant bidrag. Vi kan utvinna värdefulla föreningar ur trä tack vare en process som kallas membranfiltrering.

Låt oss skapa nya material från trä

För att utnyttja alla värdefulla föreningar i trä måste det brytas ner till dess kemiska byggstenar. Industriella anläggningar för denna process finns redan i form av massafabriker som producerar råvaror för pappers-, kartong- och textiltillverkning. Genom att införa membranteknik i massafabrikerna förvandlas de till lignocellulosabaserade bioraffinaderier", vilket gör det möjligt för oss att utvinna ännu fler användbara kemikalier som annars skulle gå till spillo. Det arbete som presenteras i denna avhandling hjälper lignocellulosabioraffinaderier att komma ett steg närmare en cirkulär ekonomi, men processen kräver avancerad teknik.

Under bearbetningen av trä löser sig en del av dess kemiska beståndsdelar i vatten. En av utmaningarna är att extrahera och koncentrera dessa föreningar för vidare användning. Ett effektivt och energisnålt sätt att göra detta är att använda membranfiltrering. Membran är mycket täta filter som kan användas för att separera molekyler i en lösning baserat på deras storlek, på ungefär samma sätt som ett filter används för att hålla tillbaka malda kaffebönor när man gör filterkaffe, men i mycket mindre skala. Det största problemet med att använda membran för denna uppgift är att de tenderar att bli igensatta under filtreringen. Detta brukar kallas "membranförorening". "membranförorening".

En närmare titt på problemet och hur det kan lösas

Jag har studerat nedsmutsning och rengöring av membran i bioraffinaderier för lignocellulosa. Jag har använt ett antal analytiska metoder för att förstå varför och hur membranen blir nedsmutsade och vad som faktiskt smutsar ner membranen. Jag analyserade membranen efter användning och efter rengöring och studerade utvecklingen av nedsmutsning under filtrering. Slutligen undersökte jag nya sätt att rengöra förorenade membran på ett miljövänligt sätt. Mitt arbete visade att en grupp föreningar, som finns i den lösning som erhålls vid mekanisk massaförbränning vid höga temperaturer, fastnade på membranytan och bildade ett tunt skikt. Detta skikt växte med tiden

och även andra komponenter inkorporerades i det. Dessa föreningar trängde också in i membranens porer. Sköljning med vatten avlägsnade det mesta av nedsmutsningen, men ett mycket tunt skikt fanns kvar. Det var möjligt att avlägsna denna kvarvarande beläggning med en miljövänlig blandning av enzymer, följt av rengöring med ett alkaliskt rengöringsmedel. Min vision är att denna forskning kommer att förbättra membranprocesserna i bioraffinaderier för lignocellulosa, vilket gör det mer attraktivt att genomföra dem. Detta skulle utgöra ett viktigt bidrag till omvandlingen av samhället från ett fossilbaserat till ett hållbart biobaserat samhälle.

Populärwissenschaftliche Zusammenfassung

Die Beherrschung von Trennverfahren ist entscheidend für die Umstellung auf erdölfreie Produkte

Der Übergang zu einer kreislauf, nicht-Erdöl-basierten Wirtschaft ist für viele WissenschaftlerInnen innerhalb den Ingenieurwissenschaften weltweit das Hauptziel, und zwar aus der Not heraus. Wir brauchen jeden möglichen Beitrag, um die uns bevorstehende Klimakrise zu verhindern. Die Herstellung von neuen erdölfreien Produkten aus Holz ist ein solcher Beitrag. Dank eines Verfahrens, das sich Membranfiltration nennt, können wir wertvolle Verbindungen aus Holz extrahieren.

Lasst uns neue Werkstoffe aus Holz herstellen

Um alle wertvollen Verbindungen im Holz zu nutzen, muss es in seine chemischen Bausteine zerlegt werden. Industrielle Anlagen für diesen Prozess gibt es bereits in Form von Zellstofffabriken, die Rohstoffe für die Papier-, Karton- und Textilproduktion herstellen. Durch den Einsatz von Membranverfahren in Zellstofffabriken werden diese zu "Lignozellulose-Bioraffinerien" umgewandelt, wodurch weitere nützliche Chemikalien gewonnen werden können, die sonst als Abfall enden würden. Die in dieser Dissertation vorgestellten Studien helfen Lignozellulose-Bioraffinerien einer vollständigen Kreislaufwirtschaft einen Schritt näher zu kommen, allerdings benötigt der Prozess moderne Technologie.

Bei der Verarbeitung von Holz lösen sich einige seiner chemischen Bestandteile in Wasser auf. Eine der Herausforderungen besteht darin, diese Verbindungen für die weitere Verwendung zu extrahieren und zu konzentrieren. Ein effizienter und energiesparsamer Weg, dies zu tun, ist die Membranfiltration. Membranen sind sehr dichte Filter, mit denen kleinste Chemikalien in einer Lösung nach ihrer Größe getrennt werden können, ähnlich einem Filter der zum Zurückhalten von gemahlenen Kaffeebohnen bei der Herstellung von Filterkaffee verwendet wird, nur in einem wesentlich kleineren Maßstab. Das größte Problem bei der Verwendung von Membranen für diese Aufgabe ist, dass sie dazu neigen, während der Filtration zu verstopfen. Dies wird gewöhnlich als "Membranverschmutzung" bezeichnet.

Ein genauerer Blick auf das Problem und wie es gelöst werden kann

Ich habe die Verschmutzung und die Reinigung von Membranen in Lignocellulose-Bioraffinerien untersucht. Hierbei verwendete ich eine Reihe von Analysetechniken, um zu verstehen, warum und wie die Verschmutzung von Membranen stattfindet und was genau die Membranen eigentlich blockiert. Dazu analysierte ich die Membranen nach Gebrauch und nach der Reinigung und erfoschte den Einfluss und die Entwick-

lung der Verschmutzung direkt während der Filtration. Schließlich untersuchte ich neue Wege, um verschmutzte Membranen auf umweltfreundliche Weise zu reinigen.

Meine Arbeit zeigt, dass sich eine Gruppe von Verbindungen, die sich während des mechanischen Aufschluss von Zellstoff bei hohen Temperaturen im Prozesswasser löst, an der Membranoberfläche festsetzt und eine dünne Schmutzschicht bildet. Diese Schicht wuchs mit der Zeit und weitere Komponenten wurde eingebaut. Außerdem drangen Schmutzstoffe in die Poren der Membranen ein. Spülen mit Wasser entfernte den größten Teil der Verschmutung, aber eine sehr dünne Schmutzschicht blieb zurück. Diese verbleibende Schicht konnte mit einer umweltfreundlichen Enzymmischung gefolgt von einer Reinigung mit einem alkalischen Reinigungsmittel entfernt werden.

Meine Vision ist, dass diese Arbeit Membranverfahren in Lignozellulose-Bioraffinerien verbessert und damit deren Einsatz attraktiver macht. Dies wäre ein wichtiger Beitrag zur Transformation der Gesellschaft von einer erdölbasierten zu einer nachhaltigen erdölfreien Gesellschaft.

List of publications

This thesis is based on the following publications, referred to in the text by their Roman numerals. The publications are appended at the end of the thesis.

I **A review of in situ real-time monitoring techniques for membrane fouling in the biotechnology, biorefinery and food sectors**

G. Rudolph, T. Virtanen, M. Ferrando, C. Güell, F. Lipnizki, M. Kallioinen
Journal of Membrane Science **2019**, 588, 117221

II **Investigations on alkaline and enzymatic membrane cleaning of ultrafiltration membranes fouled by thermomechanical pulping process water**

G. Rudolph, H. Schagerlöf, K. B. Morkeberg Krogh, A.-S. Jönsson, F. Lipnizki
Membranes **2018**, 8(4), 91

III **Analysis of ultrafiltration membrane fouling by Brunauer-Emmett-Teller nitrogen adsorption/ desorption technique**

T. Virtanen, **G. Rudolph**, A. Lopatina, B. Al-Rudainy, H. Schagerlöf, L. Puro, M. Kallioinen, F. Lipnizki
Scientific Reports **2020**, 10, 3427

IV **In situ real-time investigations on adsorptive membrane fouling by thermomechanical pulping process water with quartz crystal microbalance with dissipation monitoring (QCM-D)**

G. Rudolph, A. Hermansson, A.-S. Jönsson, F. Lipnizki
Separation and Purification Technology **2021**, 254, 117578

V **QCM-D for studying membrane fouling - opportunities and limitations on the example of process water from thermomechanical pulping**

G. Rudolph, H. Schagerlöf, A.-S. Jönsson, F. Lipnizki
Manuscript

VI **Comprehensive analysis of foulants in an ultrafiltration membrane used for the treatment of bleach plant effluent in a sulfite pulp mill**

G. Rudolph, B. Al-Rudainy, J. Thuvander, A.-S. Jönsson
Membranes **2021**, 11(3), 201

Other related publications

Focus on fouling monitoring

G. Rudolph, T. Virtanen, M. Kallioinen, F. Lipnizki
Filtration + Separation **2019**, 56(3), 25–27

Membrane processes and applications for biorefineries

F. Lipnizki, J. Thuvander, **G. Rudolph**
in: *Current Trends and Future Developments on (Bio-) Membranes*, A. Figoli, Y. Li, and M. Basile (Eds.) **2020**, 283–301

Fouling and cleaning of membranes in biorefineries

J. Thuvander, **G. Rudolph**, F. Lipnizki, A.-S. Jönsson
Poster, 7^{th} *Nordic Wood Biorefinery Conference* **2017**, 28–30 March, Stockholm, Sweden

Application potential of membrane processes in the concept of lignocellulose biorefineries

F. Lipnizki, **G. Rudolph**, J. Thuvander, B. Al-Rudainy, M. Battestini Vives
Accepted for publication

Author contributions to the appended papers.

I I developed the concept together with the co-authors. I, together with T. Virtanen, summarized and evaluated the literature, and developed the schematic figures. I and T. Virtanen wrote the paper together with the co-authors.

II I planned and performed the experiments and evaluated the results. I performed the scanning electron microscopy analysis with the help of D. Madsen. I wrote the paper together with the co-authors.

III T. Virtanen and I planned and performed the experiments, and carried out the analysis and evaluation of the results. B. Al-Rudainy performed the fouling experiments with black liquor. T. Virtanen and I wrote the paper together with the co-authors.

IV I planned and performed the experiments. A. Hermansson performed some parts of the experiments under my supervision. I performed the analysis and evaluated the results. I wrote the paper together with the co-authors.

V I planned and performed the experiments, and analyzed and evaluated the results. I wrote the paper together with the co-authors.

VI I planned, analyzed, and evaluated the ATR-FTIR. I planned and evaluated the scanning electron microscopy with energy dispersive spectroscopy analysis, and performed it with the help of D. Madsen. I wrote the paper together with the co-authors.

Abbreviations and symbols

Abbreviations

AFM	Atomic force microscopy
ATR-FTIR	Attenuated total reflectance-Fourier transform infrared spectroscopy
BET	Brunauer-Emmett-Teller
CA	Water contact angle (°)
CFV	Cross-flow velocity (m/s)
CP	Concentration polarization
EDS	Energy-dispersive X-ray spectroscopy
EPS	Extracellular polymeric substances
FDG	Fluid dynamic gauging
GGM	(O-acetyl) Galactoglucomannan
MBR	Membrane bioreactor
mCT	Micro-computed tomography
MF	Microfiltration
MW	Molecular weight (kDa)
MWCO	Molecular weight cut-off (kDa)
NF	Nanofiltration
PES	Polyethersulfone
PSU	Polysulfone
QCM-D	Quartz crystal microbalance with dissipation monitoring
rms	Root mean square
RO	Reverse osmosis

SAXS	Small-angle X-ray scattering
SEM	Scanning electron microscopy
SMP	Soluble microbial products
TMP	Transmembrane pressure (bar)
UF	Ultrafiltration
UTDR	Ultrasonic time domain reflectometry
VR	Volume reduction (g/g or %)

Symbols

K	Phenomenological coefficient – constant (s/m^2)
R_f	Resistance due to fouling (1/m)
R_{irrev}	Resistance due to irreversible fouling (1/m)
R_m	Resistance of the membrane (1/m)
R_{rev}	Resistance due to reversible fouling (1/m)
R_t	Total resistance (1/m)
V	Permeate volume (m^3)
μ	Dynamic viscosity (Pa·s)
c_b	Bulk concentration (g/L)
c_m	Concentration in the boundary layer above membrane surface (g/L)
c_p	Permeate concentration (g/L)
k	Mass transfer coefficient (g/L)
p_{feed}	Feed pressure (bar)
p_{perm}	Permeate pressure (bar)

p_{ret}	Retentate pressure (bar)
t	Time (s)
%(v/w)	Weight per volume percentage
%(w/w)	Weight percentage
$\%D_a$	Relative flux loss ratio due to adsorption (-)
$\%D_{cp}$	Relative flux loss ratio due to concentration polarisation (-)
$\%D_{pb}$	Relative flux loss ratio due to pore blocking (-)
$\Delta\pi$	Difference in osmotic pressure across the membrane (bar)
D	Dissipation (10^{-6})
f	Frequency (Hz)
f_0	Fundamental resonance frequency (Hz)
J	Flux (L/m^2·h)
n	Characteristic model constant for fouling mechanism (-)
n_0	Overtone number (-)
P	Permeability (L/m^2·h·bar)
P_a	Pure water permeability after static adsorption (L/m^2·h·bar)
P_i	Pure water permeability of a pristine membrane (L/m^2·h·bar)
P_v	Permeability at the end of filtration (L/m^2·h·bar)

Contents

1 Introduction

We are facing a climate crisis, and must develop new chemical processes that are sustainable for both us and the planet. The greatest problem is our current dependency on fossil-based products, and to overcome this, we must improve and develop products and processes that are based on non-fossil resources, namely, biomass. An important part of this transformation is the conversion of pulp and paper mills into lignocellulosic biorefineries that utilize non-fossil biomass for the simultaneous production of fibers, novel biochemicals, and energy [1]. Figure 1.1 illustrates such a plant. The main compounds found in lignocellulosic materials such as wood are cellulose, lignin, hemicelluloses, extractives, inorganics, and water. These must be separated from the process stream for further processing. Separation processes in mature chemical processes currently account for 60–80% of the process costs [2]. In the US, they account for 45–55% of the total energy demand; 80% of this being used in thermal separation processes [3]. Highly selective, electrifiable, and low-energy-demanding separation technologies are therefore key for the complete and economically feasible utilization of the valuable compounds found in wood [4].

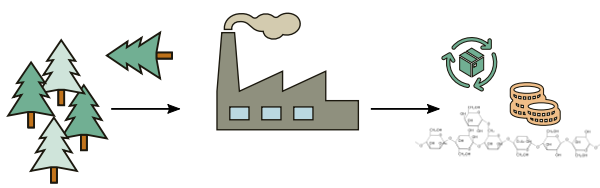

Figure 1.1 Illustration of a lignocellulosic biorefinery.

1.1 Lignocellulosic biorefineries and membrane processes

Membrane technology fulfills the requirements described above. For example, separation with membrane processes requires 90% less energy than separation by distillation

[3]. The pressure-driven membrane processes, microfiltration (MF), ultrafiltration (UF), nanofiltration (NF), and reverse osmosis (RO) are especially suitable, and have already been investigated in various processes in lignocellulosic biorefineries on both pilot and industrial scale [5–10]. However, bio-based process streams are very complex, and often cause severe membrane fouling. Figure 1.2 visualizes this challenge.

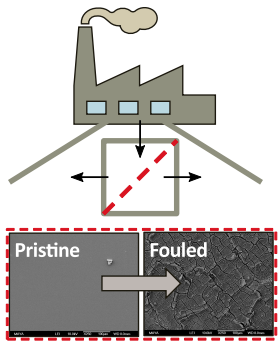

Figure 1.2 Illustration of membrane fouling in a lignocellulosic biorefinery.

Membrane fouling is defined as, "a process resulting in loss of performance of a membrane due to the deposition of suspended or dissolved substances on its external surfaces, at its pore openings, or within its pores" [11]. Fouling reduces the filtration capacity, changes the selectivity and cut-off, and shortens the membrane lifetime, thus increasing the operational costs of the process. Membrane fouling can be overcome by regular membrane cleaning, although this is sometimes not sufficient, and the fouled membranes must be replaced. It is therefore important to have a comprehensive understanding of the processes leading to membrane fouling in order to ensure that the process is economically feasible. Membrane fouling can be studied after filtration, when the membrane is removed from the module (*ex situ*) or directly during the filtration process (*in situ* and in real time). Novel, energy- and resource-efficient membrane processes and cleaning strategies can then be developed based on the knowledge gained through such investigations.

1.2 Aim and outline of this thesis

The aim of the work presented in this thesis was to gain in-depth knowledge on membrane fouling and membrane cleaning during UF processes in lignocellulosic biorefineries. The objectives were: 1) to identify suitable methods for the characterization of membrane fouling and cleaning, focusing on real-time monitoring; 2) to understand the underlying processes leading to membrane fouling with the help of the methods identified; and 3) to investigate ways of improving membrane cleaning.

The UF of thermomechanical pulping process water was used as the reference system for the investigation of process streams from other pulp and paper processes. The main experimental focus was on elucidating the adsorption mechanisms of hemicelluloses and extractives, two dominant foulants in the process streams investigated.

Membrane fouling and cleaning were studied using surface characterization methods, and analysis of the chemical composition of the fouling layer, and its impact on the inner structure of the membrane. These studies were complemented with *in situ* real-time monitoring of adsorptive fouling by quartz crystal microbalance with dissipation monitoring (QCM-D).

2 The Interplay between Membrane Fouling and Membrane Cleaning

Membrane filtration is a unit operation used in chemical engineering for the separation of liquids or gases. The membrane is a semi-permeable barrier that concentrates larger compounds of the feed in the retentate, while allowing smaller compounds to pass through and be collected in the permeate. Membrane processes have several advantages over other separation processes such as evaporation, centrifugation, drying, and filter pressing. Apart from being energy-efficient and highly selective, they can be operated continuously, at moderate temperatures and without additives, often without phase change, and have a modular design allowing easy scale-up and extension [4]. This is why membrane processes are already in use in a wide range of industrial applications such as food production, biological and chemical processing, and water and wastewater treatment. The various kinds of pressure-driven membrane processes are introduced in Section 2.1, followed by a discussion on the theoretical approaches that can be used to interpret flux data with regard to membrane fouling in Section 2.2. The most important potential foulants in process streams from lignocellulosic biorefineries are then discussed in Section 2.3. The chapter concludes with an overview of membrane cleaning and brief descriptions of typical cleaning approaches in Section 2.4.

2.1 Pressure-driven membrane processes

The most common type of membrane processes are the pressure-driven processes MF, UF, NF, and RO, where an external pressure is applied to separate the solution into a fraction with a low concentration of compounds (the permeate) and a fraction with

a high concentration of compounds (the retentate). These processes are commonly categorized by the pore size, or the molecular weight cut-off (MWCO) of the membranes used. MF membranes have the most open pores, and the MWCO becomes successively smaller in UF, NF, and RO, as can be seen in Table 2.1. The operating pressure is increased with decreasing MWCO.

Table 2.1 Overview of typical process conditions and characteristics of pressure-driven membrane processes [12]

	Operating pressure (bar)	Pore size (nm)	Nominal MWCO (Da)	Application
MF	< 2	> 100	-	Cold sterilization
UF	1–10	1–100	>1000	Protein and water purification
NF	5–40	0.5–2	200–1000	Water softening
RO	30–100	-	< 200	Desalination

Pressure-driven membrane filtration can be performed in perpendicular (dead-end) or tangential (cross-flow) mode, as illustrated in Figure 2.1. In dead-end mode, the retained compounds usually accumulate on the membrane surface forming a filter cake that increases in thickness during the course of filtration. In cross-flow mode, the feed flows tangentially over the membrane leading to higher shear forces that reduce or eliminate the build-up of a filter cake and improving the filtration capacity and product quality.

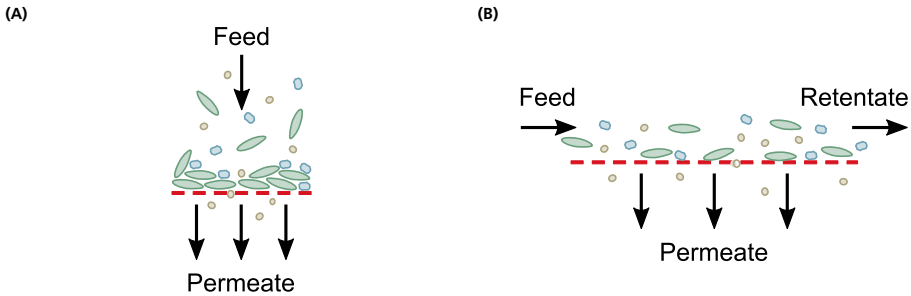

Figure 2.1 Illustration of dead-end filtration **(A)** and cross-flow filtration **(B)**. (Adapted from [13].)

In the research presented in this thesis, UF was investigated in both modes, mainly with the commercial UF membrane UFX5-pHt (Alfa Laval, Denmark). This membrane was used in the studies described in Papers II, III, IV, and V. This is an asymmetric membrane consisting of a thin polysulfone (PSU) skin layer and a polypropylene non-woven support layer, and has a nominal MWCO of 5 kDa. The PSU is modified so that the skin layer is permanently hydrophilized, which causes a relatively low

contact angle in the range 81° [14] to 51° (Paper IV). This membrane has a maximum operating pressure of 15 bar, and a maximum operating temperature of 75°C. Figure 2.2 shows an image of a cross-section of a pristine UFX5-pHt membrane obtained with X-ray micro-computed tomography (mCT) (Figure 2.2A) and an image of the surface of the membrane obtained with scanning electron microscopy (SEM) (Figure 2.2B). Other UF membranes used in this work were GR95PP (Alfa Laval, Denmark), a polyethersulfone (PES) membrane with a MWCO of 2 kDa; UP010 (Microdyn-Nadir, Germany), a PES membrane with a MWCO of 10 kDa (Paper III); and ES404 (PCI Membranes, now part of Filtration Group, UK), a PES membrane with a MWCO of 4 kDa (Paper VI). These membranes are also asymmetric, consisting of a skin layer on a porous non-woven support layer. The support layer is made of polypropylene in the GR95PP and UP010 membranes. The support layer of the ES404 membrane is proprietary information of the company.

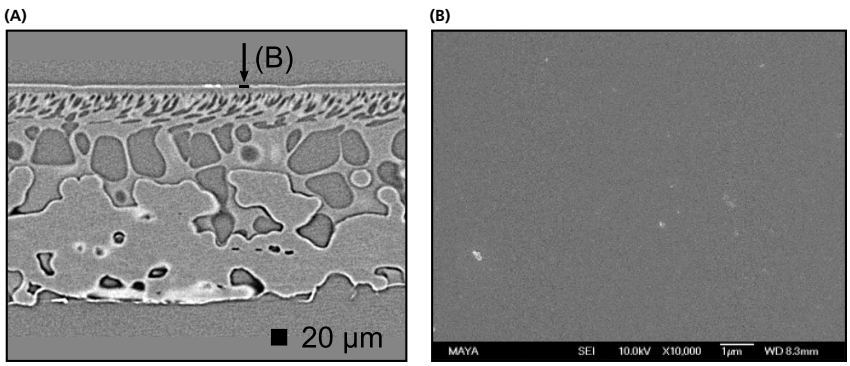

Figure 2.2 **(A)** Image of the cross-section of a pristine UFX5-pHt membrane obtained with mCT. The first 50 µm is the skin layer, and the porous structure below is the unwoven support. **(B)** Image of the surface of the membrane obtained with SEM.

2.2 Flux and membrane fouling

The filtration capacity, expressed as the flux, J, or permeability, P, is one of the three most important parameters in membrane processes. The other two are the selectivity of the membrane and the degree of membrane fouling. Darcy's law states that the flux is proportional to the applied pressure difference. In pressure-driven membrane processes, this difference is called the transmembrane pressure (TMP), and is the difference between the average of the pressure on the feed side, p_{feed}, and the pressure on the retentate side, p_{ret}, minus the pressure on the permeate side, p_{perm} (Eq. 2.1).

$$\mathrm{TMP} = \frac{p_{feed} - p_{ret}}{2} - p_{perm} \tag{2.1}$$

In a pure solvent system, the entire TMP drives the separation process, and only the hydraulic resistance of the membrane, R_m, works against it. The hydraulic resistance of a membrane can be measured empirically and depends on the characteristics of the membrane, including the pore size distribution and the membrane porosity. Based on Darcy's law, and considering the dynamic viscosity of the solvent, μ, the flux, J, can be defined as in Eq. 2.2.

$$\mathrm{J} = \frac{\mathrm{TMP}}{\mu R_m} \tag{2.2}$$

When a solution is filtered, the net driving force is (TMP - $\Delta\pi$) where $\Delta\pi$ is the osmotic pressure difference across the membrane. Retained solutes accumulate at the membrane surface due to the convective transport of solvent and solutes towards the membrane by the TMP, resulting in a concentration gradient in a boundary layer at the membrane surface. This phenomenon is known as concentration polarization (CP), and is counterbalanced by the diffusion of solutes back into the bulk phase. CP is unavoidable, but can be reversed by the elimination of the convective transport (TMP and/or J). The impact of CP can be reduced by increasing the shear rate near the boundary layer. CP is mathematically described by the film model (Eq. 2.3), where c_m is the concentration in the boundary layer just above the membrane surface, c_b the concentration in the bulk phase, c_p the concentration in the permeate, and k the mass transfer coefficient for the diffusion of solutes from the boundary layer into the bulk phase. The coefficient k depends on the operating parameters, such as the filtration temperature and the cross-flow velocity (CFV), but also on the characteristics of the solution, such as its density and viscosity.

$$\mathrm{J} = k \ln \frac{c_m - c_p}{c_b - c_p} \tag{2.3}$$

Another effect that has a more serious impact on membrane filtration is membrane fouling. Several fouling phenomena can be distinguished: adsorption, pore blocking, and cake or gel layer formation (Figure 2.3). Both CP and membrane fouling lead to an increase in resistance, thus reducing the membrane flux, and hence its capacity. Eq. 2.2 can be extended to include the resistance due to reversible fouling, R_{rev}, and irreversible fouling, R_{irrev}, leading to the resistance-in-series model (Eq. 2.4). Reversible fouling occurs during operation, but disappears after switching from the feed solution to pure solvent. This includes CP, but could also include resistance due

to cake or gel layer formation. Irreversible fouling is the result of adsorption and pore blocking and may be removed by membrane cleaning.

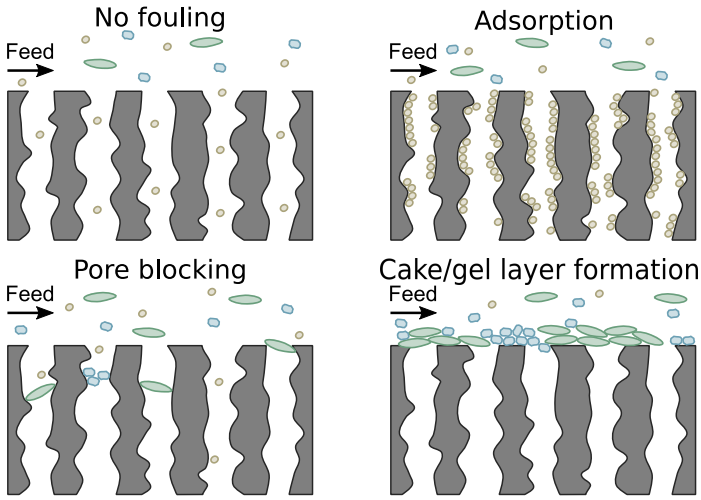

Figure 2.3 Schematic illustration of various types of fouling in membrane filtration. (Adapted from [13].)

$$J = \frac{TMP - \Delta\pi}{\mu(R_m + R_{rev} + R_{irrev})} \tag{2.4}$$

Plotting the flux as a function of TMP reveals several important points. During the filtration of a pure solvent, the flux increases linearly with TMP. However, if the feed contains solutes, the flux will stop increasing at a certain TMP and level off (Figure 2.4). At this point, the process has reached its so-called limiting flux [15]. This is the result of CP and/or fouling, and cannot be overcome by simply increasing the pressure/TMP. However, the limiting flux can be increased by increasing the shear force or the temperature, or reducing the concentration of the solute in the feed. The flux at which the curve starts to deviate from linearity is known as the critical flux [16] and indicates the onset of fouling.

It is important to understand the type of fouling in order to prevent or reduce it. Based on the type of fouling, decisions can be made on which membrane and operating conditions will give the best filtration performance. Hermia developed an approach to identify the type of fouling in dead-end filtration [17], but it was later shown that it could also be applied to the early stage of cross-flow filtration (see, for example [18]). The generalized Hermia model is stated in Eq. 2.5 [17], or modified focusing on the flux as in Eq. 2.6 [16], with K as the phenomenological coefficient in s/m^2.

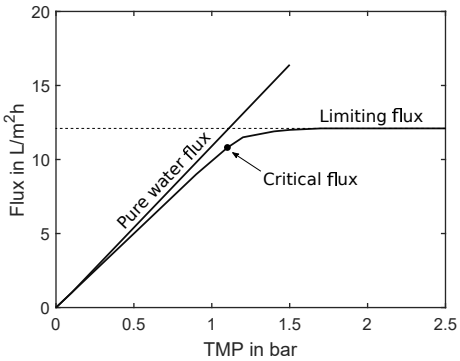

Figure 2.4 Schematic flux curves illustrating limiting and critical flux.

$$\frac{\mathrm{d}^2 t}{\mathrm{d}\, V^2} = K(\frac{\mathrm{d}t}{\mathrm{d}\, V})^{\mathrm{n}} \tag{2.5}$$

$$\frac{\mathrm{dJ}}{\mathrm{d}t} = -K\mathrm{J}^{3-\mathrm{n}} \tag{2.6}$$

Hermia distinguished between four types of membrane fouling, and the parameter n changes depending on the dominating type of fouling, as given in Table 2.2. Complete blocking describes the fouling where one foulant blocks the membrane pores and no other foulant can settle on top of that foulant. This leads to a decrease in the active membrane surface. Standard blocking is the term used to describe the adsorption of foulants on the pore walls. The volume of the pores decreases proportionally with the volume of solution filtered, and the cross-sectional area of the membrane pores thus decreases with time. Standard blocking is caused by foulants that are much smaller than the pores. Intermediate blocking describes pore blocking by a foulant when other foulants can settle on top, which means that not every foulant compound that arrives at the membrane blocks a pore. Hence, the probability of a foulant blocking a pore decreases continuously with time. This type of fouling occurs when the size of the foulant is similar to the size of the pores. Cake or gel layer formation takes place when the foulant is larger than the pores and cannot penetrate the membrane, but is instead deposited on the membrane surface.

Table 2.2 Types of fouling and the value of the characteristic model constant, n, for the four fouling mechanisms according to Hermia [17]

Fouling type	n
Complete blocking	2
Standard blocking	1.5
Intermediate blocking	1
Cake/gel layer formation	0

2.3 Potential foulants in process streams of lignocellulosic biorefineries

Process streams in lignocellulosic biorefineries contain compounds with a wide range of particle size and/or molecular weight, many of which may act as foulants. Key foulants in process waters from lignocellulosic biorefineries are cellulose fibers, lignin, wood polysaccharides such as hemicelluloses, wood extractives, proteins, and inorganic compounds. Examples of membrane fouling in membrane processes in the biorefinery sector are presented in Table 2.3. Biological fouling in the form of biofilm formation is usually not a major concern due to the harsh conditions prevailing (extreme pH and high temperatures). The concentrations of potential foulants vary depending on the wood species, the pulping process, and the chemical additives. For example, in mechanical pulping, 2–5%(w/w) of the wood biomass is dissolved in the process water [19]. The dissolved compounds are mostly hemicelluloses, lignin and lignans [20]. Wood extractives typically do not dissolve but instead often form colloids droplets [21].

In this work, mainly process water from thermomechanical pulping of spruce (from the Stora Enso Kvarnsveden Mill, Sweden) was used as the fouling solution (Papers II, III, IV, and V). The composition of this process water is presented in Table 2.4, where total dry solids includes all compounds that did not evaporate at 100°C, and ash represents inorganic compounds such as Na, Mg, or Si that were not incinerated during the analysis. The process water had a pH of 4.5.

Other process streams used in this work are black liquor from Kraft processing of a mixture of hardwood and softwood (Smurfit Kappa Piteåmill, Sweden), pressurized-hot water extract from spruce sawdust (Mustola Timber, Finland), both Paper III, and bleach plant effluent from sulfite pulping of softwood (Stora Enso Nymölla mill, Sweden)(Paper VI). All the process streams investigated contained the common wood compounds hemicelluloses, extractives, and lignin, which often cause fouling. Each of these compounds will be described in more detail below.

Table 2.3 Reported examples of fouling types, fouling mechanisms, and main foulants in membrane processes employed in the biorefinery sector (adapted from Paper I, originally modified from [22] and [23])

Process	Membrane type	Fouling type	Mechanism	Main foulant
Lignin recovery	MF, UF, NF	Organic	Cake/gel layer, pore blocking, adsorption	Lignin, extractives
Hemicelluloses recovery	MF, UF, NF	Organic	Cake/gel layer	Hemicelluloses
Inhibitor removal	NF	Organic	–	Sugars or inhibitors
Enzyme recovery	MF, UF	Organic	Cake/gel layer	Enzymes, lignocellulosic particles
Algae harvesting	UF	Biofouling	Cake layer	Algae
		Organic	Adsorption	Algogenic organic matter
Acetic acid production	MF, UF	Biofouling	Deposition	Microorganisms and fermentation broth
		Organic	Pore blocking	
Biogas production	MF, UF	Biofouling		
Bio-oil production	MF	Inorganic	Cake layer	Char
Biodiesel production	MF, UF, NF	Organic	Pore blocking	Glycerol agglomerates
Effluent, sludge, and wastewater treatment	MBR	Biofouling		EPS, SMPs, flocs, bacteria
		Organic	Cake/gel layer, pore blocking	Colloidal particles, proteins, polysaccharides, humic acids
		Inorganic	Cake layer	Ca, Al, Ba and Fe salts

MBR: Membrane bioreactor, EPS: Extracellular polymeric substances, SMP: Soluble microbial products

Table 2.4 Compositional characteristics of process water from thermomechanical pulping of spruce (analyzed according to [24, 25])

Solution	Total dry solids (mg/g)	Ash (mg/g)	Total sugars (g/L)	Acid-insoluble solids (mg/g)	Acid-soluble lignin (g/L)	Total lignin (g/L)	Extractives (mg/L)
Process water	6.35	1.85	0.63	0.35	2.61	0.88	19.9
Retentate	7.68	0.34	4.02	1.40	0.72	1.13	615.2
Permeate	5.53	1.51	0.59	0.37	2.73	0.90	10.5

2.3.1 Hemicelluloses

Hemicelluloses are wood polysaccharides with different chemical compositions and molecular sizes. They are the most abundant polysaccharides in lignocellulosic biomass after celluloses. For example, spruce stem wood contains, 10–25%(w/w)

hemicelluloses [26]. The composition of hemicelluloses depends on the type of biomass. The most common forms are (O-acetyl) galactoglucomannan (GGM), and arabinoglucuronoxylan; other forms include arabinogalactan, xyloglucan, glucans and pectins [27–29].

The most common form of hemicellulose in thermomechanical pulping process water from softwood such as spruce is GGM. Figure 2.5 shows the chemical structure of a unit of GGM. Generally, two types of GGM can be distinguished: one with a high galactose content (with a galactose:glucose:mannose ratio of about 1:1:3), and one with a low galactose content (galactose:glucose:mannose ratio of about 0.1:1:3) [30]. The latter type is also referred to as glucomannan due to its low galactose content.

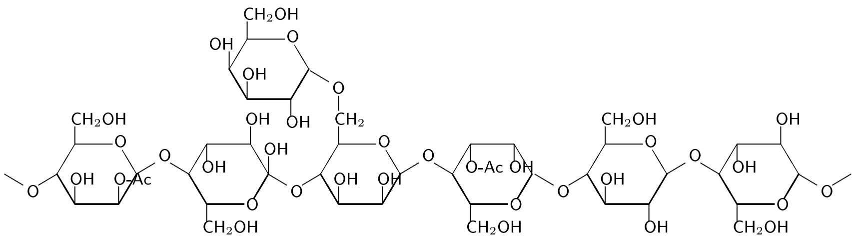

Figure 2.5 A single unit of GGM, a common hemicellulose in softwood.

GGM is composed of a backbone of (1→4) linked β-D-mannose and β-D-glucose units, and its degree of polymerization is 100 to 150, corresponding to a MW of 16 kDa to 24 kDa [30–32], however GGM can also have a MW of up to 490 kDa [33]. The determined MW of GGM depends strongly on the measurement method. This hemicellulose contains side groups of α-D-galactose units attached to some of the mannose in the backbone through (1→6) linkages [26, 30]. Some of the mannose units are O-acetylated at the C2 and C3 positions [34]. Both the galactose side groups and the acetyl groups contribute to the good solubility of GGM in water [20]. The high amount of galactose side groups is the reason why GGM with the high galactose content is even more soluble in water than glucomannan [30].

2.3.2 Wood extractives

Wood extractives, also known as wood resin, are a large group of hydrophobic, i.e., lipophilic, compounds that are soluble in natural organic solvents. They are regarded as non-structural wood constituents of low MW. Less than 10%(w/w) of dry wood usually consists of extractives [26], and around 75%(w/w) of the total extractives can be transferred into water during wood processing. Extractives can be roughly divided into five groups: 1) fatty acids, 2) resin acids, 3) sterols, 4) steryl esters, and

5) triglycerides. The chemical structures of typical compounds of each group are presented in Figure 2.6.

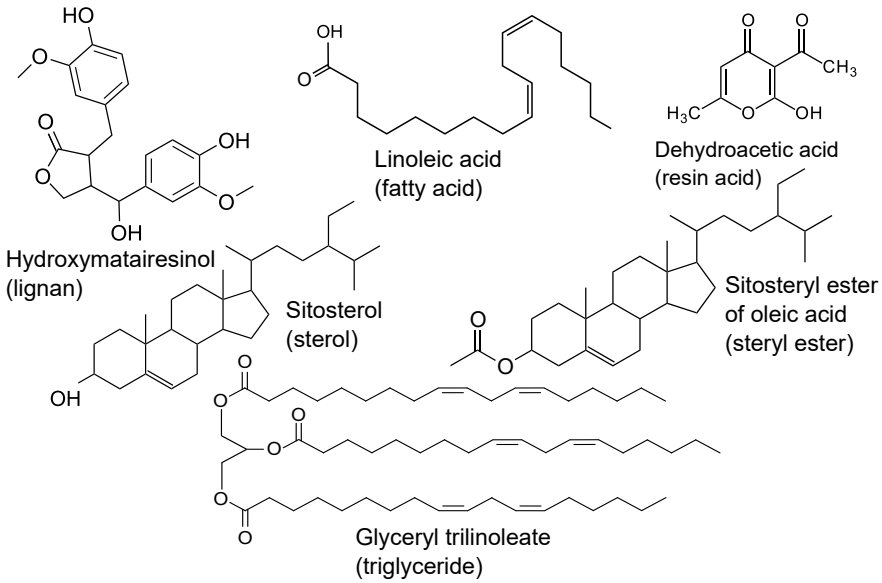

Figure 2.6 Chemical structures of compounds from typical wood extractive groups.

Only 5% of the extractives exists in dissolved form in thermomechanical pulping process water [21]; the remainder forming colloidal droplets. The core of these droplets consists of the most hydrophobic compounds, steryl esters and triglycerides, while free fatty acids, resin acids, and sterols create a thin layer around the core [35]. Carboxyl groups of fatty acids and resin acids are orientated towards the aqueous phase, allowing hydrogen bond formation on the surface of the droplets, making them electrostatically stabilized [35]. Furthermore, they are sterically stabilized by hemicelluloses or other dissolved compounds. Especially GGM acts as a stabilizer as it attaches on the surface of colloidal droplets [34]. This prevents the aggregation of the colloidal droplets with salts such as NaCl or $CaCl_2$ at acidic or neutral pH [7]. A schematic illustration of such a stabilized colloidal droplet is given in Figure 2.7. In thermomechanical pulping process water, the droplets have a spherical shape with an average diameter of 0.6 µm (range of 0.1–2 µm) [21, 36].

2.3.3 Lignin

Lignin is mainly responsible for the strength of lignocellulosic biomass and its resistance to biological and environmental degradation. It surrounds the cellulose fibrils and binds covalently to wood polysaccharides, thereby protecting the wood fibers.

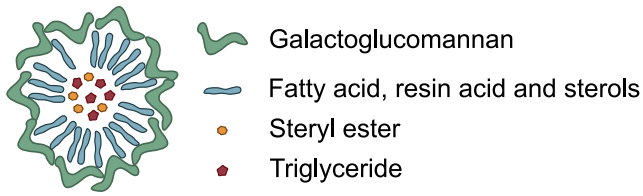

Figure 2.7 Schematic illustration of a droplet of colloidal wood extractives sterically stabilized by GGM.

Lignin is a large, highly heterogeneous polyphenolic polymer. It is made up of three types of cross-linked monomers, also known as the three monolignols: p-coumaryl alcohol, coniferyl alcohol, and sinapyl alcohol. The chemical structure of the monolignols is shown in Figure 2.8. The individual composition and structure of lignin polymers depends on the type of wood. The typical MW of lignin polymers in thermomechanical pulping process water from spruce is 2 kDa [37].

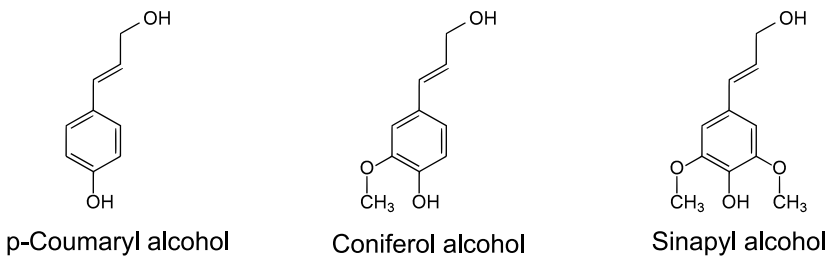

Figure 2.8 Chemical structure of the three types of monolignols making up lignin.

Lignin is often found covalently bound to hemicelluloses in the form of lignin–carbohydrate complexes in the process streams of lignocellulosic biorefineries [38]. Common linkages in these complexes are benzyl ether, benzyl ester and phenol glycosidic [39]. However, they are quickly hydrolyzed under acidic conditions. Therefore, lignin–carbohydrate complexes are found, for example, in black liquor from Kraft pulping, but they are hydrolyzed under the acidic conditions of process water from thermomechanical pulping.

2.4 Membrane cleaning

Fouled membranes must be cleaned. The point in time when membrane cleaning is required depends highly on the process. However, there are some rules of thumb: 1) when the normalized permeate flow has fallen by 10–15%; 2) when the normalized permeate quality has decreased by 10–15%; or 3) when the normalized pressure drop

over the membrane has increased by 10–15% [40].

Membrane cleaning can be performed in several ways, for example, mechanically by forward flushing, backward flushing, or by pulling foam balls through the feed channels [41]. Forward flushing means that the feed side of the membrane is rinsed with the solute or permeate at an elevated CFV. In backward flushing, the filtration process is reversed, and permeate is forced from the permeate side through the membrane back into the feed/retentate side. However, backward flushing is often not suitable for composite membranes and spiral wound modules. In such cases, or if flushing does not restore the capacity and/or selectivity of the membrane, chemical cleaning must be performed. Depending on the type of fouling, the membrane is soaked or flushed at a high CFV with an acidic or alkaline solution, usually at elevated temperatures. The success of chemical cleaning depends on the type of fouling and the foulants, the concentration and composition of the cleaning agent, the duration of cleaning, the temperature, and the fluid mechanics in the module.

Cleaning agents change the pH, and typically contain surface-active agents, sequestering agents, and disinfectants [41]. Alkaline cleaning is often performed with an agent based on sodium hydroxide (NaOH) or sodium hypochlorite (NaOCl) and is usually applied to remove organic fouling. Acidic cleaning is typically used to remove scaling, which is the kind of fouling caused by the precipitation of inorganic compounds, as these are generally more soluble in acidic solutions. Acidic cleaning is often performed with agents based on hydrochloric acid (HCl), phosphoric acid (H_3PO_4), or sulfuric acid (H_2SO_4). In general, the formation of hypochlorite (ClO^-) during cleaning, as with NaOCl cleaning, should be avoided due to concerns regarding the generation of toxic halogenated by-products [42].

In general, chemical membrane cleaning leads to the risk of membrane aging, and thus membrane lifetime reduction [43–46]. In this work, the membranes were conditioned and cleaned with a 1% solution of the alkaline cleaning agent Ultrasil 10 (Ecolab, Germany) at 50°C, either by soaking (Papers II and III), or at 2 bar TMP (Papers IV and V), or soaking in a 2% solution of the alkaline cleaning agent BanUltra 17 (Banmark, Finland) at 50°C (Paper VI).

To avoid or minimize the need for chemical cleaning, milder approaches such as enzymatic cleaning have been investigated in several industrial applications [47–51], including the cleaning of UF membranes used to treat Kraft pulping effluent in a lignocellulosic biorefinery [52]. Enzymatic cleaning does not require elevated temperatures or extreme pH and, in the ideal case, targets only specific foulants. However, the enzyme concentration is critical, as enzymes are still relatively costly compared to chemicals such as NaOH. Another important parameter when using this approach is the duration of cleaning [41].

Alkaline cleaning was compared with milder enzymatic cleaning using an enzyme cocktail of six commercially available enzymes from different classes (Paper II). The classes were β-glucanase, cellulase, mannanase, xylanase (all polysaccharide-degrading enzymes), lipase (a lipid-degrading enzyme), and cutinase (a hydrolase acting on carboxylic ester bonds). The concentration of each enzyme was 0.1%(w/v) in a citrate buffer with pH 5.8.

Regardless of the cleaning agent used, the membrane plant must be flushed with several system volumes of solvent, typically water, to remove any residual cleaning agent. This, together with the time needed for the actual cleaning process and the occasional replacement of an aged membrane, leads to significant production time losses and resource usage. The production down time resulting from membrane cleaning has been roughly estimated to be equivalent to 5–20% of the capital cost of the membrane plant, while the cost of replacing membranes was roughly estimated to be 2–5% of the capital cost of the membrane plant [53]. Thus, membrane cleaning is a trade-off between cleaning frequency, production efficiency, and membrane lifetime, and if performed appropriately can save time and money.

3 Methods of Membrane Characterization in Lignocellulosic Biorefineries

Membrane processes have been [41], and are still often designed, run or improved, based on time-consuming trial-and-error studies [54, 55], experience or rules of thumb. Flux measurements, in combination with feed, permeate, and retentate analysis, are often used to select a membrane that best meets the demands on the three decisive parameters: high capacity, high selectivity, and low fouling tendency, for a particular process. Only occasionally are membranes characterized in detail to obtain an understanding of the causes of fouling during filtration, or to tailor membrane cleaning to the foulants in question. However, detailed knowledge on the changes in the membrane during operation is required to optimize the filtration process. When a membrane is characterized with methods other than flux measurements, it is often removed from the module after filtration and analyzed *ex situ* in a so-called "membrane autopsy". Various analytical techniques can be used for this type of characterization, ranging from imaging techniques such as microscopy or tomography, analysis of the surface charge or porosity of the membrane, to chemical analysis of the fouling layer with methods such as spectroscopy, extraction in combination with chromatography, or dyeing.

The characterization of membrane fouling in membrane processes related to lignocellulosic biorefineries with *ex situ* techniques, in addition to flux measurements, started in 1995. Figure 3.1 presents the reported techniques employed for this task. Over the years, fouling analysis has become more complex and it is now common to employ more than one analytical technique when investigating membrane fouling in lignocellulosic biorefineries. The most often reported techniques are SEM, attenuated total reflectance-Fourier transform infrared spectroscopy (ATR-FTIR), energy-dispersive X-ray spectroscopy (EDS), and water contact angle (CA) measurements.

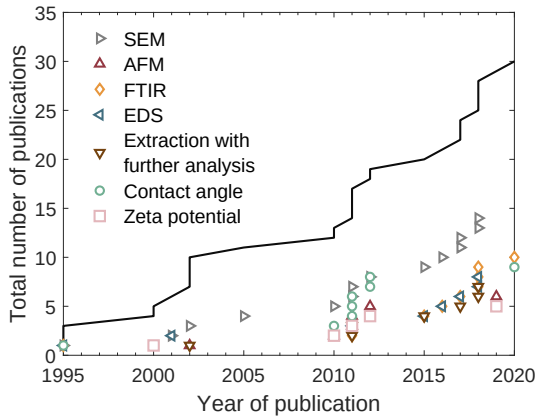

Figure 3.1 Overview of the methods reported in publications on ***ex situ*** fouling analysis of membranes used for the filtration of process streams from pulp and paper mills (lignocellulosic biorefineries) over the past 25 years. Studies in which only flux analysis was performed have been excluded. Methods were only considered if they had been applied at least three times. AFM = atomic force microscopy, CA = contact angle measurements, EDS = energy-dispersive X-ray spectroscopy, SEM = scanning electron microscopy. (Data based on [7, 52, 56–81].)

A more direct way of obtaining an understanding of the processes leading to changes in a membrane during operation, is to monitor the development of fouling and the effect of cleaning directly on the membrane in real time. Monitoring of membrane fouling processes is especially interesting since irreversible fouling often starts with early-stage adsorption of foulants on the membrane, and cannot always be detected by a reduction in flux [46] as stated in Section 2.2. Furthermore, CP, adsorptive fouling, pore blocking, or cake and gel layer formation can have a cumulative effect on the membrane performance. Imaging of membrane fouling *ex situ* usually allows higher resolution, and *ex situ* chemical analysis of the fouling layer is quite well-established, but it provides no information on early-stage fouling, the compositional changes in the fouling layer during the process, or the contribution of different foulants, or cleaning agents, to the development of the fouling layer over time.

Typical approaches that can be used for monitoring membrane processes while in operation are presented in Figure 3.2. In the context of this work, *in situ* real-time monitoring consisted of either the introduction of a probe into the membrane module (invasive) or monitoring of the process through the module (non-invasive). In-line monitoring describes the continuous analysis of feed, retentate and/or permeate streams. Both, *in situ* and in-line monitoring can be grouped together under the term online monitoring. At-line monitoring necessitates sampling followed by sample analysis, and is therefore fundamentally different from online monitoring. The main advantage of *in situ* real-time monitoring is that fouling and cleaning can be precisely monitored where and when it takes place.

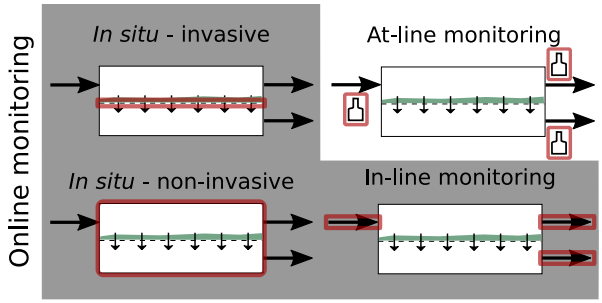

Figure 3.2 Schematic overview of approaches that can be used for monitoring membrane processes (adapted from Paper II.)

Several *in situ* real-time monitoring techniques can provide information on the chemical composition and structure of the fouling layer at a specific position, over a certain area, or for the whole module. A range of analytical techniques have been applied for the investigation of membrane fouling in processes related to lignocellulosic biorefineries (Figure 3.3). However, they have only been applied more widely in recent years. The most often applied methods are fluid dynamic gauging (FDG) and Raman spectroscopy. Other methods that have been used more than once are ultrasonic time domain reflectometry (UTDR), and null ellipsometry.

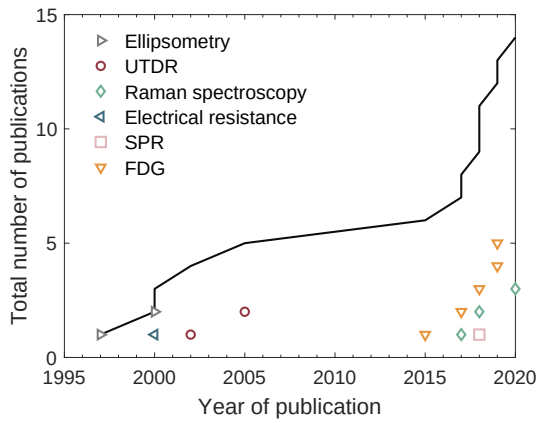

Figure 3.3 Overview of the methods reported in publications on membrane fouling monitoring in processes related to pulp and paper mills (lignocellulosic biorefineries) over the past 25 years. FDG = fluid dynamic gauging, SPR = surface plasmon resonance spectroscopy, UTDR = ultrasonic time domain reflectometry. (Data based on [62, 64, 76, 77, 80–88].)

In the work presented in this thesis, the impact of membrane fouling and the success of membrane cleaning is evaluated *ex situ* and is described in Section 3.1. Results of a survey amongst industrial membrane users and analytical equipment suppliers on the status of *in situ* monitoring of membrane fouling in industry are presented, and

QCM-D as a promising technique for monitoring of membrane fouling in lignocellulosic biorefineries is discussed in Section 3.2.

3.1 *Ex situ* analysis of membranes

The membrane surface (Paper II) and the cross-section of membranes were visually assessed using SEM (Paper VI) The membrane samples were first dried and then sputter coated with a platinum-gold mixture. To achieve a straight cut line for cross-sectional images, the membrane sample was dipped in liquid nitrogen and then broken. Although SEM only provides information on a small area of the sample, it is a relatively fast method of obtaining a first impression of the fouling status, as it enables qualitative evaluation of the fouling. A disadvantage of SEM is that sample preparation leads to changes in the structure of the fouling layer. In addition, it is very difficult to distinguish different types of foulants from each other based on microscopic examination. A much more detailed view at greater magnification, and with additional information on the surface roughness, usually given as root mean square (rms) roughness, was gained with atomic force microscopy (AFM) (Papers IV and V). AFM does not require any additional sample preparation; however, the technique is very time consuming due to the long scanning times, and the area on which information is provided is even smaller than in SEM. Since AFM images only provide information on a very small area, more than one spot per sample must be investigated. In this work, at least three spots per sample were scanned, to obtain representative data for each sample.

Information on the chemical composition of the fouling layer was obtained with ATR-FTIR (Papers II, III, V, and VI), EDS (Paper VI) and, to some extent, by sessile-drop CA (Papers II,III, IV, and V). Sample drying is required for sample preparation in all these methods. No further sample preparation was required for ATR-FTIR, making the technique rather straightforward. Furthermore, if the wavenumber of the chemical bonds is known, it is a very fast method of identifying the compounds adsorbed onto the membrane surface, especially organic foulants. However, the information is only valid for the particular spot investigated, and it is not easy to identify inorganic fouling compounds. EDS is more suitable for identifying fouling caused by inorganic compounds. This technique allows the mass of individual elements in an area to be determined at different magnifications. In this work, EDS was only used in combination with SEM. The combination of these two techniques makes it possible to overlay data from EDS on the SEM images, thus allowing certain inorganic foulants to be ascribed to structures visible in the SEM images. CA measurements were used as a simple and fast method of identifying changes in the hydrophobic characteristics of the membrane surface due to fouling. In addition, a significant difference in the left

and right CA indicates a chemically heterogeneous surface. However, it should be borne in mind that surface roughness could also cause this observation limiting the reproducibility and thus the reliability of CA measurements. Another problem is that during sample drying in a desiccator, the membrane samples sometimes curl as the skin layer shrinks more than the support layer. This presents a problem in any *ex situ* analysis, but was especially problematic in CA measurements as a very flat surface is required for reliable results.

The inner structure of the membranes was characterized using Brunauer-Emmett-Teller (BET) surface analysis (Papers III and VI). This technique utilizes the adsorption of gas molecules in the membrane pores due to pore condensation, and the desorption of gas molecules from the pores due to gas evaporation, to determine the inner pore area and inner pore volume. Measurements are normally performed at normal pressure at the boiling point of liquid nitrogen (-195.79°C). It is possible to investigate the properties of micropores with diameters down to 2 nm, mesopores with diameters of 2–50 nm, and up to macropores with diameters over 50 nm. The sample preparation for BET analysis is laborious. The sample must be completely dry to avoid outgassing of the sample during the measurements, and degassing of dried membrane samples in a degasser unit can take up to 24 h. Furthermore, the reliability of BET analysis depends on the inner area and volume of the sample, such that the reliability of the results improves with increasing inner area and inner volume of the sample. It is therefore important to have as much membrane sample as possible in the sample vial. The membrane sample thus has to be cut into very small pieces, but there is still a limit on the quantity of the sample that can be inserted into the vial.

3.2 *In situ* real-time monitoring of membrane processes

To investigate the status of membrane process monitoring in industry, a survey was conducted among industrial membrane experts and analytical equipment suppliers [53]. Interviews with industrial membrane experts revealed that not only scholars are convinced that *in situ* real-time monitoring is important for membrane processes. All 24 interviewees stated that monitoring of membrane fouling is helpful, important, or very important. However, only a few of them had already used one of the techniques available to monitor their membrane processes. In general, the responses of the industrial experts revealed that their knowledge concerning methods of monitoring membrane fouling was unfortunately rather limited. Surprisingly, instrument suppliers had not yet taken the membrane market as such into consideration, and were not aware of the expediency of their instruments for monitoring membrane processes. In fact, most of them had no knowledge of membrane processes at all.

When asked about factors affecting the success of *in situ* real-time monitoring of membrane fouling, the industrial experts stated up to sixteen factors. The four factors most often mentioned were: 1) the technique should be able to determine the composition of the fouling layer, 2) it should be easily automated, 3) it should be robust, and 4) it should be able to determine the thickness of the fouling layer. Interestingly, the potential economic advantage offered by the implementation of such a technique in the membrane process was only ranked eleventh.

To further penetrate this topic, a literature review was conducted on potential *in situ* real-time monitoring techniques for membrane fouling in lignocellulosic biorefineries and two other industrial sectors to identify techniques suitable for this task (Paper I). A broad variety of techniques was identified for *in situ* real-time monitoring of membrane fouling (and cleaning). However, despite many promising studies on laboratory scale, only a few techniques had been employed in studies on industrially relevant applications. An overview of the identified techniques and some of their properties with regards to membrane fouling in lignocellulosic biorefineries are given in Table 3.1, while the respective strengths and weaknesses of the techniques are presented in Table 3.2.

Table 3.1 Overview of techniques that could be used for ***in situ*** real-time monitoring of membrane fouling in the biorefinery sector (adapted from Paper I)

Monitoring technique	Type of information	Scale	Membrane	Operation	Area	Detection limit
Direct observation	Composition, distribution, thickness	Lab	Flat, tubular, hollow	Flow	Module	<10 μm
Laser-based techniques	Thickness	Lab	Flat	Flow	Spot	<5 μm
Image analysis	Concentration, distribution	Lab, pilot	Flat	Flow	Spot	ppm
Confocal laser scanning microscopy	Composition, distribution	Fundamental, lab	Flat	Static	Spot	20 μm
Multiphoton microscopy	Composition, distribution	Fundamental, lab	Flat	Static	Spot	20 μm
Surface plasmon resonance	Thickness	Fundamental	Flat	Flow	Spot	<10 nm
Ellipsometry	Thickness	Fundamental, lab	Flat	Flow	Spot	μm–nm
UV/Vis reflectance spectroscopy	Composition, concentration	Lab	Flat, tubular, hollow	Flow	Spot	1 mol%
Photo interrupt sensor	Thickness, distribution	Lab, pilot	Flat	Flow	Spot	10 μm
Photoacoustic spectroscopy	Thickness, composition	Fundamental, lab	Flat	Flow	Spot	<10 μm
Ultrasonic time-domain reflectometry	Thickness, distribution	Pilot, industrial	Flat, tubular, hollow, spiral	Flow	Module	<10 μm
Quartz crystal microbalance with dissipation	Thickness	Fundamental	Flat	Flow	Spot	<10 nm
Holographic interferometry	Concentration, thickness	Lab	Flat	Flow	Module	μm, mol
Optical coherence tomography	Distribution	Fundamental, lab	Flat	Flow	Spot	10 μm
Magnetic resonance imaging	Thickness, distribution	Fundamental, lab	Flat, tubular, hollow, spiral	Flow	Spot, module	μm–nm
X-ray microimaging	Distribution	Fundamental	Flat, tubular, hollow, spiral	Flow	Spot	<1 μm
Small-angle scattering	Distribution	Fundamental	Flat, tubular, hollow, spiral	Static	Spot	1 nm
Infrared spectroscopy	Composition, concentration	Fundamental, lab	Flat	Flow	Spot	1 μg/cm^2
Raman spectroscopy	Composition, concentration	Lab, pilot	Flat	Flow	Spot	100 μg/cm^2
Electrical impedance spectroscopy	Thickness, composition	Lab, pilot, industrial	Flat, tubular, hollow	Flow	Module	1 μm
Streaming potential	Thickness	Fundamental, lab	Flat, tubular, hollow	Flow	Module	<20 μm
Voltammetry and chronopotentiometry	Concentration	Lab	Flat	Flow	Spot	1 mol
Fluid dynamic gauging	Thickness, cohesive and adhesive strength	Lab, pilot, industrial	Flat	Flow	Spot	10 μm

Table 3.2 Strengths and weaknesses of the methods available for the monitoring of membrane fouling in the biorefinery sector (adapted from Paper I)

Monitoring technique	Strengths	Weaknesses
Direct observation	Simple and affordable	Only applicable to larger molecules, not proteins or polysaccharides
Laser-based techniques	Information on the thickness of a fouling layer with a resolution of ~3 μm	Foulants must reflect laser light, interference from changes in a refractive index of solution
Image analysis	Both qualitative and quantitative information	Cannot be used to determine absolute amounts of fouling
Confocal laser scanning microscopy	Protein and carbohydrate differentiation possible	Foulants must be labeled with fluorophores
Multiphoton microscopy	Fluorescence excitation in UV region	Filtration must be stopped during imaging
Surface plasmon resonance	Information on early-stage fouling on model layers	Low molecular weight compounds are difficult to detect
Ellipsometry	Information on early-stage fouling during membrane filtration	Refractive index of fouling must be different from that of the membrane
UV/Vis reflectance spectroscopy	Highly sensitive and rapid	Clear solution with low concentrations needed
Photo interrupter sensor	Fast, simple and affordable	Low concentration necessary
Photoacoustic spectroscopy	Applicable to highly scattering, optically opaque media	Fouling signal must differ from membrane signal
Ultrasonic time-domain reflectometry	No constraints regarding module type or size	Density of fouling must differ from that of the membrane
Quartz crystal microbalance with dissipation	Information on early-stage fouling on model layers	Sensitive to hydrodynamically coupled water, resulting in too high adsorbed mass
Holographic interferometry	Visualization of CP	Restricted to low flow rates
Optical coherence tomography	Applicable to opaque medium layers	Scattering events lead to intensity loss and limit scan depth
Magnetic resonance imaging	Quantification of spatial fouling distribution	Low flow rates and small molecules required <30 kDa
X-ray microimaging	Not yet applied for *in situ* real-time monitoring	Distinct difference required in electron density between components of interest
Small-angle scattering	Structural information on objects between 1 nm and 100 nm	Small scattering volume up to a thickness of 100 μm
Infrared spectroscopy	Quantification of chemical interaction between solutes and membrane	Measurements limited by interference from O–H vibrational bands from water
Raman spectroscopy	Both qualitative and quantitative information	Interference from fluorescence
Electrical impedance spectroscopy	Dielectric substructures of systems and electrochemical diffusion processes can be characterized	Conductive membrane and/or fouling needed
Streaming potential	Information on surface charge of fouling layer	Overlay of membrane and fouling layer zeta potential
Voltammetry and chronopotentiometry	Information on kinetics of ion-exchange membrane fouling	The interpretation of the results may be difficult
Fluid dynamic gauging	Information on cohesive/adhesive strength of fouling layer	Fouling layer is assumed to be locally stiff

3.2.1 Quartz crystal microbalance with dissipation monitoring

QCM-D was chosen as the method for *in situ* monitoring of membrane fouling in lignocellulosic biorefineries (Papers IV and V), based on the findings presented in Paper I and its so far underutilized potential for membrane fouling investigations. QCM-D is a useful technique for investigating adsorption and desorption processes *in situ* and in real time. The technique is illustrated in Figure 3.4. A piezoelectric quartz crystal sensor oscillates due to electric induction. The shift in resonance frequency of the sensor caused by the adsorption or desorption of mass on the sensor surface is continuously measured. This is combined with monitoring the dissipation of the oscillation when induction is removed. Together, the frequency and dissipation shift provide information on the adsorbed mass, changes in the density or viscosity of the solution, viscoelastic changes in the boundary layer, and changes in the surface free energy.

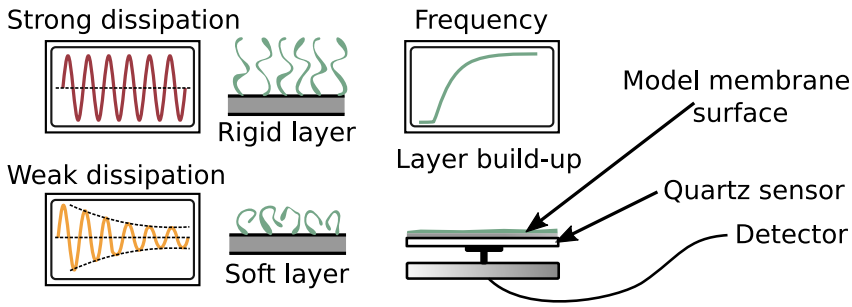

Figure 3.4 Schematic of QCM-D for ***in situ*** real-time monitoring of membrane fouling on a model membrane surface. (Adjusted from Paper I.)

QCM-D is a very useful tool to study early-stage adsorptive fouling processes. Unfortunately, it cannot directly be used for membrane processes, instead, a model surface representing the membrane must be used. This can be achieved, for example, by spin-coating a membrane polymer on the sensor surface [89–95]. An alternative approach is the formation of a self-assembled monolayer of polymer on the sensor. A comprehensive understanding of the underlying fouling mechanisms can be obtained by combining QCM-D with additional techniques such as surface imaging using AFM and chemical composition analysis using ATR-FTIR.

In the context of membrane fouling, studies involving QCM-D have so far focused on protein adsorption [91, 93, 94, 96–98], in water treatment and the production of dairy products, and on the adsorptive behavior of extracellular polymeric substances during membrane fouling in water treatment [90, 95, 99–101]. To date, only a few studies have been performed to compare findings from adsorption studies using QCM-D with results from conventional membrane fouling monitoring methods such

as flux or pressure measurements. Good agreement was found between fouling on the model surfaces and membrane fouling during the filtration process [91, 93, 99]. For example, pore plugging has been identified and confirmed by comparing results from QCM-D with flux decline during filtration [92].

In this work, QCM-D was applied to study adsorptive fouling of the membrane by thermomechanical pulping process water, and to identify the main compounds on a polysulfone surface modeling an UFX5-pHt membrane (Paper IV). The long-term adsorption from this process water was studied at different temperatures (Paper V). Furthermore, the reliability of the results from QCM-D studies was studied by comparing them with flux measurements and *ex situ* analysis of fouling during UF under similar conditions.

4 Flux and *ex situ* Analysis of Membrane Fouling in Lignocellulosic Biorefineries

The classic method of detecting fouling is by flux measurements. Theoretical approaches for the interpretation of flux data were introduced in Section 2.2. In this chapter, these approaches are applied to data from the reference system and the findings briefly discussed (Section 4.1). Thereafter, the results of *ex situ* analysis of the membrane surface (Section 4.2) and the inner structure (Section 4.3) of UF membranes used to filter several process streams from lignocellulosic biorefineries are presented.

4.1 Fouling analysis based on flux

The resistance-in-series model (Eq. 2.4) can be used to determine the contributions of reversible and irreversible fouling to the total flux decline. With a sufficient amount of data, it is possible to determine whether the increase in membrane resistance is due mainly to adsorption, pore blocking, or cake layer formation. In order to use this model, the osmotic pressure difference due to solute rejection above the membrane surface must be estimated. This is usually difficult, but in MF and UF it is reasonable to assume that $\Delta\pi$=0 bar, as osmotic effects are too small to have any substantial effect on the flux.

In this section, fouling analysis with the resistance-in-series model is exemplified by application to data from the UF of thermomechanical pulping process water with an UFX5-pHt membrane at 25°C and at 50°C in cross-flow mode (Paper v). The filtration process was run at a TMP of 0 bar or 2 bar. The dynamic viscosity of the

permeate was assumed to be water-like, i.e., 0.9 mPa·s at 25°C and 0.5 mPa·s at 50°C. For easier comparison, the permeability of the membranes (P = J/TMP) was used instead of the flux. Table 4.1 gives the permeability of new membranes P_i, after static adsorption at 0 bar TMP at 25°C and 50°C (P_a), at the end of filtration at 2 bar TMP at 25°C and 50°C (P_v), and after subsequent rinsing with deionized water.

Table 4.1 Permeability expressed as $L/m^2 \cdot h \cdot bar$, of new membranes (P_i), after static adsorption (P_a), at the end of a filtration (P_v), and after filtration and rinsing (P_f) at 25 °C and 50 °C

Permeability	25°C	50°C
P_i	65.2	62.4
P_a	54.4	53.4
P_v	1.7	0.4
P_f	21.1	7.1

Using the resistance-in-series model, the resistance of the membrane R_m, was found to be 6.20×10^{12} 1/m at 25°C and $R_m = 11 \times 10^{12}$ 1/m at 50°C. The higher resistance of the membrane at the higher temperature could be due to swelling of the membrane. Calculating the resistance due to reversible R_{rev} and irreversible R_{irrev} fouling revealed that R_{rev} was substantially higher than R_{irrev} and both increased with temperature. R_{rev} increased from 213.0×10^{12} 1/m to 1608.4×10^{12} 1/m, while R_{irrev} increased from 13.0×10^{12} 1/m to 82.2×10^{12} 1/m. The higher temperature resulted in a lower density and viscosity of the feed solution, but it also increased the mass transport of solutes to the membrane. The high concentration of solutes in the boundary layer of the membrane can lead to CP and/or cake and gel layer formation, which would be seen as an increase in R_{rev} and R_{irrev} at the higher temperature.

Dal-Cin et al. [6] reported that the resistance-in-series model could underestimate the impact of adsorptive fouling. They therefore presented an alternative approach using the basic assumptions of the resistance-in-series model combined with relative flux loss ratios based on the absolute flux decline for a given mechanism in relation to the overall flux decline (Eqs. 4.1, 4.2, 4.3) where $R_f = R_{rev} + R_{irrev}$ and $R_t = R_f + R_m$.

$$D_a = \frac{R_f}{R_t} \cdot \frac{P_i - P_a}{P_i - P_v} \tag{4.1}$$

$$\%D_{pb} = \frac{R_f}{R_t} \cdot \frac{P_a - P_f}{P_i - p_v} \tag{4.2}$$

$$\%D_{cp} = \frac{R_f}{R_t} \cdot \frac{P_f - P_v}{P_i - p_v} \tag{4.3}$$

When this method was applied to the data from the UF of thermomechanical pulping process water, the relative flux loss ratio attributed to adsorptive fouling (%D_a) decreased from 16.6% at 25°C to 1.9% at 50°C, while the relative flux loss ratio attributed to pore blocking (%D_{pb}) increased from 51.1% at 25°C to 74.2% at 50°C. Both are related to R_{irrev}. The increase in %D_{pb} indicates that membrane fouling at the higher temperature was mainly related to pore blocking. The relative flux loss ratio attributed to CP (%D_{cp}) decreased from 29.7% at 25°C to 10.8% at 50°, indicating that the contribution of reversible fouling (R_{rev}) decreased, and the membrane became severely fouled at the higher temperature. The remaining percentage is related to the membrane resistance. The poorer performance of the membrane at the higher temperature can also be seen from the flux curves in Figure 4.1, where the flux at 50°C was lower than the flux at 25°C during the whole measurement period.

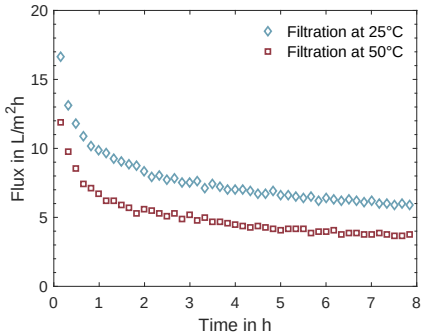

Figure 4.1 Flux of membranes fouled with thermomechanical pulping process water filtered at 25°C and at 50°C and 2 bar TMP, as a function of time.

Hermia's model (Eq. 2.5 or Eq. 2.6) can also be used for fouling analysis based on flux measurements, but is only applicable at the beginning of filtration. Figure 4.2 shows the derivative of the flux as a function of time (dJ/dt) for both the original data and the results obtained with Hermia's model. The modeled data were obtained using Eq. 2.6 by fitting a polynomial function to the data from the first 60 min and then taking the derivative of this polynomial function with respect to t. Finally, the differentiated polynomial was set equal to $k \cdot J^{3-n}$, and k was fitted with the GRG Nonlinear function in Excel (Office 365, Microsoft) by minimizing the residuals between the left-hand side and the right hand side of the equation, while n was kept constant at either 0, 1, 1.5, or 2, representing one of the four fouling types defined in Table 2.2. The best fit was found for n = 0, indicating that the dominant type of fouling was cake layer formation.

The flux analysis with Hermia's model indicated a different type of fouling than the resistance-in-series model, which indicated that flux decline was related to irreversible fouling, and increased at the higher temperature. Thus, the different flux analysis

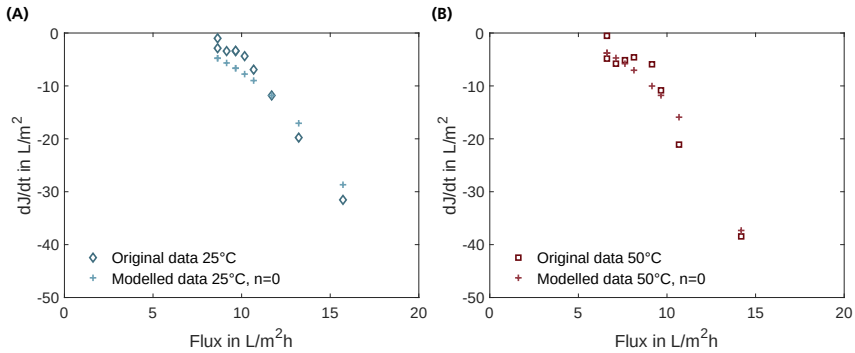

Figure 4.2 Original flux data and data obtained by fitting to Hermia's model at 25°C **(A)** and 50°C **(B)**. The value of the parameter n found to fit to the experimental data best was n = 0 for both temperatures, indicating cake layer formation. (Unpublished data.)

approaches are contradictory. The results based on the relative flux loss ratios indicated that pore blocking was the dominant type of fouling. It is likely that the kind of fouling changes with time, as suggested by Wang and Tarabara [102], starting with pore blocking and ending with cake filtration. However, this cannot be confirmed by flux analysis alone. Moreover, neither of the models provides any information on the compounds causing fouling or ways of preventing or reducing it. Thus, further analyses are required to understand fouling in more detail, and ways in which cleaning can be adapted to remove it.

4.2 Surface analysis of membrane fouling

Ex situ surface analysis is a useful method as it provides information on the structure and chemical composition of the fouling layer on the membrane surface. In this section, the results of *ex situ* analysis with SEM, AFM, SEM-EDS, ATR-FTIR and CA measurements on fouled membranes are presented and discussed.

4.2.1 SEM

SEM imaging was used to investigate the fouling of UFX5-pHt membranes resulting from dead-end filtration (schematic of the module given in Figure A.1 in the Appendix) of thermomechanical pulping process water at 2 bar TMP and 70°C (Paper II), and ES404 membranes used for the filtration of bleach plant effluent in cross-flow mode on industrial scale (Paper VI). The UFX5-pHt membrane fouled by thermomechanical pulping process water shows a fouling layer that seems to be thin with

elongated structures and many small particles 1–2 µm in size in this low-magnification image (Figure 4.3A). The extent of the fouling is obvious when this image is compared to that of the pristine membrane (Figure 2.2: note the higher magnification in this image). The visible fouling layer may be the remnants of a thin gel layer, as suggested by the flux analysis of UF of the same solution at a lower temperature in cross-flow mode. The nature of the elongated structures and small particles can only be speculated upon, but their interpretation can be facilitated as the composition of the feed solution was known. Bearing in mind the composition of thermomechanical pulping process water, the elongated objects may be wood fibers, and the particles precipitated organic or inorganic compounds. In contrast, the fouling layer caused by bleach plant effluent (Figure 4.3B) is very fractured, and seems to be much thicker than the fouling layer caused by thermomechanical pulping process water. It is possible that the fouling layer broke up during sample preparation, and a gap can be seen the center of the image, suggesting that a piece of the fouling layer broke off during sample preparation. However, it cannot be determined from this image whether the membrane is visible through the fouling layer in this opening or not.

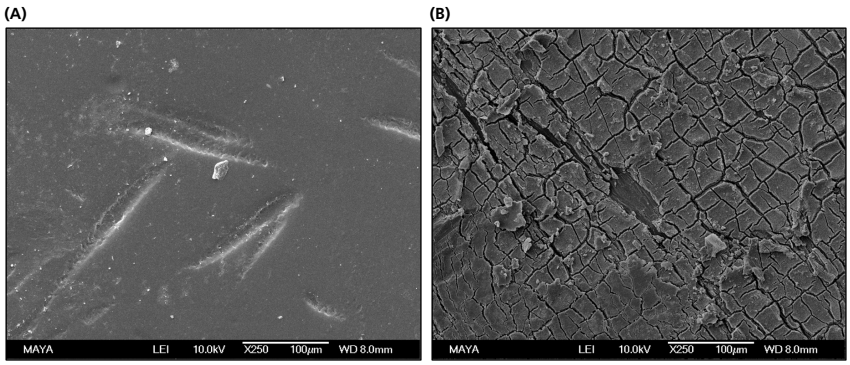

Figure 4.3 SEM images of a UFX5-pHt membrane fouled with thermomechanical pulping process water **(A)**, and the ES404 membrane fouled with bleach plant effluent from sulfite pulping **(B)**.

4.2.2 AFM

More detailed images of the surface of the UFX5-pHt membrane fouled with thermomechanical pulping process water under different operating conditions in cross-flow mode were obtained with AFM (Paper v). Figure 4.4 shows AFM images of a pristine membrane (Figure 4.4A) and membranes fouled at 25°C (Figure 4.4B) and at 50°C (Figure 4.4C). It is difficult to draw any further conclusions based on these images, but roughness analysis revealed that the roughness of the membrane fouled at 25°C (rms roughness of 2.6 nm) was similar to that of the pristine membrane (rms rough-

ness of 2.8 nm). A considerable increase in roughness was seen for the membrane fouled at the higher temperature (rms roughness of 6.6 nm).

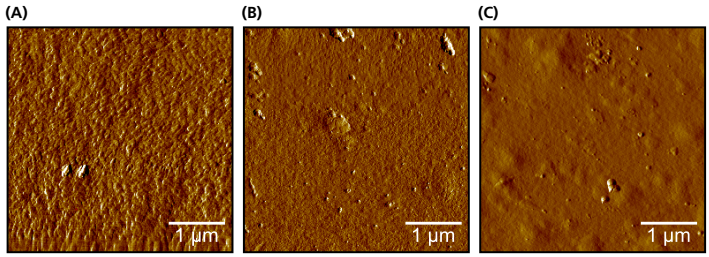

Figure 4.4 AFM images of a pristine UFX5-pHt membrane **(A)**, and UFX5-pHt membranes fouled with thermomechanical pulping process water at 25°C **(B)** and 50°C **(C)**.

The findings from AFM indicate the formation of a gel or cake layer on the membrane at the higher temperature, which is in accordance with the findings from the flux analysis (Section 4.1).

4.2.3 SEM-EDS

The combination of SEM and EDS was applied for the characterization of the ES404 membrane fouled with bleach plant effluent (Paper VI). The results are presented in Figure 4.5, where the surface and the cross-section of the fouled membrane are shown. Using the information obtained from EDS, it was possible to identify the green-yellowish fractured structure as consisting mainly of compounds with high contents of magnesium and oxygen. This is reasonable considering that magnesium is used as the cooking chemical base in the pulp mill, which leads to a high concentration of magnesium in the bleach plant effluent.

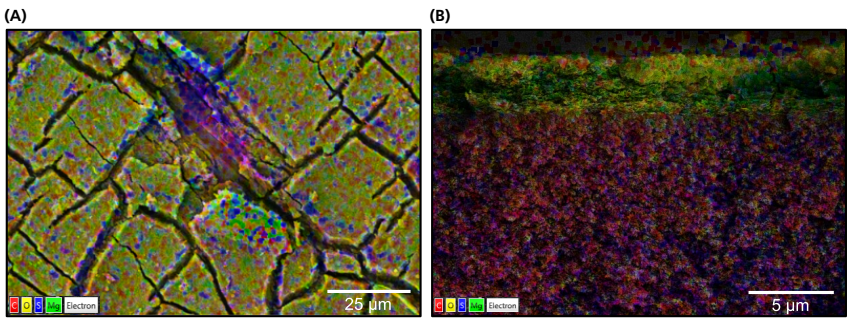

Figure 4.5 SEM-EDS images of ES404 membranes fouled with bleach plant effluent from sulfite pulping: Surface **(A)** and cross-section **(B)**.

This layer is thus likely to be a precipitate of magnesium hydroxide $Mg(OH)_2$. As cake formation by inorganic compounds (scaling) was not expected, the SEM-EDS analysis provided a very valuable insight. The reddish region in the gap in the middle of the fouling layer (Figure 4.5A), is caused by signals from carbon and sulfur, both present in the membrane polymer. This indicates that the membrane can be seen in this gap, or that the fouling layer is sufficiently thin for the signal from the membrane to be detected.

Two regions are distinguishable in the cross-sectional image (Figure 4.5B). The green-yellowish section at the top of the image contains mainly magnesium and oxygen, and can thus be ascribed to the fouling layer. This is evidence that a cake layer was formed on the surface of the membrane. Furthermore, this layer was roughly 4.5 µm. The reddish region below contains mainly carbon and sulfur, and can therefore be ascribed to the membrane. However, a line scan from the top (fouling layer and membrane) in to the membrane (not shown here) revealed that the atomic weight percentage of magnesium was highest 2 µm below the surface of the fouling layer, and declined rapidly towards the membrane surface. Further into the membrane, the magnesium content was very low. Silicon was detected further into the membrane, with a maximum content of 10% in atomic weight approximately 10 µm from the membrane surface.

4.2.4 ATR-FTIR

When inorganic compounds are only minor foulants in the process, elemental analysis with EDS does not give sufficient information and other techniques are required for the analysis of the chemical composition, such as ATR-FTIR. This was used for the analysis of fouling on UFX5-pHt membranes caused by thermomechanical pulping process water (Papers II, III, and V), fouling of the UP010 membranes by pressurized hot-water extract (Paper III), fouling of the GR95PP membranes by black liquor (Paper III), and fouling of the ES404 membrane by bleach plant effluent (Paper VI).

ATR-FTIR spectra obtained from the UFX5-pHt membranes after fouling by thermomechanical pulping process water, and from GR95PP membranes after fouling by black liquor (data from Paper III) are shown in Figure 4.6 as examples, and are briefly discussed below.

The wavenumber range from 1500 cm^{-1} to 450 cm^{-1} is called the fingerprint region as it contains most of the peaks and the pattern is unique to each sample. Many peaks in the fingerprint region can be assigned to vibrations of the bonds from the polysulfone of the membrane polymer, while others can be assigned to specific bonds in the foulants. The peak assignments are given in Table 4.2.

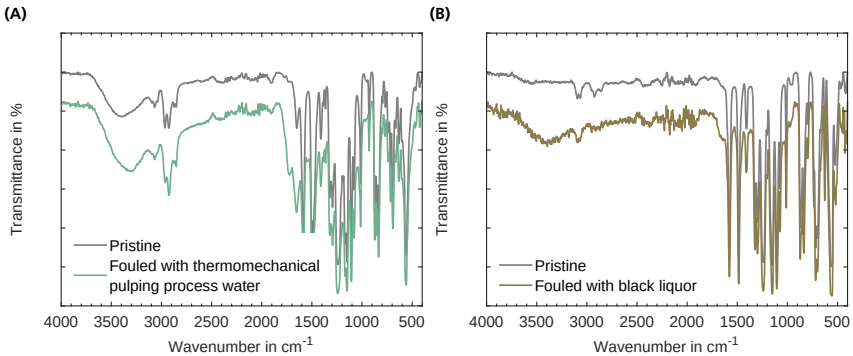

Figure 4.6 ATR-FTIR spectra of UFX5-pHt membranes fouled with thermomechanical pulping process water **(A)** and GR95PP membranes fouled with black liquor **(B)**.

A peak in the region 3600–3100 cm^{-1} can be seen in the spectrum for the thermomechanical pulping process water. The signal from O–H stretching of bonds in the hydroxyl or phenolic groups is also found in this region [103]. To avoid signals from water, all the samples were dried and stored in a desiccator for at least 24 h. However, it is still possible that some water remained in the sample, leading to the observed response. The intensity of this peak increased slightly in the fouled membrane. Based on knowledge of the feed composition, this increase in intensity might originate from weak signals from the hydroxy groups of either polysaccharides such as GGM or lignin [104–107]. The peak at 2964 cm^{-1} can be attributed to the stretching of aromatic C–H bonds, which are present in both PSU and polysaccharides [106, 108, 109]. The intensity of this peak is also increased in the fouled membrane, indicating the adsorption of polysaccharides. The peak at 1736 cm^{-1} can be assigned to the C=O carbonyl bonds in the methyl ester groups or carboxylic acid in the acetyl groups of hemicelluloses or extractives [104, 110, 111]. The peaks at 1080 cm^{-1} and 1014 cm^{-1} are attributed to the rocking of aliphatic C–C bonds and aromatic –CH bonds, respectively [112], both of which can be ascribed to polysaccharides. Similar results were found in the other investigations (Papers II, III, and V). Overall, ATR-FTIR analysis of membrane fouling by thermomechanical pulping process water indicates fouling by polysaccharides in the form of GGM and low-level fouling by extractives.

A peak in the region 3600–3100 cm^{-1} assigned to O–H stretching was observed for the membrane fouled with black liquor. Polysaccharides have not been found to be potential foulants in this process stream. Hence, the peak can be ascribed to the phenolic groups of ligneous compounds and extractives [104, 106, 107]. A peak was also seen at about 1650 cm^{-1}, which was assigned to carbonyl-containing compounds such as natural lignin or terpenoid extractives [104, 106, 107]. Furthermore, the areas

Table 4.2 Peak assignment for ATR-FTIR analysis of membrane fouling on PSU and PES membranes [104–114]

Wavenumber (cm^{-1})	Assignment
834, 873	Stretching of C–H bonds in the aromatic ring of PSU and PES
1014, 1080	Skeletal vibrations of aliphatic C–C bonds aromatic C–H bonds in PSU, PES and polysaccharides
1106, 1169	Stretching of C–O–C bonds in polysaccharides, symmetric stretching of $C–SO_2–C$ bonds in PSU and PES
1151	Symmetric stretching of $C–SO_2–C$ bonds in PSU and PES
1242	Stretching of C–O–C bonds in PSU and PES
1295	Asymmetric stretching of S=O bonds in PSU and PES
1488	Stretching of $CH_3–C–CH_3$ bonds in PSU and PES
1503	Stretching of C=C bonds in aromatic rings and stretching of C=O bonds in extractives and lignin
1576	Skeletal vibrations of C–C bonds in PSU, PES and lignin
1730	Stretching of C=O bonds in polysaccharides and extractives
2964	Stretching of C–H bonds in aromatic groups of PSU, PES and polysaccharides
3000–3600	Stretching of O–H bonds in polysaccharides and water

between the peaks at 1576 cm^{-1} and 1485 cm^{-1}, 1485 cm^{-1} and 1410 cm^{-1}, and 1410 cm^{-1} and 1320 cm^{-1}, were attenuated in the case of the fouled membrane. These regions can be attributed to skeletal vibrations of phenolic compounds such as lignin and extractives [106, 107]. ATR-FTIR analysis of the membrane fouled by the filtration of black liquor indicates that mainly lignin and extractives are attached to the membrane.

4.2.5 CA analysis

CA measurements were made in all the studies on membranes in this thesis (Papers II, III, and IV) to elucidate the hydrophilic properties of the fouling layer. For example, fouling caused by thermomechanical pulping process water reduced the CA from 71.5° to 39.5° (Paper III), indicating the attachment of hydrophilic compounds such as GGM on the membrane surface. However, as described above, the CA is also influenced by the surface roughness and chemical homogeneity of the surface, and results from CA measurements must thus be interpreted with caution, taking surface roughness measurements into consideration.

4.3 Impact of membrane fouling on the inner structure of the membrane

Ex situ surface analysis can provide important insight into membrane fouling, but it cannot reveal if or how fouling substances have penetrated the membrane during filtration. Analysis of the inner structure of the membrane is required, using, for example BET analysis. This is a method not yet commonly applied in the characterization of membrane fouling.

4.3.1 BET analysis

BET surface analysis was applied to analyze UFX5-pHt membranes fouled with thermomechanical pulping process water, GR95PP membranes fouled with black liquor and UP010 membranes fouled with pressurized hot water extract (Paper III). Further investigations were performed on UFX5-pHt membranes fouled with thermomechanical pulping process water in cross-flow mode under various operating conditions (Paper V).

The results presented in Papers III and V on fouling caused by thermomechanical pulping process water will be discussed in this section. Filtration was carried out in dead-end mode (Paper III) and cross-flow mode (Paper V). Reference values were obtained by filtering deionized water through the membranes under similar conditions.

Pores in both the skin layer and the support layer were investigated, and are included in the total pore volume. The diameters of the pores in the studied membranes ranged from 1 nm to several nm. Hence, fouling-induced changes in the micropore region (<2 nm), e.g., due to pore adsorption, and the mesopore region (2–50 nm), e.g., by cake layer formation, are of interest. Fouling during dead-end filtration caused an increase of less than 2% in the BET surface area compared to the reference (Paper III). The total pore volume showed an increase of 7% while the average pore diameter decreased by about 7%. Figure 4.7 shows the pore area and pore volume as a function of pore diameter. Only small differences were seen between the reference data and the fouled membrane. The only differences between the pristine membrane and the fouled membrane were an increase in the pore area of pores smaller than 4 nm and a slight decrease in the pore area of pores between 4 nm and 30 nm. The pore volume was similar for most pore sizes, however it increased with fouling in pores with diameters larger than 32 nm. Based on these findings, it appears that there was little adsorption of compounds in the pores, and only a thin layer was formed on the surface of the membrane, which was already previously visualized by SEM (Figure 4.3A).

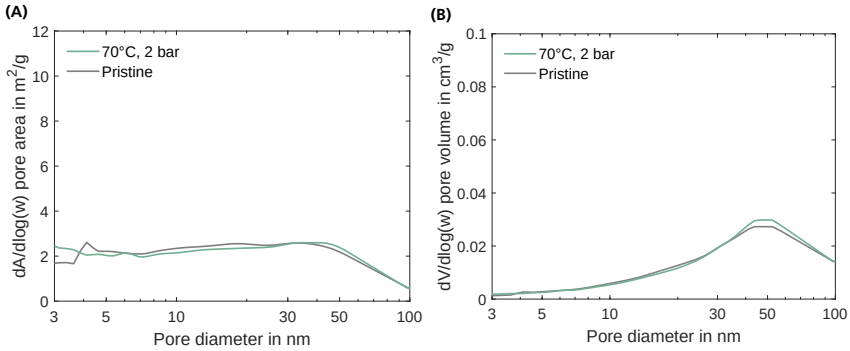

Figure 4.7 BET area **(A)** and volume **(B)** as a function of pore diameter of UFX5-pHt membranes fouled in dead-end mode.

In contrast to the results obtained following dead-end filtration, the membranes fouled in cross-flow mode showed a decrease in BET micropore area of about 50% (Paper v). This could be the result of pore blocking, in agreement with the results of flux analysis in terms of relative flux loss ratios (Section 4.1). In addition, Figures 4.8A and 4.8B show signs of considerable cake layer formation independently of temperature and TMP, supporting the results of flux analysis with Hermia's model. Both the pore area and the pore volume increased significantly in pores larger than 4 nm in diameter, which indicates the formation of a mesoporous cake or gel layer. Furthermore, the pore area and, to a limited extent, the pore volume, increased in pores smaller than 4 nm. This suggests extensive adsorptive fouling in the pores of the membrane. Interestingly, with BET analysis, no outstanding difference was seen between fouling under different operating conditions (temperature and TMP), although other analytical methods and the flux analysis showed that the operating conditions affected fouling (Sections 4.1 and 4.2).

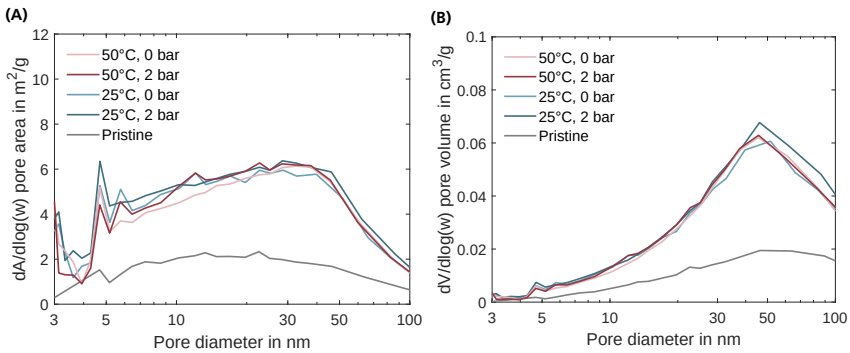

Figure 4.8 BET area **(A)** and volume **(B)** as a function of pore diameter of UFX5-pHt membranes fouled in cross-flow mode.

The observed differences between the pore area and pore volume distributions of the membranes fouled when run in dead-end mode and the membranes fouled in cross-flow mode may be due to differences in the shear forces above the membrane. According to computational fluid dynamics simulations of the dead-end module [8], at the stirring rate used here, shear rates of up to 1074 1/s can occur in close proximity to the stirrer and membrane (see Figure A.1 in the Appendix). This is considerably higher than the shear rate of about 56 1/s in the cross-flow module at the applied CFV (unpublished data, see Figure A.3 in the Appendix). The higher shear forces in the dead-end module are likely to have removed most of the cake layer, explaining the negligible differences between the reference and the fouled membrane in the mesoporous region in Figure 4.7, and the thin fouling layer visible in the SEM image in Figure 4.3A. The small increase in pore area observed in the micropores could be due to pore adsorption of dissolved extractives that are small enough to enter the pores. The volume reduction was relatively high in the dead-end filtration experiments (88%), whereas almost no volume reduction was achieved in the cross-flow filtration experiments. Volume reduction leads to an increase in the concentrations of most compounds in the bulk phase above the membrane, and in particular the salt concentration can have a negative influence. It has been reported that wood extractive colloidal droplets destabilized faster at high salt concentrations and that destabilization was more effective with shearing [115]. This would result in the colloidal droplets breaking up and dissolving in the process water, making it easier for them to enter the pores and become adsorbed on the pore walls. Moreover, they could also precipitate on the membrane surface together with other dissolved compounds such as polysaccharides, resulting in the formation of a thin layer, as seen in this work. The shear rate was much lower in cross-flow filtration, and a cake layer was therefore most likely formed. Based on the findings of ATR-FTIR, this layer appears to consist mainly of GGM.

4.4 Final remarks on flux analysis and *ex situ* fouling analysis

Flux analysis is probably the fastest way to obtain insights into the type of membrane fouling, but the results of theoretical approaches showed that flux measurements can only provide indications. Often, a combination of several types of fouling takes place during the course of filtration, the dominating form changing over time. *Ex situ* analysis of the membrane surface does not provide the same kind of information as flux analysis, but nevertheless provides important information on the chemical and structural characteristics of the fouling layer. A more reliable indication of the type of fouling can be obtained by *ex situ* analysis of the inner structure of the membrane based on BET analysis. Information on the structure and chemical composition of

the membrane surface can be obtained with SEM, SEM in combination with EDS, and ATR-FTIR. Other surface properties of the fouling layer can be determined with AFM (roughness) and CA measurements (hydrophobicity). The analysis of membranes using BET analysis provides a relatively rarely used opportunity to obtain knowledge on the effects of fouling on the membrane pores. The combination of complementary *ex situ* analysis methods allows the identification of the main foulants causing reduced capacity during UF. However, a major drawback of *ex situ* analysis is that this information can only be extracted from the membrane after the membrane operation. Thus, it is not possible to obtain information on the changes taking place on or in the membrane over time, which is of great importance if the entire membrane process (filtration, cleaning and rinsing) is be optimized.

5 *In situ* Monitoring of Membrane Fouling by Thermomechanical Pulping Process Water

This chapter presents the results of *in situ* monitoring of membrane fouling of the reference system with QCM-D. A prerequisite for this analysis is that the model system used in the QCM-D setup is comparable to the actual UF process. The model membrane surface and the membrane are characterized and compared in Section 5.1. The findings of QCM-D adsorption and desorption studies of thermomechanical pulping process water on UFX5-pHt model membranes are then presented and discussed in Section 5.2.

5.1 Model membrane surface for QCM-D *in situ* analysis

In order to use QCM-D for investigations of membrane fouling, a sufficiently thin model membrane surface must be created on the quartz sensor. This is commonly done by spin-coating. For the membrane fouling studies described in Papers IV and V, a model membrane was created by spin-coating a solution of UFX5-pHt membrane polymer dissolved in dichloromethane on a clean gold QSX301 sensor (Biolin Scientific, Sweden). The polymer film was subsequently analyzed and its properties compared with the characteristics of a pristine UFX5-pHt membrane. Since the QCM-D sensors are very delicate, ATR-FTIR and SEM analysis was done on polymer films spin-coated on pieces of gold wafers. The surface characteristics of the polymer films and the membrane are presented and compared in this section.

The CA of the spin-coated film varied between 43.6° and 83.5°, whereas the CA of the membrane varied between 50.5° and 71.5°. As discussed previously, measurements of the CA are error-prone and although the ranges of CA determined are broad, the values are similar indicating slightly hydrophilic properties.

The chemical composition of the polymer film was determined with ATR-FTIR. Figure 5.1 shows the ATR-FTIR spectra from a pristine UFX5-pHt membrane and a spin-coated polymer film. The fingerprint regions of the two samples are very similar, with peaks at the wavenumbers typical of PSU [103, 108, 113, 114]. The variation in peak intensity could be the result of difficulties in ensuring sufficient contact between the spin-coated polymer film and the ATR crystal.

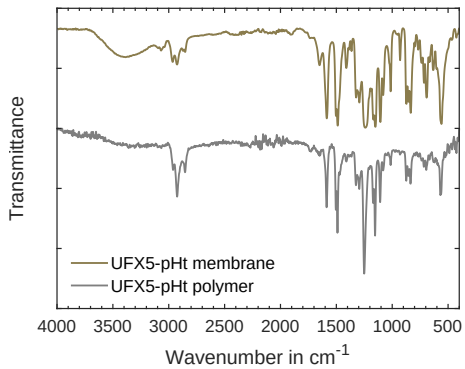

Figure 5.1 ATR-FTIR spectra of a pristine UFX5-pHt membrane and a spin-coated UFX5-pHt polymer film

AFM was used to image the surface of the polymer film and the membrane, and to determine the roughness of the two surfaces. This revealed considerable differences between different spin-coated sensors, as can be seen in Figures 5.2B and 5.2C, as well as significant differences between the polymer film and the membrane (compare with Figure 4.4A). The images presented are representative of several sensors. The polymer film shown in Figure 5.2B has a rough surface, with the appearance of a thick gel that has just stopped flowing from the center of rotation to the edge of the sensor. This seems to be a reasonable structure for a polymer film. However, the surface shown in Figure 5.2C is patterned with a network of crests and valleys.

It is not clear from the image whether the sensor was completely coated. SEM-EDS was performed at a lower magnification to investigate this further (Figure 5.3). This revealed that the crests in Figure 5.2C joined to form dark, river-like patterns of polymer, leading to roughly circular gaps, and that the surface of the gold was visible in these gaps.

There may be several reasons for the observed variation in the films. Therefore, the in-

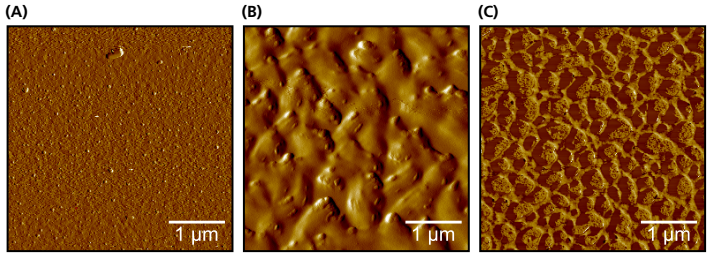

Figure 5.2 AFM images of a clean gold sensor **(A)** and two spin-coated QCM-D sensors with good coverage **(B)** and poor coverage **(C)**.

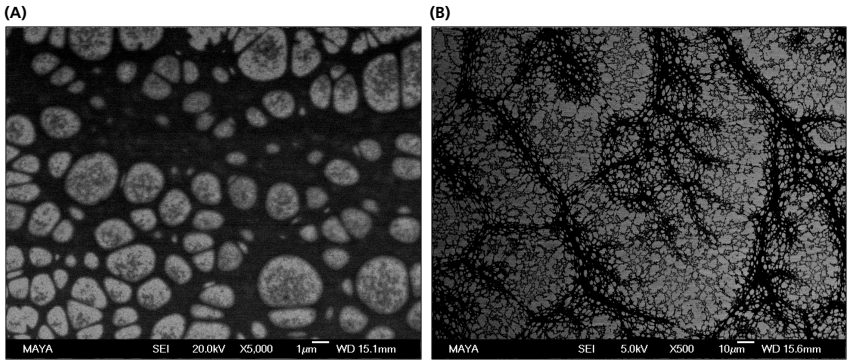

Figure 5.3 SEM images of polymer spin-coated on wafer pieces coated with gold at low **(A)** and high magnification **(B)**. (Unpublished data.)

fluence of the polymer concentration in the solvent and the hydrophobicity of the sensor surface were investigated (unpublished data). It was found that the problem was not as severe at high concentrations of the polymer (>2%(w/w)) in dichloromethane, as at low concentrations (0.5%(w/w)). However, the main cause of the problem appeared to be the hydrophobicity of the sensor surface itself. Spin-coating after ozonizing, which makes the surface much more hydrophilic, immediate rinsing with water, and subsequent drying with nitrogen helped to improve the homogeneity and smoothness of the spin-coated polymer films.

Surface roughness measurements with AFM showed that the polymer film was rougher than the membrane, but the rms roughness of the polymer film surface (5.2 nm) was of the same order of magnitude as the surface of the membrane (2.6 nm), regardless of whether the polymer film coating was good or poor.

The frequency and dissipation of each sensor were measured in Milli-Q water before and after spin-coating. The film thickness of the model membrane was estimated by assuming that the polymer film had the same density as pure polysulfone 0.24 g/mL.

The thickness of the active layer of these membranes has been determined previously by Lin et al. [116] using QCM-D and spin-coated polymer dissolved from various membranes. They found the thickness of the active layer to be between 17 nm and 150 nm. In the present work, the polymer films were found to have an average thickness of 41.2 nm (Paper v), which seems to be a reasonable value compared to the findings of Lin et al.

Overall, it can be concluded that the spin-coated polymer film had similar surface characteristics to the membrane, and can be considered an adequate model system mimicking a UFX5-pHt membrane.

5.2 *In situ* real-time monitoring of adsorptive fouling with QCM-D

A Q-Sense E4 (Biolin Scientific, Sweden) instrument was used to investigate the adsorption of compounds from thermomechanical pulping process water (Papers iv and v). The main foulants in thermomechanical pulping process water are wood polysaccharides such as hemicelluloses, and extractives [7, 61, 78]; in this application, lignin was not found to cause severe membrane fouling. To understand how these compounds cause fouling, three fractions of thermomechanical pulping process water were studied: 1) thermomechanical pulping process water that had been sieved to remove large particles such as fibers, 2) MF retentate that is rich in colloids droplets, and 3) MF permeate from which most of the colloidal droplets had been removed during MF. The adsorption of these solutions was studied at 25°C until equilibrium was reached, but at a maximal time of 2 h. After the adsorption, the QCM-D measurement cell was rinsed with Milli-Q water to flush away loosely bound compounds. In a further study (Paper v), the adsorption of thermomechanical pulping process water on the model membrane was studied for 8 h at 25°C and 50°C to investigate longterm fouling effects and the influence of temperature on the adsorption processes.

5.2.1 Adsorptive behavior of fractions of thermomechanical pulping process water

Figure 5.4 shows the change in frequency and dissipation over time caused by the adsorption of compounds from the three fouling solutions on the model membrane, and by the removal of compounds from the model membrane by rinsing with Milli-Q water. The decrease in frequency is the result of the adsorption of mass, while the increase in dissipation is the result of an increase in the softness of the attached layer.

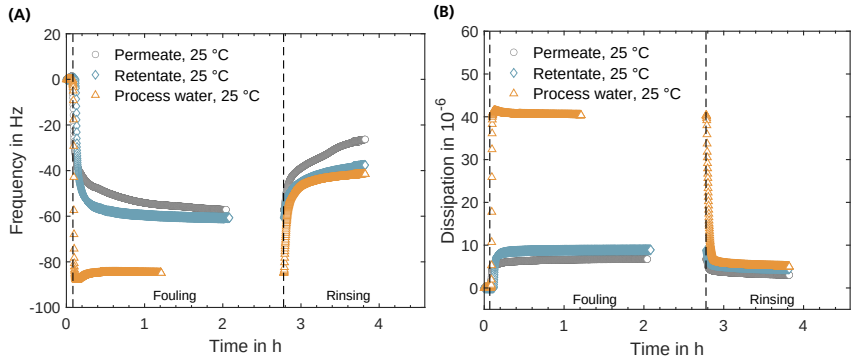

Figure 5.4 Changes in frequency **(A)**, and dissipation **(B)**, over time due to adsorption from thermomechanical pulping process water, MF permeate and MF retentate. The timescale has been adjusted so that the initiation of fouling and the start of rinsing are at t = 0 h and t = 2.8 h, respectively.

A decrease in frequency was seen as soon as the fouling solutions were introduced into the QCM-D cell, which implies very fast initial adsorption kinetics (Figure 5.4A). After 2 h, the frequency for the permeate was higher than that of the process water. The dissipation also showed a rapid change (Figure 5.4B), increasing immediately after the introduction of the fouling solutions. The dissipation for the permeate and process water appeared to reach a steady state after a very short time, but the dissipation for the permeate was slightly lower. This means the fouling layer formed by the adsorption of the permeate was slightly more rigid than the fouling layer formed by the process water.

On one hand, the difference between the progression of the frequency and dissipation curves for process water and permeate, respectively, can be explained by compositional differences. The permeate contained less extractives and other large compounds, as they had been removed by MF, and the proportion of hemicelluloses in the permeate was thus higher. On the other hand, variations in the way in which the hemicelluloses are adsorbed on the membrane surface can play a role. The alignment of the hemicelluloses plays an important role, and the degree of alignment depends on the hemicellulose structure. A less branched glucomannan, which will pass more likely through the MF membrane in the permeate, will adsorb more parallel to the surface, whereas GGM will not be able to adsorb parallel to the surface due to its galactose and acetyl side groups [20, 30]. Alignment of GGMs on the polymer surface can also be impeded by the surface roughness of the model membrane.

The comparison of the progression of the fouling curves showed that the adsorption kinetics of permeate are slower than for process water. Furthermore, it appears that the adsorption of permeate continues until the end of the experiment, while the ad-

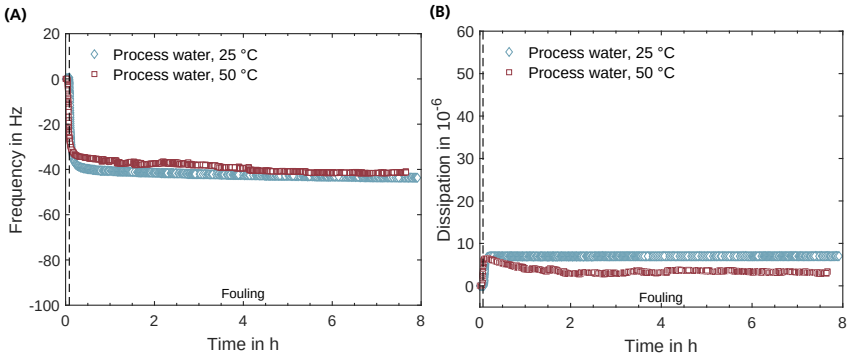

Figure 5.5 Changes in frequency **(A)**, and dissipation **(B)**, over time due to adsorption of thermomechanical pulping process water at different temperatures.

sorption kinetics of process water appear to reach equilibrium after an hour. The adsorption kinetics of the permeate can be compared to the reported adsorptive behavior of mannan on cellulose fibers reported by Hannuksela et al. [117]. They found that initial, very rapid adsorption was followed by a much slower adsorption phase, and suggested that this was due to multilayer adsorption of mannan on cellulose fibers. If this was also the case in the present study, the continuing adsorption of the permeate could be due to the longer time required for the hemicelluloses to become packed in a multilayer.

The adsorption of process water was studied for 8 h to investigate whether the adsorption kinetics actually reached equilibrium, and whether the fouling layer restructured after a longer time (Paper v). A continuous decrease in frequency was observed, which means that the adsorption kinetics of the process water did not reach equilibrium within 2 h (Figure 5.5). This is a strong indication that multilayer adsorption also occurs with process water. A similar experiment was run at 50°C, the maximum temperature of the instrument, and similar adsorption kinetics were observed. In this case, some kind of multilayer adsorption was observed too. However, dissipation monitoring at 50°C revealed a decrease in dissipation after reaching a maximum soon after fouling started. This indicates that the fouling layer is restructured at higher temperatures, most likely by the replacement of water or loosely attached compounds with smaller ones, making the fouling layer more compact and more rigid [118].

The adsorption of retentate was very different from the adsorption of the process water and the permeate (Figures 5.4 and 5.5). The adsorption kinetics of the retentate were fastest, exhibiting the lowest frequency and the highest dissipation value. However, after reaching its minimum, the frequency increased only slightly and then stabilized, while the dissipation decreased and stabilized after reaching its maximum. This suggests that the adsorbed fouling layer is considerably heavier and softer than the fouling

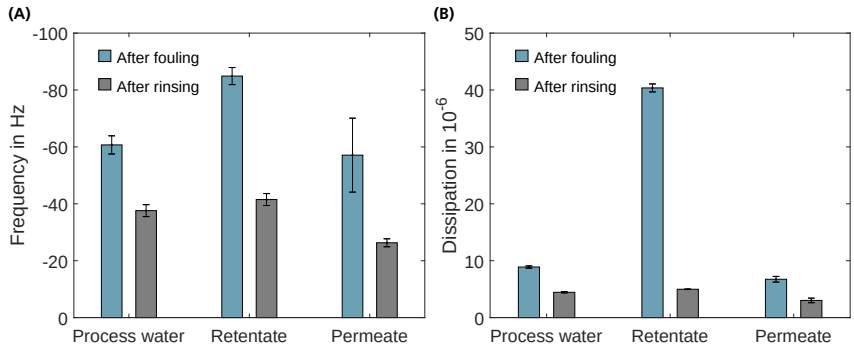

Figure 5.6 Change in frequency **(A)**, and dissipation **(B)** after fouling and after rinsing, for process water, retentate and permeate.

layers resulting from permeate at 25°C and process water at 25°C as well as 50°C.

The adsorption kinetics of the retentate can be linked to the bulk effect [119], a common phenomenon that occurs in QCM-D when studying solutions at high concentration. In addition to this phenomenon, colloidal droplets could cause the observed formation of a heavy soft layer. Close to the surface, the colloidal droplets repel each due to the charge on the hemicelluloses attached to their shells [120], but they would still be detected by the QCM-D instrument. Furthermore, the higher average molecular weight and concentration of compounds in the retentate could mean that relatively more mass adsorbs on the model membrane per attached compound (larger colloidal droplets and hemicellulose polymers).

5.2.2 Desorption of fouling from thermomechanical pulping process water by rinsing

As soon as Milli-Q water was introduced into the system, the frequency curves for all three solutions increased to a similar level, but the permeate curves continued to increase slowly with time. The dissipation decreased immediately at the beginning of rinsing, and all the curves showed similar levels (rinsing in Figure 5.4). This implies that all the solutions caused reversible fouling, which was only weakly attached, as well as irreversible fouling in the form of a thin rigid layer. A clear picture of the effects of reversible and irreversible fouling can be obtained by comparing the frequency and dissipation before and after rinsing, as shown in Figure 5.6.

Assuming that colloidal droplets also adsorb during fouling besides GGM, the lower concentration of polysaccharides resulting from rinsing could cause destabilization of the adsorbed colloidal droplets [121]. This means that the colloidal droplets open up

Table 5.1 Adsorbed mass of the studied solutions estimated with the Broadfit function in the software Dfind (Q-Sense, Sweden)

Solution	Adsorbed mass after fouling (mg/m^2)	Adsorbed mass after rinsing (mg/m^2)	Mass remaining on the surface (% total adsorbed mass)
Process water	16.4 ±5.3	9.3 ±2.1	58.8 ±6.5
Retentate	39.6 ±4.8	9.0 ±2.5	22.6 ±5.4
Permeate	13.8 ±1.9	6.4 ±0.8	46.9 ±6.0

and disintegrate and only compounds highly attracted by the GGM of the fouling layer remain attached. The strong bonds between the GGM in the outer layer of the colloidal droplets and the carboxyl groups of the fatty acids and resin acids could remain intact despite rinsing. If this group of extractives remained adsorbed, it would explain why Puro et al. [7] found more fatty acids and resin acids than lignans, sterols, steryl esters, and triglycerides in the fouling layers of polyethersulfone membranes after UF of process water and subsequent rinsing.

When comparing the mass of the fouling layers caused by the three solutions, fouling by permeate and process water had similar masses, while the mass after fouling with retentate was higher (Table 5.1). After rinsing with Milli-Q water, almost the same mass remained adsorbed on the model membrane surface for all three solutions. The adsorbed mass after rinsing estimated in this work was much less than the values reported by Weis et al. [122] and Thuvander et al. [78], who both determined the mass of the fouling layer after UF of similar solutions. In fact, the mass estimated in the present work is likely to be even lower, as QCM-D also includes hydro-dynamically coupled water in the mass. Weis et al. [122] investigated the adsorptive fouling of polysulfone and polyethersulfone membranes after UF of spent sulfite liquor and subsequent cleaning. The remaining fouling consisted mainly of extractives, with a mass of 24.4 mg/m^2 (PSU membrane) and 38.6 mg/m^2 (PES membrane). Thuvander et al. [78] determined the amount of polysaccharides by acid hydrolysis of the fouling layer of UFX5-pHt membranes after UF of thermomechanical pulping process water and MF permeate, and subsequent alkaline cleaning. Hydrolyzed monosaccharides were detected using high-performance anion-exchange chromatography. The total amount of saccharides found on the membranes was 508 mg/m^2 (process water) and 37 mg/m^2 (MF permeate).

Two factors should be considered when evaluating the differences between the estimates of the fouling layer mass reported in Paper IV and the mass of fouling layers reported in previous studies [78, 122]. Firstly, the forced convective transport during UF means that more material accumulates at the membrane surface than in the QCM-D experiments, where the transport to the surface takes place solely by dif-

fusion. Secondly, in the estimates using QCM-D, it is assumed that foulants are adsorbed homogeneously over the model membrane. This is probably a simplification, and if less material is adsorbed at the edge of the sensor than at the center, the calculated average mass of the adsorbed fouling layer per unit area will be underestimated.

5.3 Final remarks on membrane fouling caused by thermomechanical pulping process water

A schematic illustration of the way in which the fouling layer could be formed is presented in Figure 5.7. Irreversible adsorptive fouling and pore blocking by GGM takes place closest to the membrane surface. Over time, multilayer adsorption causes the build-up of reversible fouling in the form of a gel layer through the accumulation of more GGM and the embedding of colloidal droplets. The smallest compounds, such as dissolved extractives and small GGM, enter the pores and may be adsorbed on the pore walls.

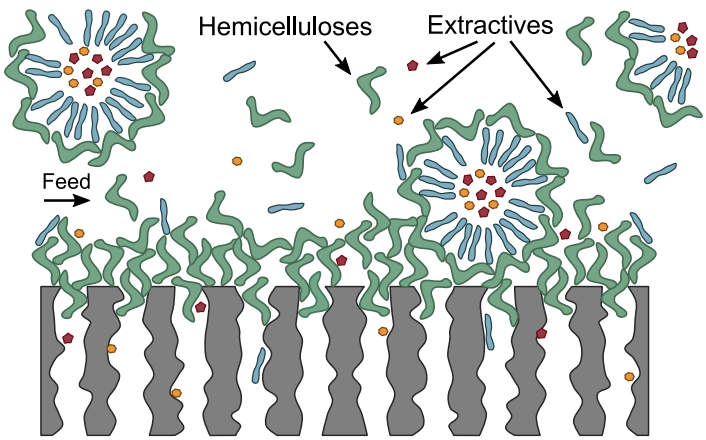

Figure 5.7 Illustration of membrane fouling during cross-flow filtration of thermomechanical pulping process water.

It was shown in this work that adsorption occurs as soon as process water comes into contact with the membrane polymer. A thin rigid layer of fouling that is irreversible is formed, with a thicker and softer layer on top of this, which is reversible. Water is lost over time, and more is lost at a higher temperature, but it reassembles incorporating colloidal droplets, leading to a denser fouling layer.

Based on the findings from the three fractions of process water investigated, is it likely that hemicelluloses and other smaller compounds that were able to pass through the

MF membrane caused the fouling. It can be speculated whether colloidal droplets are also embedded in the fouling layer. They could have become adsorbed on the polymer, as well as on GGM already adsorbed by hydrophobic, van der Waals, or electrostatic interactions [120]. Rinsing with water would destabilize them, leaving only fatty acids and resin acids behind.

Additional analysis supported the findings of the QCM-D adsorption studies. The CAs after fouling and subsequent rinsing with Milli-Q water were similar for the three solutions, and were in the range of 42°–56°. Thus, they were lower than the CA of the spin-coated polysulfone film. The transformation to a slightly more hydrophilic surface supports the hypothesis that hydrophilic GGMs remain adsorbed on the polymer film after rinsing. The results of analysis of fouled membranes using ATR-FTIR (Papers III and V) on fouled membranes support the theory of hemicelluloses as the main foulant in this process.

The flux analysis presented in Section 4.1 indicates pore blocking or gel formation as the main reason for flux decline, while the adsorption studies with QCM-D support the theory of cake or gel formation, as rinsing removed a significant part of the fouling layer. The later can also be linked to the findings of BET analysis that also indicate the formation of a cake or gel layer for cross-flow filtration (Papers III and V). The strong tendency of compounds to adsorb on the polymer film suggests additionally adsorptive fouling on the membrane surface or pore blocking at the pore entrance.

6 Membrane Cleaning following Fouling by Thermomechanical Pulping Process Water

Common membrane cleaning strategies were briefly described in Section 2.4. Alkaline and enzymatic cleaning of UFX5-pHt membranes fouled with thermomechanical pulping process water (Paper II) and alkaline cleaning of ES404 membranes fouled with bleach plant effluent from sulfite pulping (Paper VI) were investigated in this work. The findings presented in (Paper II) are discussed in this chapter, together with those from an additional study on acidic cleaning of UFX5-pHt membranes fouled with thermomechanical pulping process water by our group [123] (see Figure A.4 in the Appendix). This chapter starts with a brief general note on membrane conditioning in 6.1. The impact of alkaline membrane cleaning on the fouling layer is discussed in Section 6.2, followed by a brief discourse on acidic cleaning and its impact on the fouling layer in Section 6.3. The possibility of enzymatic cleaning of the membranes is discussed in Section 6.4.

6.1 Conditioning

Membrane cleaning is often evaluated by comparing the pure water flux, or permeability, of the membrane after fouling and rinsing, to its pure water flux after cleaning. In general, membrane cleaning is considered successful if 80–95% of the membrane permeability is recovered [124]. However, the most important parameter in a membrane process is the production flux, and membrane cleaning can thus be regarded as being successful when this is recovered [41]. A substantial increase in permeability,

well above 100% of the initial membrane permeability, indicates that the membrane has been physically damaged during cleaning. A slight increase in permeability could indicate that the permeability of the pristine membrane was incorrectly determined. New membranes are usually conditioned before use to remove storage chemicals. This is typically done by alkaline cleaning. If conditioning is inadequate, chemicals will remain in the membrane [125], and the measured permeability of the pristine membrane will be too low. During filtration, the remaining storage chemicals will be flushed out, and effective membrane cleaning will result in a higher permeability than the initial one. For this reason, membrane cleaning should not only be evaluated based on permeability. Instead, it is recommended that the success of cleaning be confirmed using *ex situ* or *in situ* methods, even if this is difficult due to the often low amount of foulants on the membrane surface or in the pores after cleaning [41].

6.2 Alkaline cleaning

It has been shown that UF of thermomechanical pulping process water leads to severe membrane fouling, mainly by organic compounds such as GGM and extractives. Alkaline cleaning is the most suitable cleaning strategy for this kind of fouling, which is why it was investigated using NaOH dissolved in deionized water, or the commercial alkaline cleaning agent Ultrasil 10. Ultrasil 10 consists mainly of NaOH, together with tensides and surfactants. The concentration of NaOH in both cleaning agents was adjusted so as to be the same.

The membrane permeability after fouling in dead-end mode at 70°C and 2 bar TMP, and after subsequent alkaline cleaning is shown in Figure 6.1. Cleaning with NaOH alone was not sufficient, as the permeability was about 45% of the initial value after one cleaning cycle. A second cleaning cycle with NaOH led to a slight increase in the permeability, but not to a satisfactory level. In contrast to cleaning with NaOH, a single cleaning cycle with Ultrasil 10 led to a permeability of roughly 110%, and a second cleaning cycle with Ultrasil 10 increased the permeability even more (roughly 130%). This increase in permeability was probably the result of insufficient membrane conditioning, as lab experiments revealed that the storage chemicals were only completely removed after five conditioning steps with a concentration of 0.5% Ultrasil 10 [126]. Conditioning was only performed once per membrane in the present work, using a higher concentration of Ultrasil 10 (1%). A reason why cleaning with Ultrasil 10 was significantly better than with NaOH alone is probably the presence of surfactants and chelating compounds in this cleaning agent. Maartens et al. [52] investigated various strategies for cleaning UF membranes fouled with process streams from pulp and paper making, and described the same positive influence of surfactants on the cleaning efficiency of the alkaline cleaning as that reported in Paper II.

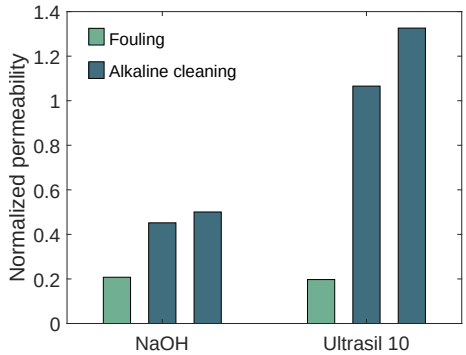

Figure 6.1 Permeability normalized to the value for the pristine membrane after fouling with thermomechanical pulping process water and subsequent cleaning with either NaOH or Ultrasil 10.

Analysis of the membrane surface with SEM revealed that despite complete recovery of the permeability, fouling was still present on the membrane surface (Figure 6.2). However, ATR-FTIR analysis indicated that almost all the fouling was removed after cleaning with Ultrasil 10. The ATR-FTIR spectrum of the cleaned membrane corresponds well with that of the pristine membrane, but a peak is still visible at a wavenumber of 1728 cm^{-1} (Figure 6.3). This peak can be ascribed to stretching of the C=O bonds of the acetyl groups in hemicelluloses [110, 127, 128]), which indicates that hemicelluloses are still present on the membrane after alkaline cleaning with Ultrasil 10. Thuvander et al. [78] analyzed the ratio of the three monosaccharides galactose:glucose:mannose in the fouling layer remaining after UF of thermomechanical pulping process water and subsequent alkaline cleaning with Ultrasil 10. They found significantly lower amounts of galactose and mannose than in the dominant type of hemicelluloses in the process water, which is GGM. This indicated that a polysaccharide other than GGM could have been adsorbed on the membrane, and they suggested that glucan caused the detected fouling. However, it is more likely that galactose and mannose are most easily removed from the fouling layer during alkaline cleaning due to alkaline hydrolysis of the glycosidic linkages in the backbone of GGM and by peeling reactions [33]. This may result in acetylated glucose remaining adsorbed on the membrane, which is also supported by the observations of Thuvander et al. [78].

6.3 Acidic cleaning

In a study related to the work described in this thesis [123], acidic cleaning of UFX5-pHt membranes fouled with MF permeate from thermomechanical pulping

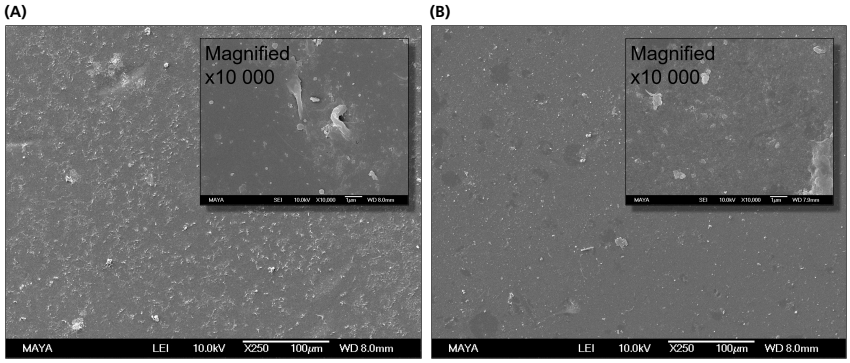

Figure 6.2 SEM images of UFX5-pHt membranes fouled with thermomechanical pulping process water and cleaned with NaOH **(A)** and Ultrasil 10 **(B)**.

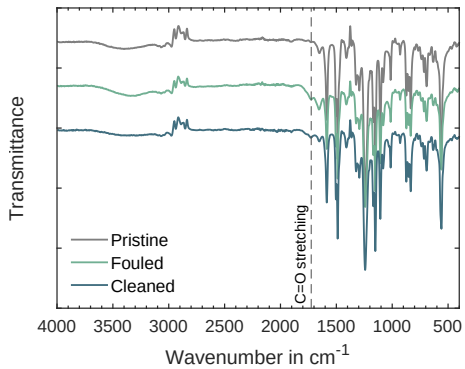

Figure 6.3 ATR-FTIR spectra of a pristine UFX5-pHt membrane, a membrane fouled with thermomechanical pulping process water and a fouled membrane after two-times cleaning with Ultrasil 10.

process water was investigated. Acidic cleaning was conducted under the same conditions as alkaline cleaning but with a 2% solution of Ultrasil 75 (Ecolab, Germany). This cleaning agent contains phosphoric acid and nitric acid. Figure 6.4 shows the change in permeability after fouling with MF permeate and cleaning with the acidic agent followed by Ultrasil 10, or vice versa. It is clear that acidic cleaning did not improve the membrane permeability significantly, regardless of whether it was performed before or after alkaline cleaning. This trend was also observed by Thuvander et al. [78], who investigated acidic cleaning with the same cleaning agent at a concentration of 0.5% Ultrasil 75 after UF of thermomechanical pulping process water. Acidic cleaning was not successful, because inorganic fouling was probably not a major problem in this application. When acidic cleaning was performed as the second and final step, the permeability was slightly reduced. This is in line with the common recommendation to conclude cleaning of polysulfone membranes with an alkaline

agent, as this affords a negative charge to the functional groups on the surface of the membrane, which usually results in the highest permeability [41]. Acidic cleaning was therefore not further investigated.

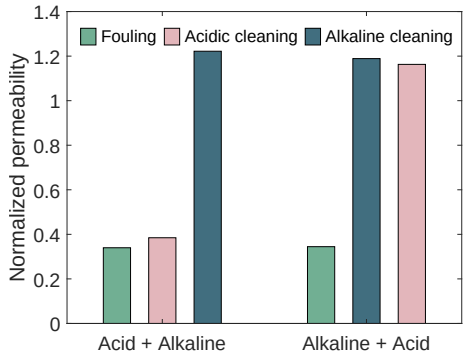

Figure 6.4 Permeability normalized to the pristine value of the membrane after fouling with thermomechanical pulping process water and either subsequent acidc cleaning followed by alkaline cleaning with Ultrasil 10 or alkaline cleaning with Ultrasil 10 followed acidic cleaning.

Even though the MF permeate of thermomechanical pulping process water was investigated in the supplementary study [123], while sieved thermomechanical pulping process water was used in the study described in Paper II, the fouling behavior was similar and can thus be compared (see MF permeate and process water in Figure 5.4 and Paper IV).

6.4 Enzymatic cleaning

Enzymatic cleaning was investigated as an environmentally sound alternative for membrane cleaning following fouling by UF of thermomechanical pulping process water (Paper II). The enzyme cocktail was designed to remove the most important foulants in the system, i.e., enzymatic hydrolysis of the dominant hemicellulose GGM, as well as lipids and the carboxylic ester bonds of extractives.

The permeability of UFX5-pHt membranes after fouling with thermomechanical pulping process water, cleaning with the enzyme cocktail only, and after subsequent alkaline cleaning with either NaOH or Ultrasil 10, is presented in Figure 6.5. The results show that a single cycle of enzymatic cleaning was not sufficient to recover the permeability of the membrane. In fact, the permeability was reduced after enzymatic cleaning. This is probably due to the adsorption of enzymes on the membrane surface, and perhaps also on the fouling layer. The permeability was fully recovered only after alkaline cleaning with Ultrasil 10. These findings are in accordance with those reported by Maartens et al. [52], who described similar observations on enzymatic

cleaning of UF membranes fouled with process water from pulp and paper making. However, ATR-FTIR analysis indicated that cleaning with the enzyme cocktail had a positive effect. Figure 6.6 shows the ATR-FTIR spectra from a pristine membrane, a fouled membrane, and a membrane cleaned enzymatically and subsequently with Ultrasil 10. It can be seen that the peak at 1728 cm^{-1}, pointing to the presence of hemicelluloses on the membrane, was absent after enzymatic cleaning followed by alkaline cleaning. This is promising, in comparison to two-cycle alkaline cleaning with Ultrasil 10 as it suggests that the combination of enzymatic cleaning and Ultrasil 10 removes hemicelluloses from the membrane surface.

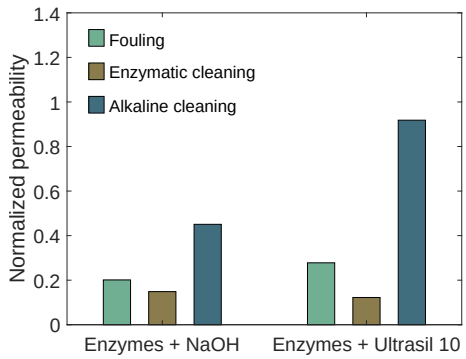

Figure 6.5 Permeability normalized to the value for the pristine membrane after fouling with thermomechanical pulping process water and subsequent cleaning with either the enzyme cocktail and NaOH or the enzyme cocktail and Ultrasil 10.

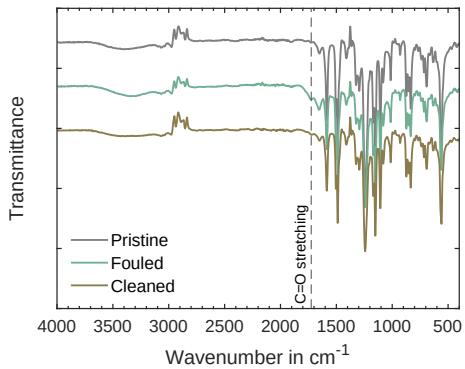

Figure 6.6 ATR-FTIR spectra from a pristine UFX5-pHt membrane, a membrane fouled with thermomechanical pulping process water and a fouled membrane after enzymatic cleaning followed by alkaline cleaning with Ultrasil 10.

The positive effect of enzymatic cleaning was even more clearly shown in a multi-cycle study, where the same membrane was repeatedly fouled and cleaned. The membrane permeability after the various fouling and cleaning steps is presented in Figure 6.7. The membrane was cleaned twice with Ultrasil 10 after the first, second and fourth

fouling cycle. After the third fouling cycle, the membrane was cleaned with the enzyme cocktail and thereafter with Ultrasil 10. It can be seen that repeated UF of thermomechanical pulping process water led to severe fouling, despite successful cleaning after the first UF cycle. However, in contrast to the results found after one cycle of fouling and cleaning (Figure 6.5), in this multi-cycle study, enzymatic cleaning resulted in an increase in membrane permeability. Subsequent alkaline cleaning resulted in a higher permeability than after cleaning in the second cycle. Despite this, the membrane was so severely fouled in the last cycle that the study had to be stopped. The positive effect of enzymatic cleaning is further proof that the adsorption of hemicelluloses is an important reason for the flux decline observed in this system.

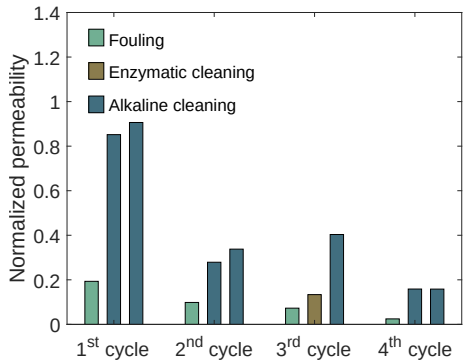

Figure 6.7 Normalized permeability after fouling with thermomechanical pulping process water and subsequent cleaning. The same membrane sample was used throughout the experiment.

In addition to measurements of the permeability and ATR-FTIR analysis, the CA of the membrane was measured and SEM-EDS analysis was performed. The CA measurements showed that the hydrophobicity of the membrane surface was significantly higher after the multi-cycle study than initially, which indicates the adsorption of hydrophobic extractives on the membrane surface. The problem of membrane fouling resulting from the adsorption of extractives during UF of process water from pulp and paper making has been pointed out previously [7, 37]. The results of the SEM-EDS analysis are presented in Figure 6.8A, which shows an image of the surface of the membrane, and in Figure 6.8B, which shows the corresponding spectra. Particles of various sizes can be seen on the membrane surface, despite the fact that the membrane had been cleaned. It is not surprising that the permeability of this membrane is very low compared to the membrane cleaned tow times with alkaline (Figure 6.2) and the pristine membrane (Figure 2.2B). EDS analysis revealed only small amounts of inorganic compounds, although iron and copper were found. Both could originate from the quick connection coupling that connects the nitrogen supply to the module providing the TMP. It is made of alloy containing iron and might have contaminated the sample during the relatively long duration of the multi-cycle study. Silicon is ex-

pected as it is a common element in wood, and gold and platinum originate from the sputter coating for SEM imaging, while sulfur originates from the polysulfone of the membrane. It is therefore clear from the EDS analysis why acidic cleaning was not successful in this case, as there was no notable fouling by inorganic compounds.

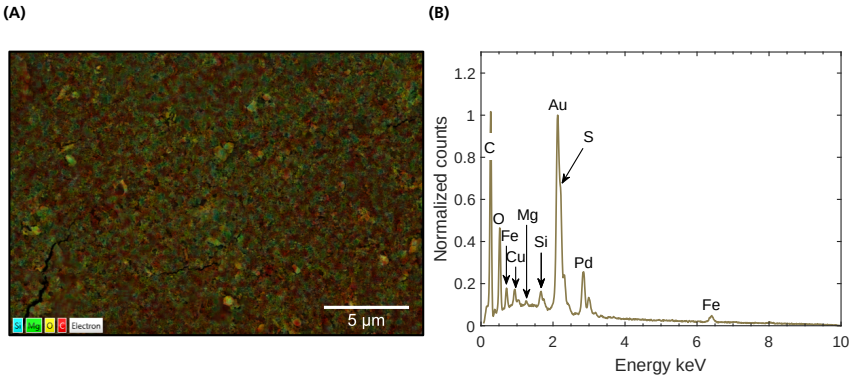

Figure 6.8 SEM-EDS image **(A)**, and spectrum **(B)** from a UFX5-pHt membrane alternately fouled with thermomechanical pulping process water and cleaned with Ultrasil 10 or the enzyme cocktail (see Figure 6.7). (Unpublished data.)

6.5 Final remarks on membrane cleaning after fouling with thermomechanical pulping process water

Membrane fouling after UF of thermomechanical pulping process water is a serious problem, and it is thus important to find a suitable cleaning strategy.

In terms of permeability recovery, it was found that alkaline cleaning with a commercial alkaline cleaning agent containing surfactants and chelating agents, such as Ultrasil 10, was best. However, *ex situ* analysis with several techniques showed that some foulants still remained on the membrane, despite the complete recovery of the permeability. This was not problematic when one cycle of fouling and cleaning was performed, but when several cycles of fouling and cleaning were performed using the same membrane, compounds accumulated on the membrane, and the permeability successively decreased. ATR-FTIR analysis together with CA measurements suggest that this was due to hemicelluloses and extractives.

Acidic cleaning was not found to be a useful cleaning strategy in this membrane process.

The more environmentally sound approach of enzymatic cleaning was found not to be effective in terms of permeability recovery when one cycle of fouling and cleaning

was performed. The membrane permeability was actually reduced when enzymatic cleaning was performed without a subsequent alkaline cleaning step. However, *ex situ* analysis indicated that enzymatic cleaning reduced the amount of polysaccharides on the membrane. Despite the fact that this had no positive effect on the permeability recovery in the single-cycle experiments, a remarkable effect was seen after enzymatic cleaning during a multi-cycle fouling and cleaning study.

It was therefore concluded that a combination of alkaline cleaning with an agent containing NaOH, surfactants and chelating agents, and enzymatic cleaning is likely to be the best approach for cleaning UF membranes following the filtration of thermomechanical pulping process water.

7 Conclusions and Future Perspectives

7.1 Conclusions

Membrane fouling and cleaning in membrane processes in lignocellulosic biorefineries have been investigated with *ex situ* and *in situ* analytical methods. Valuable insights were gained using imaging techniques such as SEM in combination with EDS. Surface roughness measurements with AFM provided further important information. CA measurements were made in most of the studies, but were found to be error-prone. ATR-FTIR has been shown to be a fast and easy method for the chemical analysis of membrane fouling and cleaning results. Information was obtained on the distribution of fouling on and in membranes using BET surface analysis, which has to date rarely been used to investigate the impact of fouling on the inner structure of membranes.

It was found that *in situ* real-time monitoring of membranes has considerable potential to deepen our knowledge on the underlying processes leading to membrane fouling and influencing membrane cleaning. QCM-D was identified as an especially promising method for the monitoring of early-stage adsorptive membrane fouling in lignocellulosic biorefineries. However, an appropriate model system is required for the successful application of QCM-D.

Most of the work presented focuses on membrane fouling of UFX5-pHt membranes by UF of thermomechanical pulping process water. The development, structure and composition of the fouling layer formed during this process were analyzed in detail. It was found that GGM together with colloidal droplets were the main causes of membrane fouling in this process. Fouling was caused by both adsorption and pore blocking. GGM is immediately adsorbed on the membrane surface, creating a thin, rigid layer. Colloid droplets then accumulate, making this layer thicker and softer.

Rinsing can remove some of the fouling, but a very thin and very rigid layer remained attached to the membrane surface as irreversible fouling. *Ex situ* analysis showed that this layer was mostly comprised of GGM and residues of extractives. Based on the results of BET analysis, it was possible to determine that the foulants also penetrate the membrane, causing a change in its inner structure. Although temperature affected the flux, no notable impact was detected on the change of the inner structure by fouling at different temperatures. The same observations were made for the TMP and CFV. However, at elevated temperatures, compaction of the fouling layer was observed over time.

Investigations on membrane fouling during UF of other relevant process solutions from lignocellulosic biorefineries identified lignin, extractives, and magnesium hydroxide as the main foulants, thus highlighting the need for cleaning strategies tailored to each individual process.

Various membrane cleaning strategies were investigated. For the reference system, it was found that cleaning with the alkaline agent Ultrasil 10 gave the best results for membranes fouled by one cycle of UF of thermomechanical pulping process water. The efficacy of a home-made enzyme cocktail was investigated as an alternative cleaning agent. When subjecting the membrane to several fouling and cleaning cycles, the combination of enzymatic cleaning followed by alkaline cleaning with Ultrasil 10 was found to give the best results in terms of the recovery of the membrane permeability. *Ex situ* analysis with ATR-FTIR showed that especially GGM seem to accumulate on the membrane when cleaned only with Ultrasil 10. However, they were successfully removed by enzymatic cleaning.

Thorough investigations of membrane fouling and membrane cleaning with *ex situ* methods in combination with *in situ* real-time monitoring techniques such as QCM-D, have led to an improved understanding of the composition, structure, and development over time of the fouling layer, enabling improvements in cleaning strategy. In particular, *in situ* real-time monitoring of membrane fouling and cleaning can assist in the optimization of membrane processes in lignocellulosic biorefineries. Based on the findings from real-time monitoring studies, operational parameters such as the timing and duration of flushing and membrane cleaning, or the most suitable type and concentration of cleaning agent, can be tailored. This will lead to prolonged membrane lifetime, a reduction in plant downtime, and a reduction in the amount of chemicals and water used, ultimately resulting in lower process costs, and promoting the wider application of membrane separation processes. The findings of this work will support the transition from the current fossil-based economy towards a bio-based circular economy.

7.2 Future perspectives

Fouling in the inner membrane structure should be investigated further to confirm the present BET analysis findings. However, this is challenging as the pores in UF membranes are on the nanometer scale. A promising approach would be to use synchrotron-radiation-based techniques such as small-angle X-ray scattering (SAXS) and X-ray computed nanotomography, or the combination of both as in X-ray ptychography, as these techniques provide sufficiently high resolution. Some initial studies have already been performed on membrane manufacturing, membrane aging by cleaning, and membrane fouling, but mainly with mCT [129–131]. Synchrotron X-ray nanotomography could be combined with image analysis to determine the pore size and volume distribution in the membrane, and thus the influence of membrane fouling and cleaning.

Furthermore, it would be interesting to monitor the adsorption of each individual foulant (GGM, colloidal droplets, lignin). The challenges in this lie in the extraction of GGM and lignin from the process streams and on the creation of model colloidal droplets. The creation of model droplets of colloidal extractives stabilized by GGM is the most difficult, but could be inspired by the work of [132] who created such model colloidal droplets. Moreover, QCM-D also detects water in the adsorbed layer, and it should be combined with other techniques, such as ellipsometry or surface plasmon resonance spectroscopy, to take the water into account. It may also be possible to investigate the effects of cleaning on the structure of the fouling layer *in situ* using liquid-state AFM.

Having obtained information in the ways outlined above, it would be easier to optimize membrane cleaning in a structured way. The impact of cleaning agent concentration, cleaning duration, and cleaning temperature could be investigated using a response surface methodology. If these cleaning parameters could be optimized, the next step would be to improve rinsing by optimizing the rinsing duration and water consumption, all of which are cost drivers and major factors for a resource-efficient process.

In situ monitoring should be more widely applied in the field of membrane science and technology. This can be achieved by supporting and increasing the exchange of knowledge and information between industrial membrane users, instrument suppliers, and membrane scientists. Figure 7.1 shows the techniques available for the determination of the thickness and chemical composition of fouling layers on different scales. It is clear that tools are needed to monitor the chemical composition of fouling on all scales, but especially on the industrial scale. Raman spectroscopy may prove useful for this, as shown recently [76, 133].

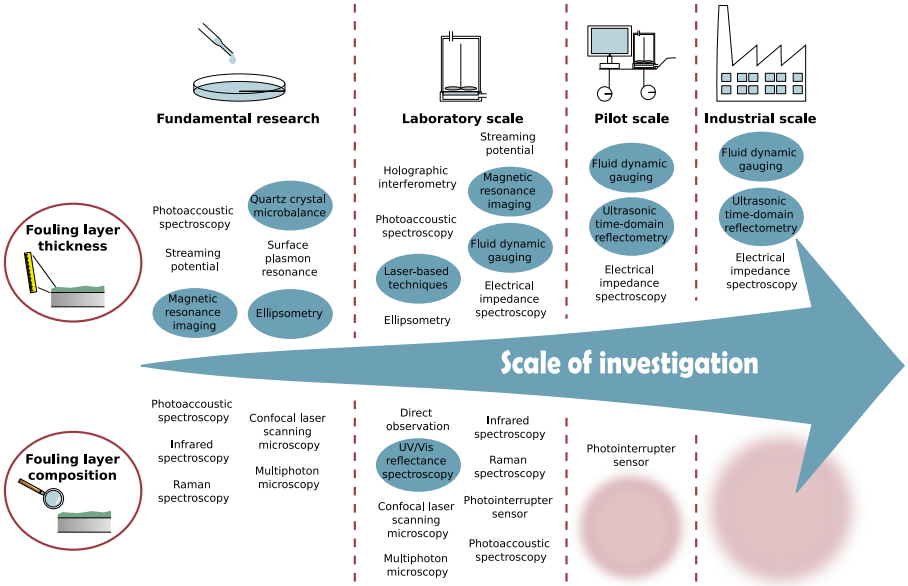

Figure 7.1 Overview of suitable techniques for ***in situ*** real-time monitoring of membrane fouling. The techniques identified as having the greatest potential for commercial application are highlighted in blue. (Figure adapted from [53].)

The ultimate goal is to improve the industrial application of membrane processes. This could be achieved by developing monitoring tools to predict the best time for membrane cleaning and, based on the feed solution and process setup, the best cleaning procedure for the separation task.

References

[1] P. Axegård. The future pulp mill –a biorefinery? Presentation at the 1st International BiorefineryWorkshop, 20-21.07.2005.

[2] J. H. Clark and F. E. I. Deswarte. *Introduction to chemicals from biomass*. Wiley series in renewable resources. Wiley, Chichester, reprint edition, 2009.

[3] D. S. Sholl and R. P. Lively. Seven chemical separations to change the world. *Nature*, 532(7600):435–437, 2016.

[4] F. Lipnizki, J. Thuvander, and G. Rudolph. Membrane processes and applications for biorefineries. In A. Figoli, Y. Li, and A. Basile, editors, *Current trends and future developments on (bio-) membranes*, pages 283–301. Elsevier B.V., Amsterdam, Netherlands, 2020.

[5] J. Thuvander, F. Lipnizki, and A.-S. Jönsson. On-site recovery of hemicelluloses from thermomechanical pulp mill process water by microfiltration and ultrafiltration. *Journal of Wood Chemistry and Technology*, 39(3):214–223, 2019.

[6] M. M. Dal-Cin, F. McLellan, C. N. Striez, C. M. Tam, T. A. Tweddle, and A. Kumar. Membrane performance with a pulp mill effluent: Relative contributions of fouling mechanisms. *Journal of Membrane Science*, 120(2):273–285, 1996.

[7] L. Puro, M. Kallioinen, M. Mänttäri, and M. Nyström. Evaluation of behavior and fouling potential of wood extractives in ultrafiltration of pulp and paper mill process water. *Journal of Membrane Science*, 368(1-2):150–158, 2011.

[8] B. Al-Rudainy, M. Galbe, and O. Wallberg. From lab-scale to on-site pilot trials for the recovery of hemicellulose by ultrafiltration: Experimental and theoretical evaluations. *Separation and Purification Technology*, 250:117187, 2020.

[9] A.-K. Nordin and A.-S. Jönsson. Case study of an ultrafiltration plant treating bleach plant effluent from a pulp and paper mill. *Desalination*, 201(1-3):277–289, 2006.

[10] O. Wallberg, A.-S. Jönsson, and R. Wimmerstedt. Fractionation and concentration of Kraft black liquor lignin with ultrafiltration. *Desalination*, 154(2):187–199, 2003.

[11] W. J. Koros, Y. H. Ma, and T. Shimidzu. Terminology for membranes and membrane processes (IUPAC Recommendation 1996). *Journal of Membrane Science*, 120(2):149–159, 1996.

[12] E. Drioli and L. Giorno, editors. *Encyclopedia of membranes*. Springer, Berlin, Heidelberg, 2016.

[13] W. Eykamp. Chapter 1 Microfiltration and ultrafiltration. In R. D. Noble and S. A. Stern, editors, *Membrane separations technology*, volume 2 of *Membrane science and technology*, pages 1–43. Elsevier B.V., 1995.

[14] B. Tanhaei, M. P. Chenar, N. Saghatoleslami, M. Hesampour, T. Laakso, M. Kallioinen, M. Sillanpää, and M. Mänttäri. Simultaneous removal of aniline and nickel from water by micellar-enhanced ultrafiltration with different molecular weight cut-off membranes. *Separation and Purification Technology*, 124:26–35, 2014.

[15] P. Aimar and V. Sanchez. A novel approach to transfer-limiting phenomena during ultrafiltration of macromolecules. *Industrial & Engineering Chemistry Fundamentals*, 25(4):789–798, 1986.

[16] R. W. Field, D. Wu, J. A. Howell, and B. B. Gupta. Critical flux concept for microfiltration fouling. *Journal of Membrane Science*, 100(3):259–272, 1995.

[17] J. Hermia. Blocking Filtration. Application to non-Newtonian fluids. In A. Rushton, editor, *Mathematical models and design methods in solid-liquid separation*, NATO ASI Series (Series E: Applied Sciences), pages 83–89. Martinus Nijhoff Publishers, Dordrecht, 1985.

[18] M. C. V. Vela, S. Á. Blanco, J. L. García, and E. B. Rodríguez. Analysis of membrane pore blocking models applied to the ultrafiltration of PEG. *Separation and Purification Technology*, 62(3):489–498, 2008.

[19] J. Sundholm. *Mechanical pulping*. Papermaking Science and Technology Series. TAPPI, Finnish Paper Engineers' Association, Helsinki, 1999.

[20] J. Thornton, R. Ekman, B. Holmbom, and F. Örså. Polysaccharides dissolved from Norway spruce in thermomechanical pulping and peroxide bleaching. *Journal of Wood Chemistry and Technology*, 14(2):159–175, 1994.

[21] M. Rundlöf, A.-K. Sjölund, H. Ström, and I. Åsell. The effect of dissolved and colloidal substances released from TMP on the properties of TMP fines. *Nordic Pulp & Paper Research Journal*, 15(4):256–265, 2000.

[22] Y. He, D. M. Bagley, K. T. Leung, S. N. Liss, and B.-Q. Liao. Recent advances in membrane technologies for biorefining and bioenergy production. *Biotechnology Advances*, 30(4):817–858, 2012.

[23] H. Li and V. Chen. Membrane fouling and cleaning in food and bioprocessing. In Z. F. Cui and H. S. Muralidhara, editors, *Membrane technology*, pages 213–254. Elsevier B.V., Amsterdam, 2010.

[24] A. Sluiter, B. Hames, R. Ruiz, C. Scarlata, J. Sluiter, and D. Templeton. Determination of sugars, byproducts, and degradation products in liquid fraction process samples: Laboratory Analytical Procedure (LAP): revised January 2008.

[25] A. Sluiter, B. Hames, R. Ruiz, C. Scarlata, J. Sluiter, D. Templeton, and D. Crocker. Determination of structural carbohydrates and lignin in biomass: Laboratory Analytical Procedure (LAP): revised July 2011.

[26] E. Sjöström. *Wood chemistry: Fundamentals and applications*. Academic Press, San Diego, 2nd ed. edition, 1993.

[27] A. Sundheq, K. Sundherg, C. Lillandt, and B. Holmhom. Determination of hemicelluloses and pectins in wood and pulp fibres by acid methanolysis and gas chromatography. *Nordic Pulp & Paper Research Journal*, 11(4):216–219, 1996.

[28] S. Willför, R. Sjöholm, C. Laine, and B. Holmbom. Structural features of water-soluble arabinogalactans from Norway spruce and Scots pine heartwood. *Wood Science and Technology*, 36(2):101–110, 2002.

[29] S. Willför, R. Sjöholm, C. Laine, M. Roslund, J. Hemming, and B. Holmbom. Characterisation of water-soluble galactoglucomannans from Norway spruce wood and thermomechanical pulp. *Carbohydrate Polymers*, 52(2):175–187, 2003.

[30] T. E. Timell. Recent progress in the chemistry of wood hemicelluloses. *Wood Science and Technology*, 1(1):45–70, 1967.

[31] J. Lundqvist, A. Teleman, L. Junel, G. Zacchi, O. Dahlman, F. Tjerneld, and H. Stålbrand. Isolation and characterization of galactoglucomannan from spruce (Picea abies). *Carbohydrate Polymers*, 48(1):29–39, 2002.

[32] H. Krawczyk and A.-S. Jönsson. Separation of dispersed substances and galactoglucomannan in thermomechanical pulp process water by microfiltration. *Separation and Purification Technology*, 79(1):43–49, 2011.

[33] J. Berglund, S. Azhar, M. Lawoko, M. Lindström, F. Vilaplana, J. Wohlert, and G. Henriksson. The structure of galactoglucomannan impacts the degradation under alkaline conditions. *Cellulose*, 26(3):2155–2175, 2019.

[34] T. Hannuksela and C. Hervé du Penhoat. NMR structural determination of dissolved O-acetylated galactoglucomannan isolated from spruce thermomechanical pulp. *Carbohydrate research*, 339(2):301–312, 2004.

[35] J. Nylund, K. Sundberg, Q. Shen, and J. B. Rosenholm. Determination of surface energy and wettability of wood resins. *Colloids and Surfaces A: Physicochemical and Engineering Aspects*, 133(3):261–268, 1998.

[36] L. H. Allen. Characterization of colloidal wood resin in newsprint pulps. *Colloid and Polymer Science*, 257(5):533–538, 1979.

[37] J. Thuvander and A.-S. Jönsson. Extraction of galactoglucomannan from thermomechanical pulp mill process water by microfiltration and ultrafiltration—Influence of microfiltration membrane pore size on ultrafiltration performance. *Chemical Engineering Research and Design*, 105:171–176, 2016.

[38] M. Lawoko, G. Henriksson, and G. Gellerstedt. Characterisation of lignin-carbohydrate complexes (LCCs) of spruce wood (Picea abies L.) isolated with two methods. *Holzforschung*, 60(2):156–161, 2006.

[39] D. Tarasov, M. Leitch, and P. Fatehi. Lignin-carbohydrate complexes: properties, applications, analyses, and methods of extraction: a review. *Biotechnology for biofuels*, 11:269, 2018.

[40] Sterlitech Corporation. Membrane chemical cleaning: why is it required and how is it performed?, 2017.

[41] G. Trägårdh. Membrane cleaning. *Desalination*, 71(3):325–335, 1989.

[42] P. Xie, C.-F. de Lannoy, J. Ma, and M. R. Wiesner. Chlorination of polyvinyl pyrrolidone–polysulfone membranes: Organic compound release, byproduct formation, and changes in membrane properties. *Journal of Membrane Science*, 489:28–35, 2015.

[43] Z. Wang. Chlorination process. In E. Drioli and L. Giorno, editors, *Encyclopedia of membranes*, pages 400–401. Springer, Berlin, Heidelberg, 2016.

[44] B. Malczewska and A. Żak. Structural changes and operational deterioration of the UF polyethersulfone (pes) membrane due to chemical cleaning. *Scientific Reports*, 9(1):422, 2019.

[45] E. Antón, J. R. Álvarez, L. Palacio, P. Prádanos, A. Hernández, A. Pihlajamäki, and S. Luque. Ageing of polyethersulfone ultrafiltration membranes under long-term exposures to alkaline and acidic cleaning solutions. *Chemical Engineering Science*, 134:178–195, 2015.

[46] M. Rabiller-Baudry, P. Loulergue, J. Girard, El Mansour El Jastimi, M., A. Bouzin, M. Le Gallic, A. Moreac, and P. Rabiller. Consequences of membrane aging on real or misleading evaluation of membrane cleaning by flux measurements. *Separation and Purification Technology*, 259:118044, 2021.

[47] A. Maartens, P. Swart, and E. P. Jacobs. An enzymatic approach to the cleaning of ultrafiltration membranes fouled in abattoir effluent. *Journal of Membrane Science*, 119(1):9–16, 1996.

[48] M. J. Muñoz-Aguado, D. E. Wiley, and A. G. Fane. Enzymatic and detergent cleaning of a polysulfone ultrafiltration membrane fouled with BSA and whey. *Journal of Membrane Science*, 117(1-2):175–187, 1996.

[49] M. Argüello, S. Álvarez, F. A. Riera, and J. R. Álvarez. Enzymatic cleaning of inorganic ultrafiltration membranes used for whey protein fractionation. *Journal of Membrane Science*, 216(1-2):121–134, 2003.

[50] C.-H. Yu, L.-C. Fang, S. K. Lateef, C.-H. Wu, and C.-F. Lin. Enzymatic treatment for controlling irreversible membrane fouling in cross-flow humic acid-fed ultrafiltration. *Journal of hazardous materials*, 177(1-3):1153–1158, 2010.

[51] Y. Li, H. Wang, S. Wang, K. Xiao, and X. Huang. Enzymatic cleaning mitigates polysaccharide-induced refouling of RO membrane: evidence from foulant layer structure and microbial dynamics. *Environmental science & technology*, 2021.

[52] A. Maartens, E.P Jacobs, and P. Swart. UF of pulp and paper effluent: membrane fouling-prevention and cleaning. *Journal of Membrane Science*, 209(1):81–92, 2002.

[53] G. Rudolph, F. Lipnizki, T. Virtanen, and M. Kallioinen. Focus on fouling monitoring. *Filtration + Separation*, 56(3):25–27, 2019.

[54] O. O. Bamigbetan. *A systematic Design Methodology for Multicomponent Membrane Systems*. Dissertation, Norwegian University of Science and Technology, 2015.

[55] C. Ba. *Design of advanced reverse osmosis and nanofiltration membranes for water purification: Design of advanced reverse osmosis and nanofiltration membranes for water purification*. Dissertation, University of Illinois at Urbana-Champaign, 2010.

[56] J. Lindau, A.-S. Jönsson, and R. Wimmerstedt. The influence of a low-molecular hydrophobic solute on the flux of polysulphone ultrafiltration membranes with different cut-off. *Journal of Membrane Science*, 106(1-2):9–16, 1995.

[57] P. Ramamurthy, R. Poole, and J. G. Dorica. Fouling of ultrafiltration membranes during treatment of CTMP screw press filtrates. *Journal of Pulp and Paper Science*, 21(2):50–54, 1995.

[58] C. Jönsson and A.-S. Jönsson. Influence of the membrane material on the adsorptive fouling of ultrafiltration membranes. *Journal of Membrane Science*, 108(1-2):79–87, 1995.

[59] M. Mänttäri, L. Puro, J. Nuortila-Jokinen, and M. Nyström. Fouling effects of polysaccharides and humic acid in nanofiltration. *Journal of Membrane Science*, 165(1):1–17, 2000.

[60] M. Mänttäri and M. Nyström. Critical flux in NF of high molar mass polysaccharides and effluents from the paper industry. *Journal of Membrane Science*, 170(2):257–273, 2000.

[61] L. Puro, J. Tanninen, and M. Nyström. Analyses of organic foulants in membranes fouled by pulp and paper mill effluent using solid-liquid extraction. *Desalination*, 143(1):1–9, 2002.

[62] J. Li. Non-invasive visualization of the fouling of microfiltration membranes by ultrasonic time-domain reflectometry. *Journal of Membrane Science*, 201(1-2):17–29, 2002.

[63] W. R. Bowen, T. A. Doneva, and H. B. Yin. Atomic force microscopy studies of membrane - solute interactions (fouling). *Desalination*, 146(1-3):97–102, 2002.

[64] R. D. Sanderson, J. Li, D. K. Hallbauer, and S. K. Sikder. Fourier wavelets from ultrasonic spectra: a new approach for detecting the onset of fouling during microfiltration of paper mill effluent. *Environmental science & technology*, 39(18):7299–7305, 2005.

[65] L. Puro, M. Kallioinen, M. Mänttäri, G. Natarajan, D. C. Cameron, and M. Nyström. Performance of RC and PES ultrafiltration membranes in filtration of pulp mill process waters. *Desalination*, 264(3):249–255, 2010.

[66] Y. Kaya, Z. B. Gönder, I. Vergili, and H. Barlas. The effect of transmembrane pressure and pH on treatment of paper machine process waters by using a two-step nanofiltration process: Flux decline analysis. *Desalination*, 250(1):150–157, 2010.

[67] Z. B. Gönder, A. Semiha, and B. Hulusi. Advanced treatment of pulp and paper mill wastewater by nanofiltration process: Effects of operating conditions on membrane fouling. *Separation and Purification Technology*, 76(3):292–302, 2011.

[68] H. Lin, B.-Q. Liao, J. Chen, W. Gao, L. Wang, F. Wang, and X. Lu. New insights into membrane fouling in a submerged anaerobic membrane bioreactor based on characterization of cake sludge and bulk sludge. *Bioresource technology*, 102(3):2373–2379, 2011.

[69] E. Koivula, M. Kallioinen, S. Preis, L. Testova, H. Sixta, and M. Mänttäri. Evaluation of various pretreatment methods to manage fouling in ultrafiltration of wood hydrolysates. *Separation and Purification Technology*, 83:50–56, 2011.

[70] E. Negaresh, A. Antony, M. Bassandeh, D. E. Richardson, and G. Leslie. Selective separation of contaminants from paper mill effluent using nanofiltration. *Chemical Engineering Research and Design*, 90(4):576–583, 2012.

[71] Z. B. Gönder, S. Arayici, and H. Barlas. Treatment of pulp and paper mill wastewater using ultrafiltration process: Optimization of the fouling and rejections. *Industrial & Engineering Chemistry Research*, 51(17):6184–6195, 2012.

[72] C. Chen, S. Mao, J. Wang, J. Bao, H. Xu, and Su, W., Dai, H. Application of ultrafiltration in a paper mill: Process water reuse and membrane fouling analysis. *BioResources*, 10(2):2376–2391, 2015.

[73] W. J. Gao, M. N. Han, Chunbao Xu, B. Q. Liao, Y. Hong, J. Cumin, and M. Dagnew. Performance of submerged anaerobic membrane bioreactor for thermomechanical pulping wastewater treatment. *Journal of Water Process Engineering*, 13:70–78, 2016.

[74] M. Haddad, S. Mikhaylin, L. Bazinet, O. Savadogo, and J. Paris. Electrochemical acidification of Kraft black liquor by electrodialysis with bipolar membrane: Ion exchange membrane fouling identification and mechanisms. *Journal of colloid and interface science*, 488:39–47, 2017.

[75] M. Gholami, B. Abbasi Souraki, A. Pendashteh, and B. M. Marzouni. Efficiency evaluation of the membrane/AOPs for paper mill wastewater treatment. *Environmental technology*, 38(9):1127–1138, 2017.

[76] T. Virtanen, S.-P. Reinikainen, M. Kögler, M. Mänttäri, T. Viitala, and M. Kallioinen. Real-time fouling monitoring with Raman spectroscopy. *Journal of Membrane Science*, 525:312–319, 2017.

[77] T. Virtanen, P. Parkkila, A. Koivuniemi, J. Lahti, T. Viitala, M. Kallioinen, M. Mänttäri, and A. Bunker. Characterization of membrane–foulant interactions with novel combination of Raman spectroscopy, surface plasmon resonance and molecular dynamics simulation. *Separation and Purification Technology*, 205:263–272, 2018.

[78] J. Thuvander, A. Zarebska, C. Hélix-Nielsen, and A.-S. Jönsson. Characterization of Irreversible fouling after ultrafiltration of thermomechanical pulp mill process Water. *Journal of Wood Chemistry and Technology*, 38(3):276–285, 2018.

[79] Y. Xu, Y. Li, and Y. Hou. Reducing ultrafiltration membrane fouling during recycled paper mill wastewater treatment using pretreatment technologies: a comparison between coagulation and Fenton. *Journal of Chemical Technology & Biotechnology*, 94(3):804–811, 2018.

[80] M. Zhou, H. Sandström, M.-P. Belioka, T. Pettersson, and T. Mattsson. Investigation of the cohesive strength of membrane fouling layers formed during cross-flow microfiltration: The effects of pH adjustment on the properties and fouling characteristics of microcrystalline cellulose. *Chemical Engineering Research and Design*, 149:52–64, 2019.

[81] T. Virtanen, G. Rudolph, A. Lopatina, B. Al-Rudainy, H. Schagerlöf, L. Puro, M. Kallioinen, and F. Lipnizki. Analysis of membrane fouling by Brunauer-Emmet-Teller nitrogen adsorption/desorption technique. *Scientific Reports*, 10(1):3427, 2020.

[82] A.-S. Jönsson, J. Lindau, R. Wimmerstedt, J. Brinck, and B. Jönsson. Influence of the concentration of a low-molecular organic solute on the flux reduction of a polyethersulphone ultrafiltration membrane. *Journal of Membrane Science*, 135(1):117–128, 1997.

[83] J. Brinck, A.-S. Jönsson, B. Jönsson, and J. Lindau. Influence of pH on the adsorptive fouling of ultrafiltration membranes by fatty acid. *Journal of Membrane Science*, 164(1-2):187–194, 2000.

[84] V. Lindstrand, A.-S. Jönsson, and G. Sundström. Organic fouling of electrodialysis membranes with and without applied voltage. *Desalination*, 130(1):73–84, 2000.

[85] T. Mattsson, W. J. T. Lewis, Y. J. M. Chew, and M. R. Bird. In situ investigation of soft cake fouling layers using fluid dynamic gauging. *Food and Bioproducts Processing*, 93:205–210, 2015.

[86] W. J. T. Lewis, T. Mattsson, Y. J. M. Chew, and M. R. Bird. Investigation of cake fouling and pore blocking phenomena using fluid dynamic gauging and critical flux models. *Journal of Membrane Science*, 533:38–47, 2017.

[87] T. Mattsson, W. J. T. Lewis, Y. J. M. Chew, and M. R. Bird. The use of fluid dynamic gauging in investigating the thickness and cohesive strength of cake fouling layers formed during cross-flow microfiltration. *Separation and Purification Technology*, 198:25–30, 2018.

[88] M. Zhou and T. Mattsson. Effect of crossflow regime on the deposit and cohesive strength of membrane surface fouling layers. *Food and Bioproducts Processing*, 115:185–193, 2019.

[89] G. Diaconu and T. Schäfer. Study of the interactions of proteins with a solid surface using complementary acoustic and optical techniques. *Biointerphases*, 9(2):029015–1–029015–6, 2014.

[90] D. L. Ferrando C., A. Nejidat, and M. Herzberg. Viscoelastic properties of extracellular polymeric substances can strongly affect their washing efficiency from reverse osmosis membranes. *Environmental Science & Technology*, 50(17):9206–9213, 2016.

[91] M. Hashino, K. Hirami, T. Ishigami, Y. Ohmukai, T. Maruyama, N. Kubota, and H. Matsuyama. Effect of kinds of membrane materials on membrane fouling with BSA. *Journal of Membrane Science*, 384(1-2):157–165, 2011.

[92] M. Hashino, K. Hirami, T. Katagiri, N. Kubota, Y. Ohmukai, T. Ishigami, T. Maruyama, and H. Matsuyama. Effects of three natural organic matter types on cellulose acetate butyrate microfiltration membrane fouling. *Journal of Membrane Science*, 379(1-2):233–238, 2011.

[93] J. T. Kim, N. Weber, G. H. Shin, Q. Huang, and S. X. Liu. The study of beta-lactoglobulin adsorption on polyethersulfone thin film surface using QCM-D and AFM. *Journal of Food Science*, 72(4):E214–21, 2007.

[94] S. X. Liu and J.-T. Kim. Application of Kevin–Voigt model in quantifying whey protein adsorption on polyethersulfone using QCM-D. *Journal of the Association for Laboratory Automation*, 14(4):213–220, 2009.

[95] M. Rückel, S. Nied, and G. Schürmann. An experimental approach to explore cleaner systems for desalination membranes. *Desalination and Water Treatment*, 31(1-3):285–290, 2012.

[96] P. Roach, D. Farrar, and C. C. Perry. Interpretation of protein adsorption: Surface-induced conformational changes. *Journal of the American Chemical Society*, 127(22):8168–8173, 2005.

[97] H. Z. Shafi, Z. Khan, R. Yang, and K. K. Gleason. Surface modification of reverse osmosis membranes with zwitterionic coating for improved resistance to fouling. *Desalination*, 362:93–103, 2015.

[98] C. Zhou, J.-M. Friedt, A. Angelova, K.-H. Choi, W. Laureyn, F. Frederix, L. A. Francis, A. Campitelli, Y. Engelborghs, and G. Borghs. Human immunoglobulin adsorption investigated by means of quartz crystal microbalance dissipation, atomic force microscopy, surface acoustic wave, and surface plasmon resonance techniques. *Langmuir*, 20(14):5870–5878, 2004.

[99] W. Ying, N. Siebdrath, W. Uhl, V. Gitis, and M. Herzberg. New insights on early stages of RO membranes fouling during tertiary wastewater desalination. *Journal of Membrane Science*, 466:26–35, 2014.

[100] X. Wang, B. Cheng, C. Ji, M. Zhou, and L. Wang. Effects of hydraulic retention time on adsorption behaviours of EPS in an A/O-MBR: biofouling study with QCM-D. *Scientific reports*, 7(1):2895, 2017.

[101] M. Piatkovsky, H. Acar, A. B. Marciel, M. Tirrell, and M. Herzberg. A zwitterionic block-copolymer, based on glutamic acid and lysine, reduces the biofouling of UF and RO membranes. *Journal of Membrane Science*, 549:507–514, 2018.

[102] F. Wang and V. V. Tarabara. Pore blocking mechanisms during early stages of membrane fouling by colloids. *Journal of colloid and interface science*, 328(2):464–469, 2008.

[103] X. Wei, Z. Wang, J. Wang, and S. Wang. A novel method of surface modification to polysulfone ultrafiltration membrane by preadsorption of citric acid or sodium bisulfite. *Membrane Water Treatment*, 3(1):35–49, 2012.

[104] K. K. Pandey. A study of chemical structure of soft and hardwood and wood polymers by FTIR spectroscopy. *Journal of Applied Polymer Science*, 71(12):1969–1975, 1999.

[105] C.-M. Popescu, M.-C. Popescu, G. Singurel, C. Vasile, D. S. Argyropoulos, and S. Willför. Spectral characterization of eucalyptus wood. *Applied spectroscopy*, 61(11):1168–1177, 2007.

[106] M. Traoré, J. Kaal, and A. Martínez Cortizas. Differentiation between pine woods according to species and growing location using FTIR-ATR. *Wood science and technology*, 52(2):487–504, 2018.

[107] N. M. Stark, D. J. Yelle, and U. P. Agarwal. Techniques for characterizing lignin. In O. Faruk and M. Sain, editors, *Lignin in polymer composites*, pages 49–66. Elsevier B.V., Waltham, MA, 2016.

[108] R. Kumar, A. M. Isloor, A. F. Ismail, S. A. Rashid, and T. Matsuura. Polysulfone–Chitosan blend ultrafiltration membranes: preparation, characterization, permeation and antifouling properties. *RSC Advances*, 3(21):7855, 2013.

[109] F. Peng, N. Jia, P. Peng, R. C. Sun, and S. J. Liu. Isolation and fractiontion of hemicelluloses from Salix Psammophila. *Cellulose Chemistry and Technology*, 46(3-4):177–184, 2012.

[110] P. Oinonen, H. Krawczyk, M. Ek, G. Henriksson, and R. Moriana. Bioinspired composites from cross-linked galactoglucomannan and microfibrillated cellulose: Thermal, mechanical and oxygen barrier properties. *Carbohydrate Polymers*, 136:146–153, 2016.

[111] H. Chen, C. Ferrari, M. Angiuli, J. Yao, C. Raspi, and E. Bramanti. Qualitative and quantitative analysis of wood samples by Fourier transform infrared spectroscopy and multivariate analysis. *Carbohydrate Polymers*, 82(3):772–778, 2010.

[112] M. Kacuráková. FT-IR study of plant cell wall model compounds: pectic polysaccharides and hemicelluloses. *Carbohydrate Polymers*, 43(2):195–203, 2000.

[113] K. Singh, S. Devi, H. C. Bajaj, P. Ingole, J. Choudhari, and H. Bhrambhatt. Optical resolution of racemic mixtures of amino acids through nanofiltration membrane process. *Separation Science and Technology*, 49(17):2630–2641, 2014.

[114] P. Veerababu, B. B. Vyas, P. S. Singh, and P. Ray. Limiting thickness of polyamide–polysulfone thin-film-composite nanofiltration membrane. *Desalination*, 346:19–29, 2014.

[115] R. Lee, K. Stack, D. Richardson, T. Lewis, and G. Garnier. Effect of shear, temperature and pH on the dynamics of salt induced coagulation of wood resin colloids. *Colloids and Surfaces A: Physicochemical and Engineering Aspects*, 396:106–114, 2012.

[116] L. Lin, C. Feng, R. Lopez, and O. Coronell. Identifying facile and accurate methods to measure the thickness of the active layers of thin-film composite membranes – A comparison of seven characterization techniques. *Journal of Membrane Science*, 498:167–179, 2016.

[117] T. Hannuksela, B. Holmbom, G. Mortha, and D. Lachenal. Effect of sorbed galactoglucomannans and galactomannans on pulp and paper handsheet properties especially strength properties. *Nordic Pulp and Paper Research Journal*, 19(2):237–244, 2004.

[118] M. C. Dixon. Quartz crystal microbalance with dissipation monitoring: Enabling real-time characterization of biological materials and their interactions. *Journal of Biomolecular Techniques*, 19(3):151–158, 2008.

[119] R. Bordes and F. Höök. Separation of bulk effects and bound mass during adsorption of surfactants probed by quartz crystal microbalance with dissipation: insight into data interpretation. *Analytical chemistry*, 82(21):9116–9121, 2010.

[120] M. T. Opedal, P. Stenius, and L. Johnsson. Review: Colloidal stability and removal of extractives from process water in thermomechanical pulping. *Nordic Pulp and Paper Research Journal*, 26(3):248–257, 2011.

[121] K. Stack, R. Lee, D. Richardson, T. W. Lewis, and G. Garnier. Complex formation and stability of colloidal wood resin pitch suspensions with hemicellulose polymers. *Colloids and Surfaces A: Physicochemical and Engineering Aspects*, 441:101–108, 2014.

[122] A. Weis, M. R. Bird, and M. Nyström. The chemical cleaning of polymeric UF membranes fouled with spent sulphite liquor over multiple operational cycles. *Journal of Membrane Science*, 216(1-2):67–79, 2003.

[123] J. Thuvander, G. Rudolph, F. Lipnizki, and A.-S. Jönsson. Fouling and cleaning of membranes in biorefineries, 2017.

[124] F. Lipnizki. Membrane cleaning: Email message, 11/02/2021.

[125] A. Arenillas, A. Drouin, E. Monnin, and P. Moulin. Glycerin removal from ultrafiltration flat sheet membranes by filtration and soaking. *Journal of Membrane Science and Research*, 3(2):102–108, 2017.

[126] J. Thuvander. Membrane conditioning: Oral, 2018.

[127] N. L. Owen and D. W. Thomas. Infrared studies of "hard" and "soft" woods. *Applied spectroscopy*, 43(3):451–455, 1989.

[128] C. Zhou, W. Jiang, Q. Cheng, and B. K. Via. Multivariate calibration and model integrity for wood chemistry using Fourier transform infrared Spectroscopy. *Journal of analytical methods in chemistry*, 2015:429846, 2015.

[129] S.-H. Lee, W.-S. Chang, S.-M. Han, D.-H. Kim, and J.-K. Kim. Synchrotron X-ray nano-tomography and three-dimensional nanoscale imaging analysis of pore structure-function in nanoporous polymeric membranes. *Journal of Membrane Science*, 535:28–34, 2017.

[130] S. Li, H. Chen, X. Zhao, L. A. Lucia, C. Liang, and Y. Liu. Impact factors for flux decline in ultra-filtration of lignocellulosic hydrolysis liquor. *Separation and Purification Technology*, 240:116597, 2020.

[131] E. Löwer, T. Leißner, and U. A. Peuker. Insight into filter cake structures using micro tomography: The dewatering equilibrium. *Separation and Purification Technology*, 252:117215, 2020.

[132] Y. Y. Tham, P. J. Molino, M. J. Higgins, K. R. Stack, D. E. Richardson, and T. W. Lewis. The study of deposition of wood extractives and model compound colloids onto chromium and cellulose surfaces using quartz crystal microbalance with dissipation (QCM-D). *Colloids and Surfaces A: Physicochemical and Engineering Aspects*, 491:1–11, 2016.

[133] T. Virtanen, S.-P. Reinikainen, J. Lahti, M. Mänttäri, and M. Kallioinen. Visual tool for real-time monitoring of membrane fouling via Raman spectroscopy and process model based on principal component analysis. *Scientific Reports*, 8(1):11057, 2018.

A Appendix

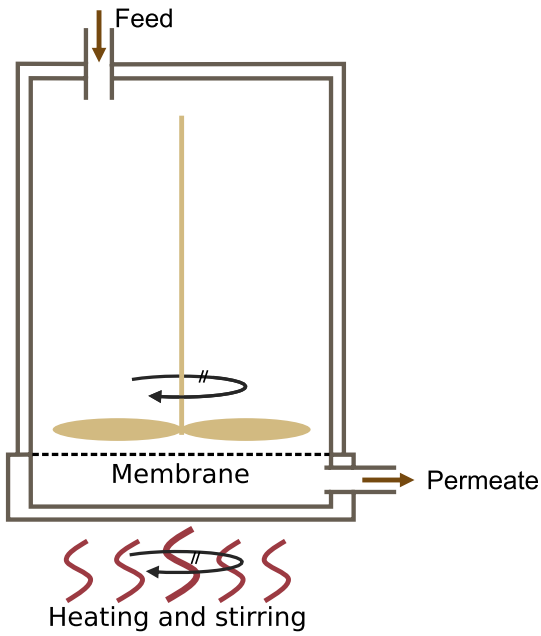

Figure A.1 Schematic of the dead-end module. TMP was generated by nitrogen gas and set with a valve connected to the feed side. The temperature and the angular velocity of the stirrer were controlled by a magnetic stirrer with a built-in heating plate.

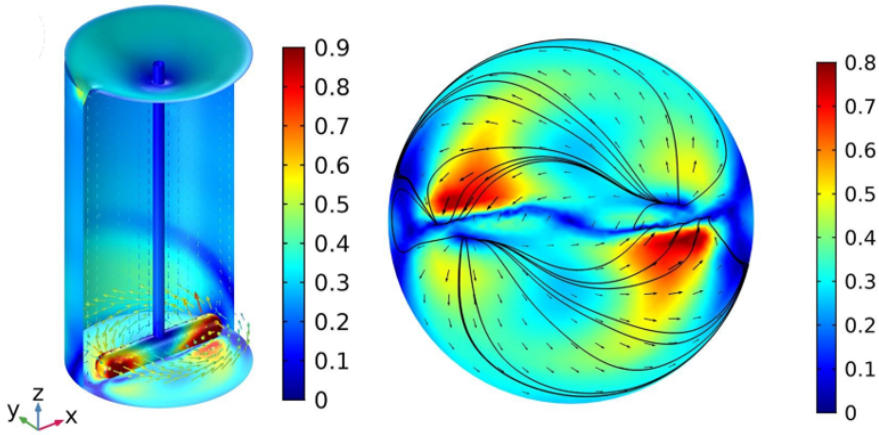

Figure A.2 Computational fluid dynamics simulations of the flow conditions in the dead-end module for a water-like solution. The gradient legends show the velocity in m/s. (Adjusted from [8].)

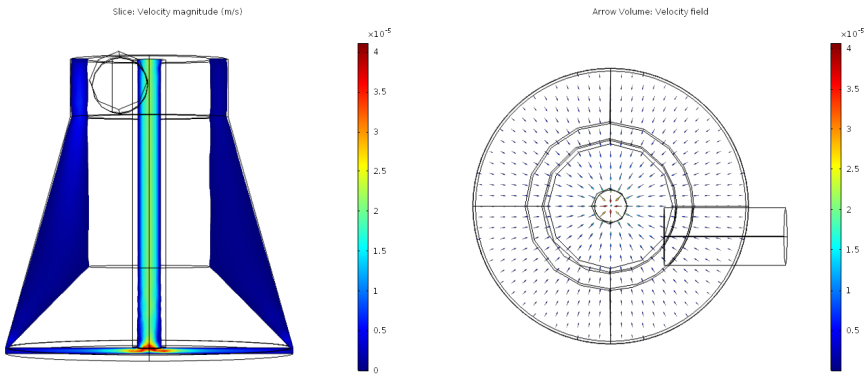

Figure A.3 Computational fluid dynamics simulations of the flow conditions in the cross-flow module for a water-like solution at 50°C. The design was done by B. Al-Rudainy, the modelling by G. Rudolph. Left: The color gradient legend indicates the velocity magnitude in the module with red being the highest and blue being the lowest value. Right: Arrows and the color gradient legend indicating the direction and the strength of the volume flow, respectively.

Fouling and cleaning of membranes in biorefineries

Johan Thuvander, Gregor Rudolph, Frank Lipnizki and Ann-Sofi Jönsson
Department of Chemical Engineering, Lund University, P.O. Box 124, SE-221 00 Lund, Sweden

Background

- Wood compounds like cellulose, hemicelluloses and lignin have great potential as biobased value-added products
- Microfiltration (MF) and ultrafiltration (UF) will play important roles as separation processes in biorefineries

Challenges

- **Fouling** is a great obstacle in the introduction of membrane processes in biorefineries: it reduces flux and alters retention
- **Cleaning** reduces negative effects of fouling but requires chemicals, harsh cleaning conditions and causes downtime, and thus has a negative impact on process costs

Aim: Tailored cleaning protocols to maintain a high filtering capacity while reducing the amount of cleaning agents and process downtime

Methods

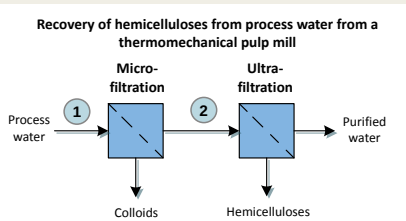

Solution	Dry solids	Ash	Hemicelluloses	Lignin
1	6.7 g/L	1.0 g/L	2.0 g/L	0.8 g/L
2	5.4 g/L	0.9 g/L	1.3 g/L	0.8 g/L

Treatment	Operation conditions	
	MF	UF
Fouling	60 L, 0.8 bar, 80 °C, 2.0 m/s, 14 h	6 L, 2.0 bar, 75 °C, 0.02 m/s, 17 h
Cleaning	0.5 bar, 50 °C, 2.0 m/s, 1 h	2.0 bar, 50 °C, 0.2 m/s, 1 h

Cleaning	Cleaning agent
Alkali	1.0 wt% Ultrasil 10, containing sodium hydroxide and tensides
Acid	2.0 wt% Ultrasil 75, containing phosphoric acid and nitric acid
Chlorine	0.1 wt% sodium hydroxide and 250 ppm sodium hypochlorite

Pure water flux after fouling and cleaning

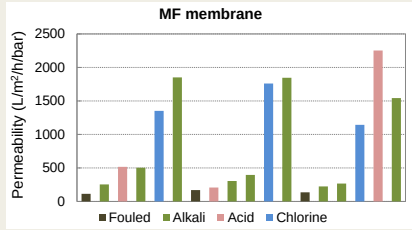

- Acidic and alkaline cleaning are insufficient as sole cleaning methods
- Chlorine cleaning is needed to recover membrane permeability
- Chlorine cleaning is more efficient after acidic and alkaline cleaning

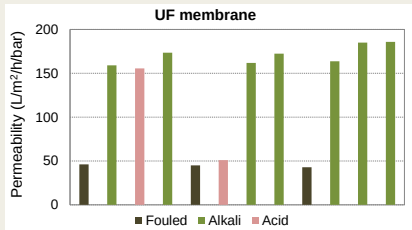

- Acidic cleaning is insufficient as sole cleaning method
- Alkaline cleaning recovered permeability effectively
- Slightly overall increased permeability due to continuous removal of membrane storage preservatives during the cleaning procedure

Outlook

- Examine fouling and cleaning with in situ methods (QCM-D, Ellipsometry, Raman spectroscopy, ToF-SIMS) to obtain a deeper insight into interactions at membrane surfaces
- Investigate the possibility to replace chlorine with hydrogen peroxide during cleaning of MF membranes
- Examine enzymatic cleaning of UF membranes
- Develop tailored cleaning protocols adapted for specific operation conditions and feed composition

Contacts:

Johan.Thuvander@chemeng.lth.se
Gregor.Rudolph@chemeng.lth.se

Figure A.4 Poster from the 7th Nordic Wood Biorefinery Conference in Stockholm, 2017 [123].

Scientific Publications

Paper I

A review of in situ real-time monitoring techniques for membrane fouling in the biotechnology, biorefinery and food sectors

G. Rudolph, T. Virtanen, M. Ferrando, C. Güell, F. Lipnizki, M. Kallioinen

Journal of Membrane Science **2019**, 588, 117221

Paper II

Investigations on alkaline and enzymatic membrane cleaning of ultrafiltration membranes fouled by thermomechanical pulping process water

G. Rudolph, H. Schagerlöf, K. B. Morkeberg Krogh, A.-S. Jönsson, F. Lipnizki

Membranes **2018**, 8(4), 91

Paper III

Analysis of ultrafiltration membrane fouling by Brunauer-Emmett-Teller nitrogen adsorption/ desorption technique

T. Virtanen, **G. Rudolph**, A. Lopatina, B. Al-Rudainy, H. Schagerlöf, L. Puro, M. Kallioinen, F. Lipnizki

Scientific Reports **2020**, 10, 3427

Paper IV

In situ real-time investigations on adsorptive membrane fouling by thermo-mechanical pulping process water with quartz crystal microbalance with dissipation monitoring (QCM-D)

G. Rudolph, A. Hermansson, A.-S. Jönsson, F. Lipnizki

Separation and Purification Technology **2021**, 254, 117578

Paper v

QCM-D for studying membrane fouling - opportunities and limitations on the example of process water from thermomechanical pulping

G. Rudolph, H. Schagerlöf, A.-S. Jönsson, F. Lipnizki

Manuscript

Paper VI

Comprehensive analysis of foulants in an ultrafiltration membrane used for the treatment of bleach plant effluent in a sulfite pulp mill

G. Rudolph, B. Al-Rudainy, J. Thuvander, A.-S. Jönsson

Membranes **2021**, 11(3), 201